Nonlinear modulational stability of periodic traveling-wave solutions of the generalized Kuramoto-Sivashinsky equation

Blake Barker, Mathew A. Johnson, Pascal Noble, Luis Miguel Miguel Rodrigues, Kevin Zumbrun

Nonlinear modulational stability of periodic traveling-wave solutions of the generalized Kuramoto–Sivashinsky equation

Blake Barker* Mathew A. Johnson† Pascal Noble‡
L.Miguel Rodrigues§ Kevin Zumbrun¶

March 16, 2012

Keywords: Periodic traveling waves; Kuramoto-Sivashinsky equation; Nonlinear stability.

2000 MR Subject Classification: 35B35, 35B10.

Abstract

In this paper we consider the spectral and nonlinear stability of periodic traveling wave solutions of a generalized Kuramoto-Sivashinsky equation. In particular, we resolve the long-standing question of nonlinear modulational stability by demonstrating that spectrally stable waves are nonlinearly stable when subject to small localized (integrable) perturbations. Our analysis is based upon detailed estimates

*Indiana University, Bloomington, IN 47405; bhbarker@indiana.edu: Research of B.B. was partially supported under NSF grants no. DMS-0300487 and DMS-0801745.

†Department of Mathematics, University of Kansas, 1460 Jayhawk Boulevard, Lawrence, KS 66045; matjohn@math.ku.edu: Research of M.J. was partially supported by an NSF Postdoctoral Fellowship under DMS-0902192.

‡Université de Lyon, Université Lyon I, Institut Camille Jordan, UMR CNRS 5208, 43 bd du 11 novembre 1918, F - 69622 Villeurbanne Cedex, France; noble@math.univ-lyon1.fr: Research of P.N. was partially supported by the French ANR Project no. ANR-09-JCJC-0103-01.

§Université de Lyon, Université Lyon 1, Institut Camille Jordan, UMR CNRS 5208, 43 bd du 11 novembre 1918, F - 69622 Villeurbanne Cedex, France; rodrigues@math.univ-lyon1.fr: Stay of M.R. in Bloomington was supported by the French ANR Project no. ANR-09-JCJC-0103-01.

¶Indiana University, Bloomington, IN 47405; kzumbrun@indiana.edu: Research of K.Z. was partially supported under NSF grant no. DMS-0300487.

of the linearized solution operator, which are complicated by the fact that the (necessarily essential) spectrum of the associated linearization intersects the imaginary axis at the origin. We carry out a numerical Evans function study of the spectral problem and find bands of spectrally stable periodic traveling waves, in close agreement with previous numerical studies of Frisch–She–Thual, Bar–Nepomnyashchy, Chang–Demekhin–Kopelevich, and others carried out by other techniques. We also compare predictions of the associated Whitham modulation equations, which formally describe the dynamics of weak large scale perturbations of a periodic wave train, with numerical time evolution studies, demonstrating their effectiveness at a practical level. For the reader's convenience, we include in an appendix the corresponding treatment of the Swift-Hohenberg equation, a nonconservative counterpart of the generalized Kuramoto-Sivashinsky equation for which the nonlinear stability analysis is considerably simpler, together with numerical Evans function analyses extending spectral stability analyses of Mielke and Schneider,

Contents

1 Introduction

Localized coherent structures such as solitary waves play an essential role as elementary processes in nonlinear phenomena. Examples of this are multi-bump solutions in reaction diffusion equations, which are constructed by piecing together well-separated solitary waves [E], or the limiting case of infinite, periodic wave trains. A similar situation occurs in nonlinear dispersive media described by a KdV equation where exact multi-bump and periodic solutions exist. In this paper, we consider *periodic solutions* of an *unstable dissipative- dispersive* nonlinear equation, namely a generalized Kuramoto-Sivashinsky (gKS) equation

$$u_t + \gamma\partial_x^4 u + \varepsilon\partial_x^3 u + \delta\partial_x^2 u + \partial_x f(u) = 0, \quad \gamma, \delta > 0, \tag{1.1}$$

where $f(u)$ is an appropriate nonlinearity and $\varepsilon, \gamma \in \mathbb{R}$ are arbitrary constants with $\gamma > 0$. In the case $f(u) = \frac{u^2}{2}$, equation (1.1) is a canonical model

for pattern formation that has been used to describe, variously, plasma instabilities, flame front propagation, turbulence in reaction-diffusion systems and nonlinear waves in fluid mechanics [S1, S2, K, KT, CD, PSU].

Equation (1.1) may be derived formally either from shallow water equations [YY] or from the full Navier-Stokes system [W] for $0 < \gamma = \delta \ll 1$. Here δ measures the deviation of the Reynolds number from the critical Reynolds number above which large scale weak perturbations are spectrally unstable. For this latter application, what we have in mind is the description of chaotic motions in thin film flows down an incline [CD]. Indeed, periodic traveling waves are some of the few simple solutions in the attractor for the classic ($\varepsilon = 0$) Kuramoto-Sivashinsky equation, a generic equation for chaotic dynamics, and there is now a huge literature on these solutions (and their bifurcations, in particular period doubling cascades) and their stability; see [FST, KE, K, CD]. As ε increases, the set of stable periodic waves, and presumably also their basin of attraction appears (numerically) to enlarge [CDK, BaN], until, in the $|(\gamma, \delta)| \to 0$ limit, they and other approximate superpositions of solitary waves appear to dominate asymptotic behavior [CD, PSU, BJRZ, BJNRZ2].

Since $\delta > 0$ it is easily seen via Fourier analysis that all constant solutions of (1.1) are unstable, from which it follows that all asymptotically constant solutions (such as the solitary waves) are also unstable. Nevertheless, one can still construct multi-bump solutions to (gKS) on asymptotically large time $O(\delta^{-1})$ by gluing together solitary waves, provided that the distance between them is not too large [PSU]. One possible interpretation of this is that there exist stable periodic wave trains nearby the solitary wave. Indeed, it has been known, almost since the introduction of the classical Kuramoto-Sivashinsky equation (1.1) ($\varepsilon = 0$) in 1975, that there exists a spectrally stable band of periodic solutions in parameter space; see for example the numerical studies in [CKTR, FST]. These stable periodic wave trains may be heuristically viewed as a superposition of infinitely many well separated solitary waves. In [EMR], the existence of such a band of stable periodic traveling waves was justified for the equation (1.1) with *periodic boundary conditions* and in the singular KdV limit $|(\gamma, \delta)| \to 0$.

Although numerical time-evolution experiments suggest that these spectrally stable waves are nonlinearly stable as well (see [CD]), up to now this conjecture had not been rigorously verified. In this paper, relying heavily on the recent infusion of new tools in [JZ1, JZN, BJRZ, BJNRZ1, BJNRZ2] in the context of general conservation laws and the St. Venant (shallow water) equations, we prove the result, previously announced in [BJNRZ3], that *spectral modulational stability of periodic solutions of* (1.1), defined in

the standard sense, *implies linear and nonlinear modulational stability to small localized* (integrable) *perturbations*; that is, a localized perturbation of a periodic traveling wave converges to a periodic traveling wave that is modulated in phase. The first such nonlinear result for any version of (1.1), this closes in particular the 35-year old open question of nonlinear stability of spectrally stable periodic waves of the classical Kuramoto-Sivashinsky equation ($\varepsilon = 0$) found numerically in [FST].

With these improvements in nonlinear theory, we find this also an opportune moment to make a definitive discussion of the generalized Kuramoto-Sivashnisky equation (and Swift-Hohenberg equations) in terms of existence, nonlinear theory, and numerical spectral stability studies, all three, across all parameters, both connecting to and greatly generalizing the variety of prior works [FST, KE, K, CD, M1, Sc, CDK, BaN]. We thus carry out also a numerical analysis of the spectrum in order to check the spectral assumptions made in our main theorem. Since the spectrum always contains the origin, due to both translational invariance and the conservative form of the equations, this stability is at best marginal, a circumstance that greatly complicates both numerical and analytical stability analyses.

Our numerical approach is based on complementary tools; namely Hills method and the Evans function. On the one hand, we use SpectrUW numerical software [CDKK] based on Hills method, which is a Galerkin method of approximation, in order to obtain a good overview of location of the spectrum: the periodic coefficients and eigenvectors are expanded using Fourier series, and then a frequency cutoff is used to reduce the problem to finding eigenvalues of a finite dimensional matrix. It is known that Hills method converges faster than any algebraic order [JZ5]; moreover, in practice, it gives quickly a reliable global qualitative picture. However, the associated error bounds are of abstract nature, with coefficients whose size is not a priori guaranteed. Further, near the critical zone around $\lambda = 0$, the resolution of this method is not in practice sufficient to guess at stability, let alone obtain satisfactory numerical verification.

Thus, in order to get more reliable pictures near the origin and guarantee the spectral stability of periodic wave, we use on the other hand an Evans function approach, computing a winding number to prove that there is or is not unstable spectrum in the part of the unstable (positive real part) complex half plane excluding a small neighborhood of the origin, then using Cauchy's integral formula to determine the Taylor expansions of the spectral curves passing through the origin. This method, though cumbersome for approximating global spectrum, is excellent for excluding the existence of spectra on a given region, and comes with error bounds that can in

a practical sense be prescribed via the tolerance of the Runga–Kutta 4-5 scheme used to evaluate the Evans function by solution of an appropriate ODE; see [Br, Z1, BJNRZ1] for general discussion of convergence of Evans function methods. Furthermore, under generic assumptions, the numerical protocol introduced in Section 2.1.3 below detects sideband stability and instability of the underlying periodic wave train without the need of lengthy spectral perturbation expansion calculations, thus adding what we believe is a valuable new method to the numerical toolbox for analyzing the spectral stability of periodic wave trains. For relations between Hill's method, Fredholm determinants, and the periodic Evans function of Gardner, see [JZ5, Z2].

In order to validate our numerical method, we check benchmarks from the Kuramoto-Sivashinsky equation ($\varepsilon = 0, f(u) = u^2/2$) and the Swift Hohenberg equation. We obtain very good agreement with existing numerical works. In particular, we recover and extend stability boundaries found numerically for KS in [FST] and analytically for Swift-Hohenberg in [M1, Sc]. Then we perform an all-parameters study linking in particular the Kuramoto-Sivashinsky equation $\varepsilon \to 0$ $\gamma = \delta = 1$ to KdV equation $\varepsilon = 0, \gamma = \delta \to 0$ by homotopy, again obtaining excellent agreement with existing results of [CDK, BaN]. A rigorous proof of spectral stability of periodic traveling wave solutions of (1.1), in the spirit of [M1, Sc], or a numerical proof (interval arithmetic) would be a very interesting direction for future work, particularly in an interesting parameter regime such as the canonical KDV limit $|(\gamma, \delta)| \to 0$ studied in [PSU]. In this regard, we point to the recent singular perturbation analysis of this limit in [BaN] and [JNRZ4], the second relying on and completing the first, reducing the problem of rigorous validation of stability/instability as $|(\gamma, \delta)| \to 0$ to computer-verified evaluation of the signs of certain elliptic integrals associated with KdV.

As we will see, our main theorem indicates that the long time dynamics of a localized perturbation of a given periodic traveling wave of (1.1) is governed by a space-time dependent phase modulation $\psi(x, t)$, which in turn satisfies in some sense a set of modulation equations. Moreover, it is well known that, in the neighborhood of the origin, the spectrum of the linearization about a given periodic wave train is strongly related to some local well-posedness properties of the associated linearized Whitham system; this set of modulation equations may be derived via a nonlinear optics expansion (WKB), and formally govern the evolution of weak large scale perturbations of the underlying wave train.

In [FST], the authors derive for the classic Kuramoto-Sivashinsky equation ($\varepsilon = 0$) a second order modulation equation in the phase ψ of the

form $\psi_{tt} - a\psi_{xx} = b\psi_{txx}$, which is indeed an alternative formulation of the linearized Whitham equations; more generally, the Whitham equations for (1.1) consist of a system of two first-order conservation laws [NR2]. The signs of the coefficients a and b depend implicitly on the underlying wave train, and determine the spectral stability in the low frequency/low wave number regime; see again [NR2]. The fact that Whitham's equations determines (a part of) the spectral stability of periodic wave trains in the low frequency regime has also been established for viscous conservation laws in [Se], for generalized KdV equations in [JZ4] and [BrJZ], and for the shallow water equations with a source term in [NR1].

Here, in terms of the modulation equations we have two requirements for low-frequency modulational stability: reality of the characteristics of the first order part (in [FST], positivity of sound speed squared; more generally, positivity of a certain discriminant); and positivity of the various diffusion parameters associated with different characteristic modes (which are equal in the classic case [FST], but in general distinct [NR1, NR2]).

We point out that the justification of such Whitham equations has become an important direction of research in the last decade, with important and fundamental results being given, for example, in the context of the reaction diffusion equations [DSSS] and the Shallow water equations [NR1]. In this paper, we carry out numerical time evolution studies that illustrate this correspondence with the Whitham equations; see section 2.3. In the forthcoming paper [JNRZ1], the authors provide a rigorous justification of Whitham's equations in the context of viscous conservations laws, which applies in particular to equation (1.1). The approach proposed there extends readily to other second and higher order parabolic equations such as the Cahn-Hilliard equation, general fourth order thin film models, and to general systems of quasilinear $2r$-parabolic equations such as the Swift Hohenberg equation.

The paper is organized as follows: in the current section, we introduce the assumptions of our main theorem, both on the set of periodic traveling wave solutions of (1.1) and on the spectrum of the linearization of (1.1) about such a wave. After stating our main theorem we continue with section 2 where we, among other things, check numerically that the spectral stability assumptions of our main theorem are satisfied for some families of periodic traveling wave solutions of (1.1). In particular, we show that there exist bands in parameter space of spectrally stable periodic traveling waves and verify that these bands agree in particular asymptotic limits with previous numerical studies [FST, CDK, BaN]. Section 3 is dedicated to the proof of the main theorem of our paper: that is, that spectral modulational

stability implies linear and nonlinear modulational stability to small localized perturbations. The proof is an adaptation of the analysis recently given for the St. Venant equations and the case of general, second order, viscous conservation laws; see [JZN, JZ1].

For completeness, we present in Appendix A a survey of the existence theory in the periodic context in a variety of asymptotic regimes; small amplitude, near the classic Kuramoto-Sivashinsky equation ($\varepsilon \to 0$, $\gamma = \delta = 1$), and near the KdV equation ($\varepsilon = 1$, $\gamma = \delta \to 0$). In Appendix B, we prove a nonlinear stability result, analogous to our main theorem, in the case of the Swift-Hohenberg equation. The nonconservative nature of this equation makes the nonlinear stability analysis considerably simpler than that presented in Section 3, and the reader unfamiliar with the techniques of Section 3 may find it helpful to read the Swift-Hohenberg analysis as a precursor to Section 3. Also in Appendix B we conduct a numerical study similar to but less detailed than that given in Section 2. In particular, this numerical study complements and extends the analytical results of [M1, Sc]. In Appendices C and D, we describe, respectively, computational statistics and the shooting algorithm [BJNRZ1] used to estimate the Evans function at a given frequency pair (λ, ξ). Finally, in Section E, we estimate the rate of growth of perturbations of unstable waves lying near stability boundaries of hyperbolic vs. diffusive type.

1.1 Equations and assumptions

Consider the generalized Kuramoto-Sivashinsky (gKS) equation given in (1.1), written here in the form

$$\partial_t u + \partial_x^4 u + \varepsilon \partial_x^3 u + \delta \partial_x^2 u + \partial_x f(u) = 0 \tag{1.2}$$

with $f \in C^2(\mathbb{R})$ and $\delta > 0$. The main goal of this paper is to establish that spectrally stable (in a sense made precise in (D1)–(D3), Section 1.1.3) periodic traveling wave solutions to (1.2) are nonlinearly stable with respect to small localized perturbations. As (1.2) is conservative, the stability analysis is an adaptation of that of [JZ1, JZN] in the second-order viscous conservation law and hyperbolic-parabolic system cases, respectively. The main new aspect here is to show that the principles contained in these previously considered cases extend to equations with higher-order derivatives.

It should be noted that this analysis applies also, with slight modifications, to more general quasilinear equations (see [JZN]), to the Cahn-Hilliard equation, and to other fourth-order models for thin film flow as discussed,

for example, in [LP, BMS, Ho].[1] Indeed, the argument and results extend to arbitrary $2r$-order parabolic systems, so are essentially completely general for the diffusive case. (As already seen in [JZ1], they can apply also to mixed-order and relaxation type systems in some cases as well.)

We emphasize here as in the introduction above that if one considers rather the generalized Swift-Hohenberg equation

$$\partial_t u + \partial_x^4 u + \varepsilon \partial_x^3 u + \delta \partial_x^2 u + f(u) = 0, \tag{1.3}$$

considered here as a non-conservative counterpart of (1.2), the verification of nonlinear stability of spectrally stable periodic traveling waves is considerably less complicated. Indeed, this is reminiscent of the distinction between general second-order parabolic conservation laws and systems of reaction diffusion equations; see [JZ1] and [JZ2]. To aid in the understanding of the forthcoming analysis of the conservative equation (1.2), therefore, we present in Appendix B the proof of the analogous nonlinear stability result for periodic traveling wave solutions of (1.3). Our approach there recovers and slightly extends the results of Schneider [Sc], yielding the same heat kernel rate of decay with respect to localized perturbations while removing the assumption that nearby periodic waves have constant speed.

1.1.1 Traveling-wave equation and structural assumptions

Throughout, we consider traveling wave solutions of (1.2) or, equivalently, stationary solutions of the traveling gKS equation

$$\partial_t u - c\partial_x u + \partial_x^4 u + \varepsilon \partial_x^3 u + \delta \partial_x^2 u + \partial_x f(u) = 0 \tag{1.4}$$

for some wave speed $c \in \mathbb{R}$. Such profiles are necessarily solutions of the traveling wave ODE

$$-cu' + u'''' + \varepsilon u''' + \delta u'' + f(u)' = 0, \tag{1.5}$$

which, integrated once, reads

$$-cu + u''' + \varepsilon u'' + \delta u' + f(u) = q, \tag{1.6}$$

where $q \in \mathbb{R}$ is a constant of integration. It follows that periodic solutions of (1.2) correspond to values $(X, c, q, b) \in \mathbb{R}^6$, where X, c, and q denote period, speed, and constant of integration, and $b = (b_1, b_2, b_3)$ denotes the

[1] In these cases, which concerned scalar equations, periodic waves were shown to be unstable in a wide variety of circumstances.

values of (u, u', u'') at $x = 0$, such that the values of (u, u', u'') at $x = X$ of the solution of (1.5) are equal to the initial values (b_1, b_2, b_3).

Following [Se, JZ1], we make the following technical assumptions:

(H1) $f \in C^{K+1}(\mathbb{R})$, $K \geq 5$.

(H2) The map $H : \mathbb{R}^6 \to \mathbb{R}^3$ taking $(X, b, c, q) \mapsto (u, u', u'')(X; b, c, q) - b$ is full rank at $(\bar{X}, \bar{b}, \bar{c}, \bar{q})$, where $(u, u', u'')(\cdot; b, c, q)$ is the solution of (1.6) such that
$$(u, u', u'')(0; b, c, q) = b.$$

By the Implicit Function Theorem, conditions (H1)–(H2) imply that the set of periodic solutions in the vicinity of the $\bar{X}$-periodic function $\bar{u} = u(\cdot; \bar{b}, \bar{c}, \bar{q})$ forms a smooth 3-dimensional manifold

$$\{\ (x,t) \mapsto U(x - \alpha - c(\beta)t; \beta) \mid (\alpha, \beta) \in \mathbb{R} \times \mathcal{U}\ \}, \quad \text{with } \mathcal{U} \subset \mathbb{R}^2. \tag{1.7}$$

Remark 1.1. As noted in [JZN], the transversality assumption (H2) is necessary for our notion of spectral stability; see (D3) in Section 1.1.3 below. Hence, there is no loss of generality in making this assumption.

1.1.2 Linearized equations and the Bloch transform

To begin our stability analysis we consider the linearization of (1.4) about a fixed periodic traveling wave solution $\bar{u} = U(\cdot; \bar{\beta})$, where we assume without loss of generality $\bar{X} = 1$. To this end, consider a nearby solution of (1.4) of the form
$$u(x,t) = \bar{u}(x) + v(x,t)$$
where $v(\cdot, t) \in L^2(\mathbb{R})$ is small in some topology (to be defined precisely later), corresponding to a small localized perturbation of the underlying solution $\bar{u}$. Directly substituting this into (1.4) and neglecting quadratic order terms in v leads us to the linearized equation

$$\partial_t v = Lv := \partial_x\left((c-a)v\right) - \partial_x^4 v - \varepsilon\partial_x^3 v - \delta\partial_x^2 v, \qquad a := f'(\bar{u}),\ c := \bar{c}. \tag{1.8}$$

Seeking separated solutions of the form $v(x,t) = e^{\lambda t}v(x)$, $v \in L^2(\mathbb{R})$ and $\lambda \in \mathbb{C}$ yields the eigenvalue problem

$$\lambda v = Lv \tag{1.9}$$

considered on the real Hilbert space $L^2(\mathbb{R})$.

As the coefficients of L are 1-periodic functions of x, Floquet theory implies that the spectrum of the operator L, considered here as a densely defined operator on $L^2(\mathbb{R})$, is purely continuous and, in particular, $\lambda \in \sigma(L)$ if and only if the spectral problem (1.9) has a bounded eigenfunction of the form

$$v(x;\lambda,\xi) = e^{i\xi x} w(x;\lambda,\xi) \tag{1.10}$$

for some $\xi \in [-\pi,\pi)$ and $w \in L^2_{\mathrm{per}}([0,1])$. Following [G1, S1, S2], we find that substituting the ansatz (1.10) into (1.9) leads one to consider the one-parameter family of Bloch operators $\{L_\xi\}_{\xi\in[-\pi,\pi)}$ acting on $L^2_{\mathrm{per}}([0,1])$ via

$$\left(L_\xi w\right)(x) := e^{-i\xi x} L\Big[e^{i\xi\cdot} w(\cdot)\Big](x). \tag{1.11}$$

Since the Bloch operators have compactly embedded domains $H^4_{\mathrm{per}}([0,1])$ in $L^2_{\mathrm{per}}([0,1])$, their spectrum consists entirely of discrete eigenvalues which, furthermore, depend continuously on the Bloch parameter ξ. It follows then by standard considerations that

$$\sigma_{L^2(\mathbb{R})}(L) = \bigcup_{\xi\in[-\pi,\pi)} \sigma_{L^2_{\mathrm{per}}([0,1])}\left(L_\xi\right);$$

see [G1] for details. More precisely, the spectrum of L can be characterized by the union of countably many surfaces $\lambda(\xi)$ such that $\lambda(\xi) \in \sigma(L_\xi)$ for each $\xi \in [-\pi,\pi)$.

Given a function $u \in L^2(\mathbb{R})$ we now recall its inverse Bloch-representation

$$u(x) = \int_{-\pi}^{\pi} e^{i\xi\cdot x} \check{u}(\xi,x) d\xi, \tag{1.12}$$

where $\check{u}(\xi,x) := \sum_k e^{2\pi i k x} \hat{u}(\xi+2\pi k)$ are 1-periodic functions and $\hat{u}(\cdot)$ denotes the Fourier transform of u, defined here as

$$\hat{u}(z) = \frac{1}{2\pi}\int_{\mathbb{R}} e^{-i\omega z} u(\omega) d\omega.$$

Denote by $\mathcal{B} : u \mapsto \check{u}$ the Bloch transform operator taking $u \in L^2(\mathbb{R})$ to its Bloch transform $\check{u} \in L^2([-\pi,\pi); L^2_{\mathrm{per}}([0,1]))$.[2] For a given linear operator L with 1-periodic coefficients, it can readily be verified that $\mathcal{B}\left(Lu\right)(\xi,x) =$

[2] Here, and elsewhere, we are adopting the notation $\|f\|_{L^q([-\pi,\pi),L^p([0,1]))} := \left(\int_{-\pi}^{\pi} \|f(\xi,\cdot)\|^q_{L^p([0,1])} d\xi\right)^{1/q}$.

$L_\xi\left[\check{u}(\xi,\cdot)\right](x)$ hence the associated Bloch operators L_ξ may be viewed as operator-valued symbols under $\mathcal{B}$ acting on $L^2_{\rm per}([0,1])$. Furthermore, the identity $\mathcal{B}\left(e^{Lt}u\right)(\xi,x) = e^{L_\xi t}\left[\check{u}(\xi,\cdot)\right](x)$ naturally yields the inverse representation formula

$$e^{Lt}u_0 = \int_{-\pi}^{\pi} e^{i\xi\cdot x} e^{L_\xi t}\left[\check{u}_0(\xi,\cdot)\right](x)d\xi \tag{1.13}$$

relating behavior of the linearized equation (1.9) to that of the diagonal Bloch operators L_ξ.

The representation formula (1.13) suggests that bounds on the linear solution operator e^{Lt} acting on some function in $L^2(\mathbb{R})$ may be obtained from bounds on the associated operators $e^{L_\xi t}$ acting on $L^2_{\rm per}([0,1])$. To facilitate these estimates, we notice by Parseval's identity that the Bloch transform $u \mapsto \mathcal{B}(u) = \check{u}$ is an isometry in L^2, i.e.

$$\|u\|^2_{L^2(\mathbb{R})} = 2\pi \int_{-\pi}^{\pi}\int_0^1 |\check{u}(\xi,x)|^2\, dx\; d\xi = 2\pi \|\check{u}\|^2_{L^2([-\pi,\pi);L^2([0,1]))}, \tag{1.14}$$

More generally, we have for any one-parameter family of 1-periodic functions $f(\xi,\cdot)$, $\xi \in [-\pi,\pi)$, the generalized Hausdorff-Young inequality

$$\Big\| \int_{-\pi}^{\pi} e^{i\xi\cdot} f(\xi,\cdot)d\xi \Big\|_{L^p(\mathbb{R})} \le (2\pi)^{\frac{1}{p}} \|f\|_{L^q([-\pi,\pi),L^p([0,1]))} \tag{1.15}$$

valid for any $q \le 2 \le p$ and $\frac{1}{p} + \frac{1}{q} = 1$; this is readily obtained interpolating Parseval's identity with Triangle Inequality (case $q = 1$, $p = \infty$), see [JZ1]. It is in the context of the above functional framework that we will obtain our crucial linearized estimates; see Section 3.2 below.

1.1.3 Spectral stability assumptions

Taking variations in a neighborhood of $\bar{u}$ along the 3-dimensional periodic solution manifold (1.7) in directions for which the period does not change, we find that the generalized kernel of the Bloch operator L_0 is at least two-dimensional by assumption (H2); see [NR2] for more details. Following [JZ1] then, we assume along with (H1)–(H2) the following *spectral diffusive stability* conditions:

(D1) $\sigma(L) \subset \{\ \lambda \in \mathbb{C} \mid \mathrm{Re}(\lambda) < 0\ \} \cup \{0\}$.

(D2) $\sigma(L_\xi) \subset \left\{\ \lambda \in \mathbb{C} \;\middle|\; \mathrm{Re}(\lambda) \le -\theta|\xi|^2\ \right\}$, for some $\theta > 0$ and any $\xi \in [-\pi,\pi)$.

(D3) $\lambda = 0$ is an eigenvalue of L_0 of algebraic multiplicity two.

Assumptions (H1)-(H2) and (D3) imply that there exist two eigenvalues of the form

$$\lambda_j(\xi) = -ia_j\xi + o(|\xi|) \tag{1.16}$$

of L_ξ bifurcating from $\lambda = 0$ at $\xi = 0$; see Lemma 3.1 below. Following [JZ1], we make the following non-degeneracy hypothesis:

(H3) The coefficients a_j in (1.16) are distinct.

Hypothesis (H3) ensures the analyticity of the functions $\lambda_j(\cdot)$; again, see Lemma 3.1 below for details.

Continuing, we notice that when $f(u) = \frac{u^2}{2}$ the Galilean invariance of (1.1), along with assumptions (H1)-(H2) and (D3), implies that the zero-eigenspace of L_0 admits a non-trivial Jordan chain of height two [NR2]. Indeed, in this case it is readily checked that the map

$$\mathcal{G}_c u(x,t) = u(x - ct, t) + c$$

sends solutions of (1.4) to solutions of (1.1) so that, in particular, variations in wave speed are period-preserving. It follows that the periodic solution manifold (1.7) can be parameterized as

$$\left\{ (x,t) \mapsto U(x - \alpha - ct; c, b) \;\middle|\; (\alpha, c, \beta) \in \mathbb{R}^2 \times \mathcal{I} \right\}, \quad \text{with } \mathcal{I} \subset \mathbb{R}. \tag{1.17}$$

that is, wave speed serves as a non-degenerate local coordinate on (1.7). Noting that $(\partial_t - (L - c\partial_x))\mathcal{G}_c = \mathcal{G}_c(\partial_t - L)$, we remark that variations along the periodic manifold (1.17) correspond to solutions of the (formal) linearized equation $(\partial_t - (L - c\partial_x))v = 0$ and find, setting $\bar{u} = U(\cdot; \bar{c}, \bar{b})$, that

$$(\partial_t - (L - \bar{c}\partial_x)) \left(\partial_c [\mathcal{G}_c U(\cdot; c, \bar{b})]_{|c=\bar{c}} \right) = 0.$$

Since $\partial_c[\mathcal{G}_c \bar{u}(\cdot; c, \bar{b})]_{|c=\bar{c}} = \mathcal{G}_{\bar{c}}(-t\bar{u}_x) + \mathcal{G}\partial_c U_{|(c,b)=(\bar{c},\bar{b})}$ and $\partial_c U_{|(c,b)=(\bar{c},\bar{b})}$ is periodic of period 1, this verifies the existence of a Jordan chain of height two (recall, the height is at most by (D3)) ascending above the translation mode $\bar{u}_x$.

For general nonlinearities f, however, the existence of such a Jordan block does not immediately follow from assumptions (H1)-(H2) and (D3). Indeed, setting $\beta = (\beta_1, \beta_2) \in \mathbb{R}^2$ in (1.7), we find, taking variations along (1.7) in β_j near $\bar{u} = U(\cdot; \bar{\beta})$, that

$$L\partial_{\beta_j} U|_{\beta=\bar{\beta}} = -\partial_{\beta_j} c|_{\beta=\bar{\beta}} \bar{u}_x. \tag{1.18}$$

As the function $\partial_{\beta_1} X(\bar\beta)\partial_{\beta_2} U(\cdot;\bar\beta) - \partial_{\beta_2} X(\bar\beta)\partial_{\beta_1} U(\cdot;\bar\beta)$ is periodic of period $X(\bar\beta) = 1$[3], we see that the existence of a non-trivial Jordan block requires the additional non-degeneracy hypothesis[4]

$$\det\left(\frac{\partial(c,X)}{\partial(\beta_1,\beta_2)}(\bar\beta)\right) \neq 0. \tag{1.19}$$

For a much more thorough and precise discussion on this topic in the context of general systems of conservation laws, please see the forthcoming work [JNRZ1]; see also Remark 1.3 and Lemma 3.1 below. Throughout this work, we assume that such a Jordan block exists by enforcing our final technical assumption:

(H4) The eigenvalue 0 of L_0 is nonsemisimple, i.e., $\dim\ker L_0 = 1$.[5]

Remark 1.2. The coefficients a_j are the characteristics of an associated Whitham averaged system formally governing slowly modulated solutions; see [NR2]. Thus, as discussed in [OZ4, JZ1, JZN], (D1) implies weak hyperbolicity of the Whitham averaged system (reality of a_j), sometimes used as a formal definition of modulational stability; condition (H4) holds generically, and corresponds to the assumption that speed c is non-stationary along the manifold of nearby stationary solutions, see Lemma 3.1; and condition (D2) corresponds to "diffusivity" of the large-time ($\sim$ small frequency) behavior of the linearized system, and holds generically given (H1)–(H4), (D1), and (D3), see also [S1, S2].

Remark 1.3. As noted in [NR2, JNRZ1], the conservative structure of (1.1) implies that, assuming (H1) and (D3), one can take $\beta = (X, M)$ in (1.7), where $M = X^{-1}\int_0^X U(s;\beta)ds$ denotes the mean mass of the associated wave. Indeed, following the computations of [OZ3] we find under these assumptions that for $|\lambda| \ll 1$

$$D_0(\lambda) = \Gamma\det\left(\frac{\partial(k,M)}{\partial(\beta_1,\beta_2)}(\bar\beta)\right)\lambda^2 + \mathcal{O}(|\lambda|^3),$$

[3]Here, we notice by (D3) that $\bar\beta$ can not be a critical point of the period X. Indeed, if $dX(\bar\beta) = 0$ then $\partial_{\beta_1} U(\cdot;\bar\beta)$ and $\partial_{\beta_1} U(\cdot;\bar\beta)$ would both be 1-periodic, hence $\lambda = 0$ would be an eigenvalue of L_0 of algebraic multiplicity three by (1.18).

[4]For more general systems, this requirement would be replaced with the condition that the gradients of the wave speed and period be linearly independent at $\bar\beta$.

[5]The degenerate case where (1.19), hence (H4), fails can be treated as in [JZ3].

where $\Gamma \neq 0$ is a constant, $k = X^{-1}$ denotes wave number and $D_0(\cdot)$ represents the Evans function[6] for the Bloch operator L_0, from which our claim follows by assumption (D3). Using this parameterization of the manifold (1.7), condition (1.19) reduces to

$$\partial_M c\,(\bar{\beta}) \neq 0$$

corresponding to *linear phase coupling* in the language of [JNRZ1]. In particular, notice that in the case $f(u) = \frac{u^2}{2}$ one can use Galilean invariance to show

$$\partial_M c\,(\bar{\beta}) = 1,$$

yielding another verification of (H4), assuming (H1)-(H2) and (D1)-(D3), in this case.

1.2 Main result

With the spectral assumptions discussed in the previous section, we are now prepared to state the main theorem of this paper.

Theorem 1.1. *Let $\bar{u}$ be any steady 1-periodic solution of* (1.4) *such that (H1)–(H4) and (D1)–(D3) hold. Then there exist constants $\varepsilon_0 > 0$ and $C > 0$ such that for any $\tilde{u}_0$ with $\|\tilde{u}_0 - \bar{u}\|_{L^1(\mathbb{R})\cap H^K(\mathbb{R})} \leq \varepsilon_0$, where K is as in assumption (H1), there exist $\tilde{u}$ a solution of* (1.4) *satisfying $\tilde{u}(\cdot,0) = \tilde{u}_0$ and a function $\psi(\cdot,t) \in W^{K,\infty}(\mathbb{R})$ such that for all $t \geq 0$ and $2 \leq p \leq \infty$ we have the estimates*

(1.20)

$$\begin{aligned}
\|\tilde{u}(\cdot + \psi(\cdot,t),t) - \bar{u}\|_{L^p(\mathbb{R})} &\leq C\,(1+t)^{-\frac{1}{2}\left(1-\frac{1}{p}\right)}\,\|\tilde{u}(\cdot,0) - \bar{u}(\cdot)\|_{L^1(\mathbb{R})\cap H^K(\mathbb{R})}\,,\\
\|(\psi_t,\psi_x)(\cdot,t)\|_{L^p(\mathbb{R})} &\leq C\,(1+t)^{-\frac{1}{2}\left(1-\frac{1}{p}\right)}\,\|\tilde{u}(\cdot,0) - \bar{u}(\cdot)\|_{L^1(\mathbb{R})\cap H^K(\mathbb{R})}\,,\\
\|\tilde{u}(\cdot + \psi(\cdot,t),t) - \bar{u}\|_{H^K(\mathbb{R})} &\leq C\,(1+t)^{-\frac{1}{4}}\,\|\tilde{u}(\cdot,0) - \bar{u}(\cdot)\|_{L^1(\mathbb{R})\cap H^K(\mathbb{R})}\,,\\
\|(\psi_t,\psi_x)(\cdot,t)\|_{H^K(\mathbb{R})} &\leq C\,(1+t)^{-\frac{1}{4}}\,\|\tilde{u}(\cdot,0) - \bar{u}(\cdot)\|_{L^1(\mathbb{R})\cap H^K(\mathbb{R})}\,.
\end{aligned}$$

Moreover, we have the $L^1(\mathbb{R})\cap H^K(\mathbb{R}) \to L^\infty(\mathbb{R})$ nonlinear stability estimate

$$\|\tilde{u}(\cdot,t) - \bar{u}\|_{L^\infty(\mathbb{R})}\,,\ \ \|\psi(\cdot,t)\|_{L^\infty(\mathbb{R})} \leq C\,\|\tilde{u}(\cdot,t) - \bar{u}\|_{L^1(\mathbb{R})\cap H^K(\mathbb{R})} \tag{1.21}$$

valid for all $t \geq 0$.

[6] Recall that the algebraic multiplicity of the root of the Evans function at $\lambda = 0$ agrees with the algebraic multiplicity of the eigenvalue $\lambda = 0$ of the associated linear operator: see [G1].

Theorem 1.1 asserts asymptotic $L^1 \cap H^K \to L^p$ convergence of the modulated solution $\tilde{u}(\cdot+\psi(\cdot,t),t)$ toward $\bar{u}$, but only bounded $L^1 \cap H^K \to L^\infty$ nonlinear stability of the unmodulated solution $\tilde{u}(\cdot)$ about $\bar{u}$.

Remark 1.4. It may seem more natural to introduce ψ via $v(x,t) = \tilde{u}(x,t) - \bar{u}(x+\psi(x,t))$ However, in doing so one introduces in the equation for v terms involving only ψ and thus not decaying in time. For this reason we work instead with $v(x,t) = \tilde{u}(x+\psi(x,t),t) - \bar{u}(x)$, that is, $\tilde{u}(x,t) = \bar{u}(Y(x,t)) + v(Y(x,t),t)$, where Y is such that $Y(x,t) + \psi(Y(x,t),t) = x$, $Y(y+\psi(y,t),t) = y$. Notice that we insure the existence of such a map Y by keeping, for any t, $\|\psi(\cdot,t)\|_{L^\infty(\mathbb{R})}$ bounded and $\|\psi_x(\cdot,t)\|_{L^\infty(\mathbb{R})}$. It should be stressed, however, that

$$Y(x,t) = x - \psi(x,t) + \mathcal{O}\left(\|\psi(\cdot,t)\|_{L^\infty(\mathbb{R})}\|\psi_x(\cdot,t)\|_{L^\infty(\mathbb{R})}\right)$$

so that we are not so far from the natural (but inappropriate) approach; see [JNRZ1] for a detailed discussion. Notice, moreover, that introducing the map Y above enables one to go back to the original unknown $\tilde{u}(x,t)$.

The proof of Theorem 1.1 is presented in Section 3. As noted earlier, the proof of the corresponding theorem for periodic traveling wave solutions of the (non-conservative) Swift-Hohenberg equation (1.3) is considerably less complicated than that of Theorem 1.1; the reader unfamiliar with the methods of this paper may thus wish to consult Appendix B before proceeding to the proof of Theorem 1.1.

While it is generally accepted that the structural hypotheses (H3)-(H4) and (D3) should generically hold, it is unclear a priori whether there exist periodic traveling wave solutions of (1.2) that satisfy the spectral diffusive stability assumptions (D1)-(D2). While an analytical verification of these conditions seems beyond the scope of our current machinery, due to the complexity of the governing equations, we provide a numerical study of this topic in Section 2 below giving convincing evidence of existence of stable bands of periodic waves. We view the rigorous numerical or analytical proof of spectral stability in some interesting regime as the primary remaining open problem in this area of investigation. See in particular [BaN] and [JNRZ4] for progress toward a numerical proof in the KdV limit $|(\gamma,\delta)| \to 0$.

2 A numerical study: spectral stability and time evolution

In this section, we address numerically the issue of spectral stability of periodic traveling wave solutions of (1.1). Our numerical study is based on

complementary tools, namely, Hill's method and Evans function computations; see [BZ, BJNRZ1]. On the one hand, we use SpectrUW numerical software [CDKK], based on Hill's method, which is a Galerkin method of approximation. More precisely, the coefficients of the linear operators L_ξ (defined by (1.11)) together with periodic eigenvectors are expanded by using Fourier series and then a frequency cutoff is used to reduce the problem to finding eigenvalues of a finite matrix. It is known that Hill's method converges "globally" very fast, but with rates not particularly guaranteed in fixed areas; this method is used here to obtain a good localization of the spectrum. In order to test rigorously the spectral stability, we use an Evans function approach: after bounding the region where unstable spectra might exist, we compute a winding number along various contours to localize the spectrum. In some sense, Hill's method helps to find suitable contours to test the spectral stability. To analyze stability near the origin, we also compute a Taylor expansion of the critical eigenvalues bifurcating from the origin at the $\xi = 0$ state. The method of moments (to be described in section 2.1.5) then guarantees the stability of these critical eigenvalues in the neighborhood of $(\lambda, \xi) = (0, 0)$. While most of the results of this section are numerical, we point out that the numerics are well-conditioned with rigorous error estimates; see [BJZ, Z1, BHZ2] for more details.

Throughout this section, both for definiteness and in order to compare with some previous numerical results (see e.g. [BaN, FST, CDK]), we consider (1.1) unless otherwise specified with the specific nonlinearity $f(u) = \Lambda\frac{u^2}{2}, \Lambda > 0$, i.e. the equation

$$\partial_t u + \delta\partial_x^2 u + \varepsilon\partial_x^3 u + \gamma\partial_x^4 u + \Lambda u\partial_x u = 0 \tag{2.1}$$

with various values of $\varepsilon, \delta, \gamma, \Lambda$. If one introduces the characteristic amplitude U, length scale L and time scale $T = L/\Lambda U$, equation (2.1) is alternatively written as

$$\partial_{\tilde{t}}\tilde{u} + \tilde{u}\partial_{\tilde{x}}\tilde{u} + \frac{\varepsilon}{\Lambda UL^2}\partial_{\tilde{x}}^3\tilde{u} + \frac{\delta}{\Lambda UL}\partial_{\tilde{x}}^2\tilde{u} + \frac{\gamma}{\Lambda UL^3}\partial_{\tilde{x}}^4\tilde{u} = 0. \tag{2.2}$$

As a result, one can always assume $\Lambda = 1$ in (2.1). Depending on applications and numerical purposes, one can remove two of the three other parameters in the study of (2.1). We have chosen here two reduced parameterizations of the problem. On the one hand, we first choose some $\bar{\varepsilon}$ then, setting $\bar{\varepsilon} = \varepsilon/\Lambda UL^2$ and $\gamma = \Lambda UL^3$ into (2.2), one finds that it is equivalent to choose $\gamma = 1$ and ε is a fixed parameter and let δ vary as a free parameter in (2.1). On the other hand, letting $L^2 = \gamma/\delta$ and $U^2 = (\varepsilon/\Lambda L^2)^2 + (\delta/\Lambda L)^2$,

one finds that it is equivalent to choose[7] $\gamma = \delta$ and $\delta^2 + \varepsilon^2 = 1$ in (2.1). This latter case is particularly of interest since it is found in thin film theory[8] and since *all* equations (2.1) can be reduced to this particular form through rescaling; that is we cover *all* the values of parameters $\varepsilon, \delta, \gamma$. However this form of the equation may lead to a singularly perturbed problem as $\delta \to 0$; that is why we have also focused on the first form of (2.1) with $\gamma = 1$ even if, to cover all cases, we need then to introduce two families, one with ε fixed to 0 and the other one with ε fixed to some arbitrary positive value.

The plan of the study is as follows. As a first (testing) step, we consider the spectral stability case $\gamma = 1$ and ε fixed. In this test case, we give all the details of our numerical approach: we first compute a priori bounds on possible unstable eigenvalues and then describe our numerical Galerkin/Evans functions based approach. In order to compare our results with the existing literature, specifically the results in [FST], we first carry out a numerical study in the case of the classical Kuramoto-Sivashinsky equation ($\varepsilon = 0$, $\gamma = 1$). We follow this with a numerical study for the generalized KS equation when $\varepsilon = 0.2$ and $\gamma = 1$. Next, we switch to the "thin film scaling" $\gamma = \delta$, $\delta^2 + \varepsilon^2 = 1$ and show numerically that there are (sometimes several) bands of stable periodic traveling waves for all choices of the model parameters, comparing to previous numerical studies of [BaN] and [CDK]

We end this section with a discussion of time-evolution studies nearby various periodic traveling wave profiles numerically computed and compare with the dynamics predicted by the associated Whitham averaged system.

2.1 Spectral stability analysis: $\gamma = 1$, ε fixed

2.1.1 Continuation of periodic traveling waves

Let us consider periodic traveling wave solutions of (2.1) in the simple case $\gamma = 1$ and ε is fixed. After integrating once, traveling waves of the form $u(x,t) = u(x - ct)$ are seen to satisfy the first order nonlinear system of ODE's

$$\begin{pmatrix} u \\ u' \\ u'' \end{pmatrix}' = \begin{pmatrix} u' \\ u'' \\ cu - \varepsilon u'' - \delta u' - \frac{u^2}{2} + q \end{pmatrix} \tag{2.3}$$

[7] Notice that, applying the transformation $(x,u) \mapsto (-x,-u)$ if necessary, we may always take $\varepsilon \geq 0$ in (2.1). Thus, here we set $\varepsilon = \sqrt{1-\delta^2}$ or $\delta = \sqrt{1-\varepsilon^2}$.

[8] Where the equation is designed to investigate formation of patterns of size 1 at a threshold of instability and therefore is scaled as $\gamma = \delta$ so that, for constant states, the most linearly-unstable perturbation has frequency 1.

for some constant of integration $q \in \mathbb{R}$. Noting that we can always take $c = 0$ by Galilean invariance, we find two fixed points in the associated three-dimensional phase space given by

$$U_-(q) = \begin{pmatrix} -\sqrt{2q} \\ 0 \\ 0 \end{pmatrix} \quad \text{and} \quad U_+(q) = \begin{pmatrix} \sqrt{2q} \\ 0 \\ 0 \end{pmatrix}.$$

Following the computations of Section A.1, we find that the fixed point $U_+(q)$ undergoes a Hopf bifurcation when $\varepsilon\delta_{\text{Hopf}}(q) = \sqrt{2q}$; see Figure 1(a) when $\varepsilon = 0.2$. Moreover, near this bifurcation point we find a two dimensional manifold of small amplitude periodic orbits of (2.3) parameterized by period and the integration constant q. Observe that due to the presence of the destabilizing second order and stabilizing fourth order terms in (1.2), an easy calculation shows that the equilibrium solution $U_+(q) = \sqrt{2q}$, and in fact all constant solutions, are linearly unstable to perturbations of the form $v(x,t) = e^{\lambda t + ikx}$, $\lambda \in \mathbb{C}$, $k \in \mathbb{R}$, with $|k| \ll 1$, while linearly stable to such perturbations when $|k| \gg 1$. As a result we find that all small amplitude periodic orbits of (2.3) emerging from the Hopf bifurcation correspond to spectrally unstable periodic traveling waves of (2.1).

Not surprisingly, we are able to numerically continue this two parameter family of small amplitude periodic orbits to obtain periodic orbits of (2.1) with large amplitude. Furthermore, in the natural three-dimensional phase space of (2.3) and for ε fixed, we are able to find a one-parameter family of periodic orbits of (2.3) with fixed period X by continuing the periodic orbits emerging from the Hopf point $U_+(q)$ with respect to the integration constant q; see Figure 1(b) for $\varepsilon = 0.2$ and $X = 6.3$. Notice that in order to keep the period X fixed, one naturally has to vary the modeling parameter δ with respect to q.

What is perhaps surprising, however, even though by now well known [FST, CDK], is that there appears numerically to be a small band of spectrally stable periodic traveling waves within this one-parameter family, outside of which all waves are spectrally unstable; see Figure 2 and Figure 3. Our immediate goal is to substantiate this claim with careful numerical procedures completed with rigorous error bounds. Although, due to machine error, the justifications we discuss do not constitute a proof, given the rigorous error bounds involved, our claims could in principle be translated into a numerical proof with the help of interval arithmetic. This would be an interesting direction for further investigation.

Remark 2.1. As well explored in the literature (see for example [CDK]), there occur a number of period doubling bifurcations as parameters are varied, which might in principle be difficult to follow by continuation. However, this difficulty is easily avoided by rescaling so as to fix the period, while letting other parameters vary instead. This is our reason for computing with fixed period as we do.

2.1.2 High-frequency analysis

We begin our study of the spectrum of the linear operator L, obtained by linearizing (2.1) about a fixed periodic traveling wave solution, by eliminating the possibility that the associated Bloch operators L_ξ admit arbitrarily large unstable eigenvalues. As the resulting estimates are independent of the Bloch frequency ξ, this allows us to reduce our search for unstable spectrum of L into a fixed compact domain in λ. For generality, here we consider (1.1) with a general (smooth, say) nonlinearity f rather than the quadratic nonlinearity leading to the formulation in (2.1) and $\gamma = 1$.

Letting $\bar{u}$ be a fixed $\bar{X}$-periodic solution of (1.2), for each $\xi \in [-\pi/\bar{X}, \pi/\bar{X})$ we must study the eigenvalue problem

$$\lambda u + (\partial_x + i\xi)\left(f'(\bar{u})u\right) + \varepsilon(\partial_x + i\xi)^3 u + \delta(\partial_x + i\xi)^2 u + (\partial_x + i\xi)^4 u = 0$$

considered on $L^2_{\text{per}}([0, \bar{X}])$ We restrict ourselves to rational Bloch frequencies, that is to cases where $\xi\bar{X}/(2\pi) \in \mathbb{Q}$, (recall that the spectra of L_ξ is continuous in ξ) and thus this is equivalent with studying the family of eigenvalue problems

$$\lambda u + \left(f'(\bar{u})u\right)' + \varepsilon u''' + \delta u'' + u'''' = 0 \tag{2.4}$$

considered on $L^2_{\text{per}}([0, n\bar{X}])$ for each $n \in \mathbb{N}$. In this latter formulation, we have the following estimates on the modulus of possible unstable eigenvalues.

Lemma 2.2. *Let $n \in \mathbb{N}$ be arbitrary, and suppose that there exists a function $u \in L^2_{\text{per}}([0, n\bar{X}])$ which satisfies (2.4) for some $\lambda \in \mathbb{C}$. Then λ must satisfy the estimates*

$$\text{Re}(\lambda) \leq \frac{1}{2}\|f''(\bar{u})\bar{u}'\|_{L^\infty([0,\bar{X}])} + \frac{\delta^2}{4}, \tag{2.5}$$

and

(2.6)

$$\text{Re}\lambda + |\text{Im}\lambda| \leq \frac{1}{2}\left(\|f''(\bar{u})\bar{u}'\|_{L^\infty([0,\bar{X}])} + \|f'(\bar{u})\|^2_{L^\infty([0,\bar{X}])} + \delta^2 + \frac{(1+2\varepsilon^2)^2}{2}\right).$$

In particular, the above estimates are independent of n.

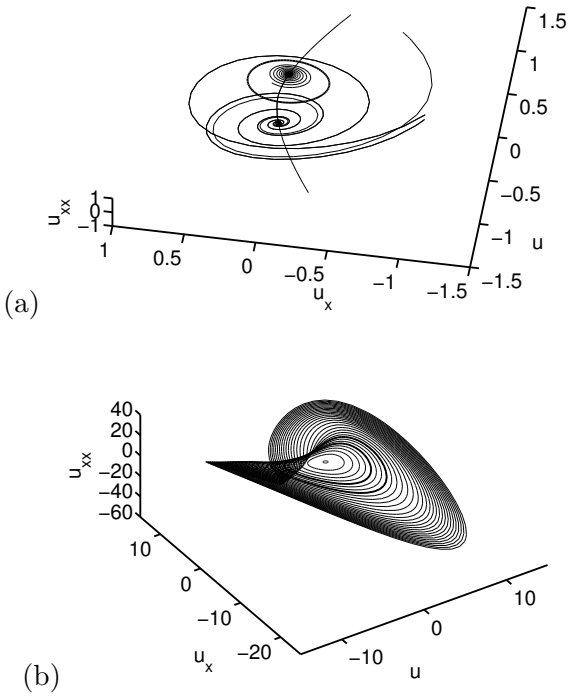

Figure 1: (a) Here, we plot a few of the trajectories in the phase portrait of the (2.3) for $\varepsilon = 0.2$, $q = 0.04$, and $\delta \approx 1$. The periodic trajectory bifurcating from the nearby unstable equilibrium solution $U_+(q)$ is plotted in bold, and has period $X = 6.3$. (b) This figure depicts the one-parameter family (up to translations) of periodic orbits of period $X = 6.3$ and wave speed $c = 0$ emerging from the unstable equilibrium solution $U_+(q)$. Here, $\varepsilon = 0.2$ and q (and accordingly $\delta = \delta(q)$) varies from 1 (corresponding to the orbits near the Hopf bifurcation) to 30 by unit steps. The bold periodic orbits near the center correspond to the lower and upper stability boundaries: in particular, all periodic traveling wave solutions of (2.1) corresponding to periodic orbits of (2.3) between these bold orbits are spectrally stable with respect to small localized perturbations.

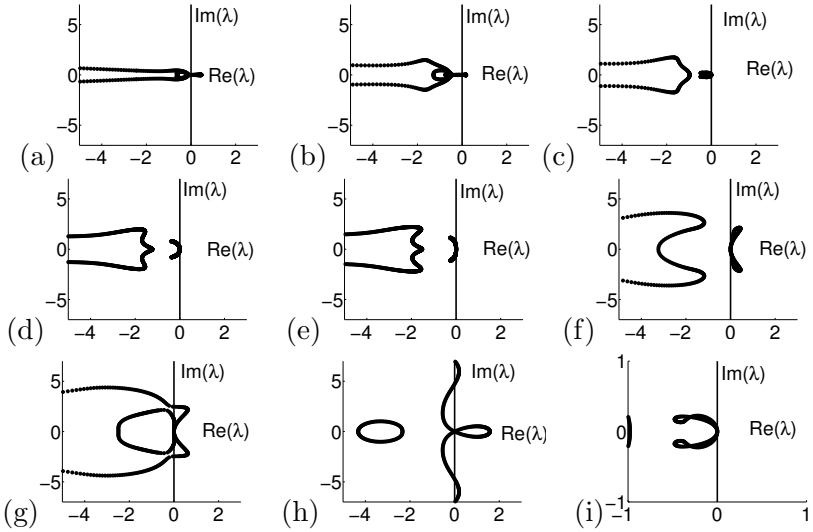

Figure 2: A numerical sampling of the continuous spectrum of the linearization of (2.1) when $\varepsilon = 0.2$, plotted here as $\mathrm{Re}(\lambda)$ vs. $\mathrm{Im}(\lambda)$, about the periodic traveling wave profiles on the periodic manifold depicted in Figure 1(b) for (a) $q = 1$, (b) $q = 4$, (c) $q = 5$, (d) $q = 6$, (e) $q = 7$, (f) $q = 12$, (g) $q = 13.8$, and (h) $q = 30$. Moreover in (i) we zoom in near the origin in the spectral plot given in (c). All pictures here were generated with the Galerkin based SpectrUW package developed at the University of Washington [CDKK].

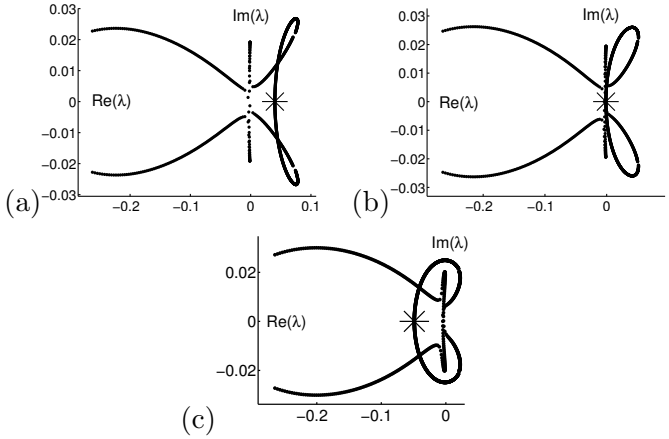

Figure 3: Here, we zoom in near the origin in the λ-plane near, but just below, the lower stability boundary when considering 6.3-periodic stationary solutions of (2.1) in the case $\varepsilon = 0.2$. The three figures correspond to (a) $q = 4.4$, (b) $q = 4.5$, and (c) $q = 4.6$. We find that prior to stability, a real anti-periodic eigenvalue (corresponding to $\xi = -\pi$, and marked with a large star) crosses through the origin and then the rest of the unstable spectrum crosses the imaginary axis away from the origin. This crossing of a real anti-periodic eigenvalue corresponds to a period doubling bifurcation; see [KE] for more details on period-multiplying bifurcations for KS. The spectral curves were generated by computing the roots of the Evans function using the method of moments described in Section 2.1.5. In particular, the transition to stability is not signaled by an eigenvalue crossing through the origin.

Proof. By taking the real part of the complex scalar product of (2.4) with u, one obtains

(2.7)
$$\mathrm{Re}(\lambda)\|u\|^2_{L^2_{per}([0,n\bar{X}])} = -\frac{1}{2}\int_0^{n\bar{X}} (f'(\bar{u}))'|u|^2(x)dx + \delta\|u'\|^2_{L^2_{per}([0,n\bar{X}])} - \|u''\|^2_{L^2_{per}([0,n\bar{X}])}.$$

Then, use the Sobolev interpolation bound

$$\|u'\|^2_{L^2_{per}([0,n\bar{X}])} \leq \frac{1}{2C}\,\|u''\|^2_{L^2_{per}([0,n\bar{X}])} + \frac{C}{2}\,\|u\|^2_{L^2_{per}([0,n\bar{X}])}, \quad C>0,$$

with $C = \frac{\delta}{2}$ to deduce (2.5). Next, by taking the imaginary part of the complex scalar product of (2.4) with u, one obtains

$$\mathrm{Im}(\lambda)\|u\|^2_{L^2_{per}([0,n\bar{X}])} = \mathrm{Im}\langle u', f'(\bar{u})u\rangle_{L^2_{per}([0,n\bar{X}])} + \varepsilon \mathrm{Im}\langle u', u''\rangle_{L^2_{per}([0,n\bar{X}])},$$

then

$$\begin{aligned}|\mathrm{Im}(\lambda)|\|u\|^2_{L^2_{per}([0,n\bar{X}])} \leq\ & \|f'(\bar{u})\|_{L^\infty([0,\bar{X}])}\|u\|_{L^2_{per}([0,n\bar{X}])}\|u'\|_{L^2_{per}([0,n\bar{X}])} \\ & + \varepsilon\|u'\|_{L^2_{per}([0,n\bar{X}])}\|u''\|_{L^2_{per}([0,n\bar{X}])}.\end{aligned}$$

By using Young's inequality, one finds

$$|\mathrm{Im}(\lambda)|\|u\|^2_{L^2_{per}([0,n\bar{X}])} \leq \frac{1}{2}\|f'(\bar{u})\|^2_{L^\infty([0,\bar{X}])}\|u\|^2_{L^2_{per}([0,n\bar{X}])} + \frac{1+\varepsilon D}{2}\|u'\|^2_{L^2_{per}([0,n\bar{X}])} + \frac{\varepsilon}{2D}\|u''\|^2_{L^2_{per}([0,n\bar{X}])}$$

valid for any $D>0$. By using again the above Sobolev interpolation bound, one finds

(2.8)
$$\begin{aligned}|\mathrm{Im}(\lambda)|\|u\|^2_{L^2_{per}([0,n\bar{X}])} \leq\ & \left(\frac{1}{2}\|f'(\bar{u})\|^2_{L^\infty([0,\bar{X}])} + \frac{C(1+\varepsilon D)}{4}\right)\|u\|^2_{L^2_{per}([0,n\bar{X}])} \\ & + \left(\frac{1+\varepsilon D}{4C} + \frac{\varepsilon}{2D}\right)\|u''\|^2_{L^2_{per}([0,n\bar{X}])},\end{aligned}$$

where now $C, D>0$ are arbitrary constants. From (2.7), one also deduces that

(2.9)
$$\mathrm{Re}(\lambda)\|u\|^2_{L^2_{per}([0,n\bar{X}])} \leq \frac{1}{2}(\|f''(\bar{u})\bar{u}'\|_{L^\infty([0,\bar{X}])} + \delta^2)\|u\|_{L^2([0,n\bar{X}])} - \frac{1}{2}\|u''\|^2_{L^2([0,n\bar{X}])}.$$

Choosing now $D = 2\varepsilon$, $C = 1 + D\varepsilon$ and adding (2.8) and (2.9) yields

$$\mathrm{Re}(\lambda) + |\mathrm{Im}(\lambda)| \leq \frac{1}{2}\Big(\|f''(\bar{u})\bar{u}'\|_{L^\infty([0,\bar{X}])} + \|f'(\bar{u})\|^2_{L^\infty([0,\bar{X}])} + \delta^2 + \frac{(1+2\varepsilon^2)^2}{2}\Big),$$

as claimed. □

Remark 2.3. Notice that by choosing different constants C and D above, along with a different choice of the Young's scaling in (2.9), various other bounds of the form (2.6) can be obtained which could be beneficial in certain parameter regimes. Specifically, given any constants $C_1, C_2, C_3, \alpha, \beta, A > 0$ such that

$$\frac{\delta}{2C_1} - 1 + A\left(\frac{C_2}{4\alpha}\|f'(\bar{u})\|_{L^\infty([0,\bar{X}])} + \frac{\varepsilon\beta C_3}{4} + \frac{\varepsilon}{2\beta}\right) = 0$$

we obtain the inequality

$$\mathrm{Re}(\lambda)+A|\mathrm{Im}(\lambda)| \leq \frac{1}{2}\|f''(\bar{u})\bar{u}'\|_{L^\infty([0,\bar{X}])}+\frac{\delta C_1}{2}+\frac{A}{2}\left(\|f'(\bar{u})\|_{L^\infty([0,\bar{X}])}\left(\alpha+\frac{1}{2\alpha C_2}\right)+\frac{\varepsilon\beta}{2C_3}\right).$$

The inequality (2.6) corresponds to the choices

$$C_1 = \delta, \quad C_2 = C_3 = \frac{1}{1+2\varepsilon^2}, \quad \alpha = \|f'(\bar{u})\|_{L^\infty([0,\bar{X}])}, \quad \beta = 2\varepsilon, \quad A = 1,$$

while an example of an alternative bound, which may be useful for large $\varepsilon > 0$, is given by

(2.10)

$$\mathrm{Re}(\lambda)+\frac{1}{2\varepsilon^2}|\mathrm{Im}(\lambda)| \leq \frac{1}{2}\left(\|f''(\bar{u})\bar{u}'\|_{L^\infty([0,\bar{X}])} + \delta^2 + \frac{1}{\varepsilon^2}\left(\frac{1}{4}\|f'(\bar{u})\|^2_{L^\infty([0,\bar{X}])} + \frac{4}{3\varepsilon^2}\right)\right)$$

corresponding to the choices

$$C_1 = \delta, \quad C_2 = C_3 = \frac{3\varepsilon^2}{4}, \quad \alpha = \frac{1}{2}\|f'(\bar{u})\|_{L^\infty([0,\bar{X}])}, \quad \beta = \frac{2}{\varepsilon}, \quad A = \frac{1}{2\varepsilon^2}.$$

By Lemma 2.2, for fixed modeling parameters ε and δ and a periodic profile $\bar{u}$ of (1.2), there exists a real number $R_0 = R_0(\varepsilon, \delta, \bar{u})$ such that the unstable (and marginally stable) spectrum of the associated linearized operator L satisfies

$$\sigma(L) \cap \{\ \lambda \in \mathbb{C} \mid \mathrm{Re}(\lambda) \geq 0\ \} \ \subset\ B(0, R_0). \tag{2.11}$$

This reduces to a compact set the region in the spectral plane where we need to search for unstable spectra of L. In order to verify the spectral stability hypotheses (D1)–(D3) and (H3) we use the periodic Evans function and basic analytic function theory, the necessary details of which we review in the next section.

2.1.3 Low- and mid-frequency analysis: Evans function and numerical methods

We now begin our search for unstable spectra of L in the ball $B(0, R_0)$, where R_0 is given by the high-frequency bounds in the previous section. To this end, we use a complex-analytic function, known as the periodic Evans function [G1], that is well-suited to the task at hand. First, let $\bar{u}$ be a fixed $\bar{X}$-periodic traveling wave solution of (2.1), $\bar{X}$ arbitrary, and notice that the associated spectral problem (1.9) can be rewritten as a first order system of the form

$$\mathbf{Y}'(x;\lambda) = \mathbb{H}(x,\lambda)\mathbf{Y}(x;\lambda), \quad \mathbf{Y} \in \mathbb{C}^4 \tag{2.12}$$

and that $\lambda \in \sigma(L)$ if and only if (2.12) admits a non-trivial solution satisfying

$$\mathbf{Y}(x+\bar{X};\lambda) = e^{i\xi\bar{X}}\mathbf{Y}(x;\lambda), \quad \forall x \in \mathbb{R}$$

for some $\xi \in [-\pi/\bar{X}, \pi/\bar{X})$.[9] Letting $\Psi(x,\lambda)$ be a matrix solution of (2.12) with initial condition $\Psi(0,\lambda) = \mathbf{I}$ for all $\lambda \in \mathbb{C}$, we follow Gardner [G1] and define the periodic Evans function for our problem to be

$$D(\lambda,\xi) := \det\left(\Psi(\bar{X},\lambda) - e^{i\xi\bar{X}}\mathbf{I}\right), \quad (\lambda,\xi) \in \mathbb{C}^2, \tag{2.13}$$

where for later convenience we allow for possibly complex Bloch frequencies ξ in the above definition. By construction, then, $\lambda \in \sigma(L)$ if and only if there exists a $\xi \in [-\pi/\bar{X}, \pi/\bar{X}) \subset \mathbb{R}$ such that $D(\lambda,\xi) = 0$. More precisely, for a fixed $\xi \in [-\pi/\bar{X}, \pi/\bar{X})$ the roots of the function $D(\cdot,\xi)$ agree in location and algebraic multiplicity with the eigenvalues of the Bloch operator L_ξ [G1].

Since $\mathbb{H}(\cdot,\lambda)$ clearly depends analytically on λ, it follows that the Evans function is a complex-analytic function of both λ and ξ, hence our search for unstable spectra of L may by reformulated as a problem in analytic function theory. Indeed, for a fixed ξ the number of eigenvalues of L_ξ within the bounded component of a closed contour Γ, along which $D(\cdot,\xi)|_\Gamma$ is non-vanishing, can be calculated via the winding number

$$n(\xi;\Gamma) := \frac{1}{2\pi i}\oint_\Gamma \frac{\partial_\lambda D(\lambda,\xi)}{D(\lambda,\xi)}\, d\lambda.$$

[9] Here, we have allowed the domain of ξ to depend on the period $\bar{X}$. This choice is to ensure that, when linearizing about a constant state, the dispersion relation $D(\lambda,\xi) = 0$ agrees with that obtained by the standard Fourier transform, where D denotes the periodic Evans function defined below in (2.13). This differs from the convention of Gardner [G1] and some others in which the Evans function is parametrized instead by the Floquet number $\bar{\zeta} := e^{i\bar{X}\xi} \in S^1$, a quantity with domain independent of $\bar{X}$.

Given a fixed contour Γ then, notice as $n(\cdot;\Gamma)$ is a continuous function with integer values, it is locally constant and hence can only change values when a root of $D(\cdot,\xi)$ crosses through Γ. With these preparations in mind, we now outline the general scheme of our numerical procedure to verify the spectral stability hypotheses (D1)–(D3) and (H3). As noted below, for numerical efficiency, the following steps are sometime carried out in a slightly different order. Of course then, there are several consistency checks that follow to justify various assumptions made. For similar reasons, it is at times advantageous to execute a particular step in a slightly different way than suggested here; more will be said about this below. Nevertheless, the general idea of the numerical procedure is contained in the following steps, to be completed for fixed.

Step 0: First, numerically determine set $\mathcal{D} := \{\, q \,|\, \partial_\lambda^2 D(0,0) = 0\}$ by looking for sign changes[10] of $\partial_\lambda^2 D(\lambda,0)$ for $\lambda > 0$, where here $D(\lambda,0)$ denotes the Evans function for $\xi = 0$ obtained by linearizing about the periodic profile $\bar{u}$ with parameter q.

Then away from this degenerate parameter set $\mathcal{D}$, we may complete the following steps.

Step 1: First, determine using the bounds of Lemma 2.2 an $R_0 > 0$ satisfying (2.11).

Step 2: Let $0 < r_0 < R_0$, $\Omega_0 := B(0,R_0) \setminus B(0,r_0)$, and set

$$\begin{aligned} \Gamma_0 &:= \partial\left(\Omega_0 \cap \{\lambda \in \mathbb{C} \,|\, \mathrm{Re}(\lambda) \geq 0\}\right), \\ \Gamma_1 &:= \partial\left(B(0,R_0) \cap \{\lambda \in \mathbb{C} \,|\, \mathrm{Re}(\lambda) \geq 0\}\right); \end{aligned} \tag{2.14}$$

see Figure 4. Now, verify that for some $0 < k_0 \ll 1$ the following two conditions hold:

(a) $n(\xi,\Gamma_0) = 0$ for all $\xi \in [-\pi/\bar{X}, \pi/\bar{X})$.
(b) $n(\xi,\Gamma_1) = 0$ for $k_0 \leq |\xi| \leq \pi/\bar{X}$;

see Figure 5 below.

Step 3: Verify that for some $r_0 < r_1 < R_0$, $n(\xi, \partial B(0,r_1)) = 2$ for $|\xi| < k_0$.

Step 4: Finally, Taylor expand the two critical modes for $|\xi| \ll 1$ as

$$\lambda_j(\xi) = \alpha_j \xi + \beta_j \xi^2 + \mathcal{O}(|\xi|^3), \quad j = 1,2 \tag{2.15}$$

[10] Since the map $q \mapsto \partial_\lambda^2 D(0,0)$ is real valued, this is sufficient to find the zeros.

and numerically verify that $\alpha_j \in \mathbb{R}i$, the α_j are distinct, and $\mathrm{Re}(\beta_j) < 0$. Notice that such an expansion exists by Lemma 3.1.

If the criteria of each of the above steps are satisfied, then we conclude (numerically) that the wave is *stable*. We emphasize here the simplicity and generality of the above numerical protocol, hence being directly applicable to many model problems. In particular, the above numerical method does not require an often lengthy and problem specific spectral perturbation expansion near the neutral stability mode $(\lambda, \xi) = (0, 0)$.

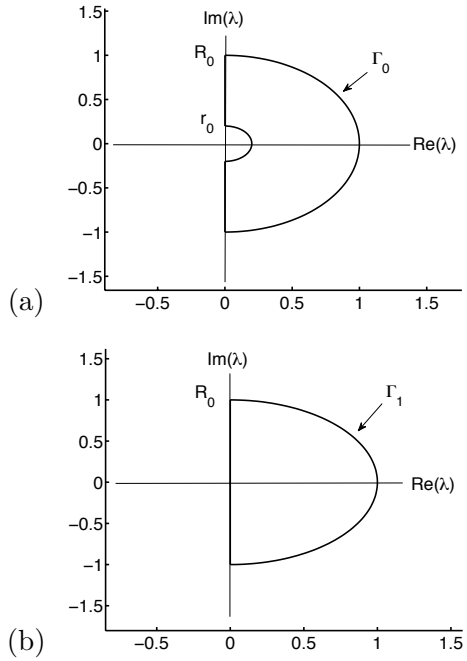

Figure 4: Illustrations of the curves Γ_0 (a) and Γ_1 (b). These pictures are not drawn to reflect the actual dimensions used in the study, but to be a visual aid.

Remark 2.4. The set $\mathcal{D}$ introduced in Step 0 above is precisely the parameter set in which hypothesis (H2) is valid; see [NR2, JNRZ1] for details. In particular, Step 0 is a useful test for co-periodic instability corresponding to bifurcation of periodic solution to a new branch. From a numerical standpoint, it should be noted that Step 3 of the above procedure will fail, producing an infinite loop in the algorithm, on the set $\mathcal{D}$. In general, given a

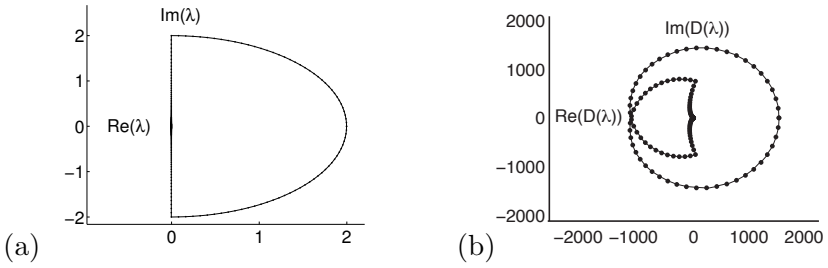

Figure 5: Sample Evans function output, demonstrating the calculation of $n(\xi, \Gamma_0)$ in Step 2 of the above numerical protocol. We view in (a) a domain contour of form Γ_0 defined in Step 2 above on which we evaluate the Evans function, and in (b) the associated range for $\xi = 0$. Here, $\varepsilon = 0$, $q = 5$, $X = 6.3$, and $\delta = 1.4627$. In particular, we see that $n(0, \Gamma_0) = 0$ in this case.

numerical tolerance $0 < \gamma \ll 1$, the algorithm is only guaranteed to be well-conditioned off of a γ-neighborhood of $\mathcal{D}$ since this guarantees we are away from a degenerate boundary case where $\partial_\lambda^2 D(0,0)$ is too small. This will produce sharp stability boundaries in the region where $\partial_\lambda^2 D(0,0)$ is small. Such degenerate boundaries, while seemingly not occurring in the present case, do occur in the non-conservative Swift-Hohenberg equation studied in Appendix B.

Remark 2.5. It is clear that some care must be taken in choosing the low-frequency cutoff k_0 in the above procedure, as it must be chosen small enough to ensure that the conditions on α_j and β_j in Step 4 are sufficient to guarantee that $\mathrm{Re}(\lambda_j(\xi)) < 0$ for $|\xi| < k_0$; that is, the cubic order remainder term must be small enough for $|\xi| < k_0$ as to not dominate the $\mathcal{O}(|\xi|^2)$ terms determined by Taylor expansions (2.15). To analyze how small k_0 must be, assume $|\xi| < k_0$ and note that Taylor's theorem implies

$$\lambda_j(\xi) = \alpha_j \xi + \beta_j \xi^2 + \frac{\xi^3}{2} \int_0^1 (1-s)^2 \lambda_j'''(s\xi) ds.$$

Letting $K \gg k_0$ and setting[11] $M_j = \max_{|\zeta|=K} |\lambda_j(\zeta)|$, where k_0 is given in

[11] In our numerics, we utilized the method of moments to determine the number M_j; see Section 2.1.5 below for details.

Step 3 above, it follows by basic interior estimates that for all $s \in [0,1]$

$$|\lambda_j'''(s\xi)| = \left| \frac{3!}{2\pi i} \int_{\partial B(0,K)} \frac{\lambda_j(\zeta)}{(\zeta - s\xi)^4} d\zeta \right| \leq \frac{6M_jK}{(K-k_0)^4}.$$

In particular, upon verifying that $\mathrm{Re}(\alpha_j) = 0$ and $\mathrm{Re}(\beta_j) < 0$ for $j = 1, 2$, we can guarantee $\mathrm{Re}(\lambda_j(\xi)) < 0$ for $|\xi| < k_0$ provided that k_0 satisfies the inequality

$$k_0 < \frac{(K-k_0)^4}{K} \cdot \min_{j=1,2} \frac{|\mathrm{Re}(\beta_j)|}{M_j}. \tag{2.16}$$

This serves as a consistency check in the above numerical procedure: if the chosen k_0 does not satisfy the stated bound then one must choose a new k_0 which does satisfy the bound and repeat Steps 1–4 with this new k_0.

2.1.4 Numerical determination of Taylor coefficients

Concerning Step 4 in the above procedure, we now explain how the coefficients α_j and β_j in (2.15) can be obtained from the Evans function. First, assuming that Steps 1-3 have been verified, the analyticity of the Evans function implies that $D(\cdot,\cdot)$ can be Taylor expanded to third order as

$$D(\lambda,\xi) = a_0\lambda^2 + a_1\lambda\xi + a_2\xi^2 + a_3\lambda^3 + a_4\lambda^2\xi + a_5\lambda\xi^2 + a_6\xi^3 + \mathcal{O}(|\lambda|^4 + |\xi|^4)$$

where the coefficients $a_0, \ldots, a_6 \in \mathbb{C}$ can be calculated from the Evans function via the formula

$$\partial_\lambda^r \partial_\xi^s D(0,0) = \frac{r!s!}{4\pi^2 r!} \oint_{\partial B(0,h)} \oint_{\partial B(0,h)} D(\mu,k)\mu^{-r-1}k^{-s-1} d\mu\, dk \tag{2.17}$$

where $h > 0$ is sufficiently small. Substituting the expansions in (2.15) into the equation $D(\lambda_j(\xi),\xi) = 0$ and equating second-order terms, we find that the α_j are roots of the polynomial $a_0z^2 + a_1z + a_2 = 0$. In particular, we can take

$$\alpha_j = \frac{-a_1 + (-1)^{j+1}\sqrt{a_1^2 - 4a_0a_2}}{2a_0} \tag{2.18}$$

noting that (strong) hyperbolicity of the associated Whitham averaged system is equivalent to the discriminant condition

$$a_1^2 - 4a_0a_2 < 0, \tag{2.19}$$

which is easily checked. Furthermore, equating third-order terms in $D(\lambda_j(\xi), \xi) = 0$ implies that

$$\beta_j = -\frac{a_3\alpha_j^3 + a_4\alpha_j^2 + a_5\alpha_j + a_6}{2a_0\alpha_j + a_1} \tag{2.20}$$

where we note that the denominator is non-zero by the definition of the α_j and the discriminant condition (2.19).

2.1.5 Method of moments

Finally, we describe how to numerically obtain bounds on the numbers $M_j := \max_{|\xi|=K} |\lambda_j(\xi)|$. From the above discussion, the computation of these quantities is important to determine the sign of eigenvalues in the neighborhood of the origin. Here, the idea is to use the Evans function to track the spectral curves $\lambda_j(k)$ as functions of k by using what we refer to as the method of moments. We need to locate two eigenvalues: to this end, we define the first and second moments of the spectral curves $\lambda_j(\xi)$ as

$$m_1(\xi) := \sum_{j=1,2} \lambda_j(\xi) \quad m_2(\xi) := \sum_{j=1,2} \lambda_j(\xi)^2.$$

Note that these moments can be directly computed through the Evans function via the formula

$$m_l(\xi) = \frac{1}{2\pi i} \oint_{\partial B(0,R)} \frac{\lambda^l \partial_\lambda D(\lambda, \xi)}{D(\lambda, \xi)} \, d\lambda.$$

for $R > 0$ sufficiently large so as $\lambda_j(\xi) \in B(0, R)$ for all $|\xi| = K$. Once the moments $m_l(\xi)$ are computed for a fixed ξ, by using a simple Stieltjes trapezoid method, for example, the corresponding numbers $\lambda_j(\xi)$ can be easily recovered via the formula

$$\lambda_j(\xi) = \frac{m_1(\xi) + (-1)^j \sqrt{2m_2(\xi)^2 - m_1(\xi)^2}}{2}, \quad j = 1, 2$$

from which the numbers M_j can easily be determined. This method of moments readily extends to an arbitrary number of eigenvalues; see [BZ, BJNRZ1]). In order to avoid the ambiguity for the choice of λ_1 and λ_2 above, we substitute (2.16) by

$$k_0 < \frac{(K - k_0)^4}{KM} \cdot \min_{j=1,2} |\mathrm{Re}(\beta_j)|.$$

where $M = \max_{j=1,2} \max_{|\xi|=K} |\lambda_j(\xi)|$.

2.1.6 Numerical results

The above numerical procedures provide a direct and well-conditioned way to numerically verify the spectral stability hypotheses (H3) and (D1)–(D3). We now apply this procedure to two cases.

First case: $\gamma = 1, \varepsilon = 0$

The case $\varepsilon = 0$ corresponds to the "classic" Kuramoto-Sivashinsky equation, which has received a great amount of numerical and analytical attention over the years. In particular, stability boundaries are well known for this equation. We state our results first in this special case for verification of our method against these previously known results. Let us now carefully describe the implementation of the numerical procedure for the special case of (2.1) for the periodic traveling waves parameterized by $q = 5$, and $X = 6.3$. For numerical efficiency, we proceed in our explicit example by slightly modifying both the content and order of the steps of the above numerical procedure. As a first step, we notice that when $\varepsilon = 0$ and $q = 5$, a periodic orbit of (2.3) with period $X = 6.3$ exists when $\delta = 1.4627$, and so we fix δ at this value throughout this discussion. The corresponding solution $\bar{u}$ of (2.1) then satisfies $\|\bar{u}\|_{L^\infty(\mathbb{R})} < 4.6509$ and $\|\bar{u}'\|_{L^\infty(\mathbb{R})} < 6.4856$ so that, appealing to Lemma 2.2, we find that any unstable spectra of the associated linearization L about $\bar{u}$ lies in the ball $B(0, \tilde{R})$ with

$$\tilde{R} = \frac{1}{2}\left(\|f''(\bar{u})\bar{u}'\|_{L^\infty(\mathbb{R})} + \|f'(\bar{u})\|^2_{L^\infty(\mathbb{R})} + \delta^2 + \frac{(1+2\varepsilon^2)^2}{2} \right)$$

Next, we set $R_0 = 15.478 > \tilde{R}$ and $r_0 = 1$ and define Γ_0 and Γ_1 as in (2.14). Using 153 evenly spaced points in λ, thereby assuring relative error between successive points varies by less than 0.2, we compute that $n(\xi; \Gamma_0) = 0$ for 1000 evenly spaced points in ξ in the interval $\xi \in [-\pi/6.3, \pi/6.3]$, where here we use the scaled lifted polar coordinate method (described in Appendix D) to compute the Evans function $D(\cdot, \xi)$; see [BJNRZ1].

Now, for numerical efficiency we deviate slightly from the basic numerical method described above and proceed to compute the Taylor expansions (2.15) of the critical modes near the origin. Notice that as there are generically two such branches of spectra bifurcating from the origin at $\xi = 0$, there is in general no problem with making this assumption at this point: at the end of our numerical test, we will do a consistency check to verify that there were indeed only two branches to start with. Using the unscaled lifted polar method (described in Appendix D) to compute the Evans function, we obtain the values of α_j and β_j which are recorded in the $q = 5$ row of Table

1. Here, we have used (2.17) with 300 points on the λ-contour, yielding relative error between successive values of α_j and β_j less than 0.1 and 0.01, respectively, and 1000 points on the k-contour, yielding relative error less than 0.2 in successive steps. From the above Taylor coefficients β_j, we can use Remark 2.5 to determine an appropriate low-frequency cutoff k_0. Here, we choose $K = 0.5$, $R = 2$ and choose k_0 such that the inequality in (2.16) holds; a brief calculation shows that $k_0 = 0.018365$ suffices. With these choices, we use 427 points in the λ-contour, assuring relative error between successive points varies less than 0.2 and verify that $n(\xi; \Gamma_1) = 0$ for 1000 evenly spaced values of ξ satisfying $k_0 \leq |\xi| \leq \pi/6.3$.

Finally we must verify that there are indeed only two spectral branches bifurcating at $\xi = 0$ from the origin. Following Step 3 of the above procedure, we must simply find an $r_1 \in (r_0, R_0)$ such that $n(\xi; \partial B(0, r_1)) = 2$ for all $|\xi| \leq k_0$. We note, however, that computing the Evans function $D(\lambda, \xi)$ for a given ξ becomes increasingly more difficult and less accurate as $\mathrm{Re}(\lambda)$ becomes increasingly more negative; see [BJNRZ1] for more details. As a result, we find it more useful to compute the winding number corresponding to the contour[12]

$$\tilde{\Gamma} := \partial \left\{ \lambda \in \mathbb{C} \;\middle|\; \mathrm{Re}(\lambda) \geq -2 \max_{j=1,2} |\mathrm{Re}(\beta_j)| k_0^2 \;\text{ and }\; \left| \lambda - 2 \max_{j=1,2} |\mathrm{Re}(\beta_j)| k_0^2 \right| \leq 2 r_0 \right\},$$

from which we find, as expected, $n(\xi; \tilde{\Gamma}) = 2$ for 1000 evenly spaced values of ξ satisfying $|\xi| \leq k_0$ where again we use 427 points along the λ-contour to evaluate the Evans function, ensuring relative error less than 0.2 between successive points. This observation, together with the (now justified) Taylor expansions computed above, implies that no unstable spectra can exist for any Bloch-frequency ξ.

From the above arguments, we conclude with great numerical certainty that the underlying periodic traveling wave associated with $q = 5$, $\varepsilon = 0$ and period $X = 6.3$ is spectrally stable to small localized perturbations, in the sense of (D1)–(D3) and (H3). This procedure can then be repeated for different values of q, holding $\varepsilon = 0$, the period (X=6.3) and the wave speed ($c = 0$) fixed, and the results of these computations are tabulated in Table 1. In particular, our numerics indicate that, as expected, there is a band of spectrally stable periodic traveling wave solutions, corresponding to different values of q, of (2.1) with $\varepsilon = 0$ and fixed period $X = 6.3$.

[12]Notice that by the previously computed Taylor expansions, we expect $\min_{|\xi| \leq k_0} \mathrm{Re}(\lambda_j(\xi)) \geq -2 \max_j |Re(\beta_j)| k_0^2 = -0.0031727$.

Comparison with previous results. As there is a well known approximate stability boundary in the case $\varepsilon = 0$ provided in [FST], it seems worthwhile to compare the results of Table 1 to theirs. In [FST], the authors consider 2π-periodic solutions of the equation

$$\partial_t u + u\partial_x u + \partial_x^2 u + \nu\partial_x^4 u = 0, \quad \nu > 0. \tag{2.21}$$

Going to Fourier space, it is clear that when $\nu > 1$ all Fourier modes of the solution are linearly damped and hence the solution converges to a spatially homogeneous state as $t \to \infty$. However, when $\nu < 1$ there will be a finite number of excited modes leading to a non-uniform solutions. Setting $\nu = 1-\eta$ then, a stability analysis is conducted for 2π-periodic solutions of (2.21) with $0 < \eta < 0.69$. In particular, the authors find that such solutions are spectrally stable for $\eta \in (\eta_1, \eta_2)$ with $\eta_1 \in (0.25, 0.3)$ and $\eta_2 \in (0.4, 0.45)$ In order to compare these results to those provided in Table 1, we notice that by setting $\alpha = \frac{6.3\nu^{2/7}}{2\pi}$ and introducing the new variables $\bar{u} = \alpha^{-3}\nu^{-1/7}u$, $\bar{x} = \alpha\nu^{-2/7}x$, and $\tilde{t} = \alpha^4\nu^{-1/7}$ the 2π-periodic solutions of (2.21) correspond to 6.3-periodic solutions of the equation

$$\partial_{\bar{t}}\bar{u} + \bar{u}\partial_{\bar{x}}\bar{u} + \rho\partial_{\bar{x}}^2\bar{u} + \partial_{\bar{x}}^4\bar{u} = 0$$

where $\rho = \left(\frac{2\pi}{6.3}\right)^2\nu^{-1}$. Letting $\nu = 1-\eta$ then, the results of [FST] suggest we should have stability for $\rho \in (\delta_1, \delta_2)$ where $\delta_1 \in (1.32623, 1.42096)$ and $\delta_2 \in (1.65778, 1.80849)$ in our ρ-parametrization: these predictions are consistent with the data in Table 1 where we find $\delta_1 \approx 1.411$ and $\delta_2 \approx 1.701$.

Remark 2.6. It is worth mentioning that the numerical method of [FST] is completely different from ours, so that the close agreement between results gives a useful check on both sets of numerics. Specifically, for frequencies (ξ, λ) bounded away from the origin, they use a Galerkin method similar to that used by us to generate figures using SPECTRUW; that is, they compute the spectra of a truncated infinite-dimensional matrix. In the numerically delicate small-frequency regime, they approximate the spectra by perturbation expansion around critical modes, as we do. However, they accomplish this in a different way, by direct spectral perturbation expansion of the underlying linearized operator about the wave. They point out also the relation between this spectral expansion and the formal modulation (i.e., Whitham) equations expected to govern asymptotic behavior. Though the numerics of [FST] are well-conditioned, and based on sound functional-analytic principles, there is no attempt made there to estimate numerical computation error. Indeed, for this type of method, this seems to us a complicated task.

By contrast, Evans-function/winding number methods come effectively with built-in error bounds, given by the ODE tolerance and the requirements of Rouchés Theorem to guarantee validity of the winding number.

Second case: $\gamma = 1, \varepsilon = 0.2$

This choice corresponds to a generalized Kuramoto-Sivshinsky equation: the purpose here was to see whether we have the same qualitative picture of a band of spectrally stable periodic traveling waves. Here $X = 6.3$ is fixed. Employing our above numerical procedure, in an analogous fashion as for the $\varepsilon = 0$ case considered above, we summarize our findings in Table 2. As before, we find a range of values of the integration constant q associated with periodic traveling wave solutions of (2.1) which are spectrally stable to small localized perturbations, in the sense that (D1)–(D3) and (H3) hold; see also Figure 1 (b).

2.2 A full parameter study: $\gamma = \delta$, $\varepsilon^2 + \delta^2 = 1$

Finally, we conclude our spectral stability analysis by considering stability of periodic traveling wave solutions of the generalized Kuramoto-Sivashinsky equation, under the particular scaling

$$\partial_t u + \partial_x(u^2/2) + \varepsilon\partial_x^3 u + \delta(\partial_x^2 u + \partial_x^4 u) = 0, \tag{2.22}$$

and $\varepsilon^2 + \delta^2 = 1$. It should be emphasized that the singular limit $\delta \to 0$ of (2.22) arises naturally in the study of small amplitude roll-waves on the surface of a viscous liquid thin film running down an inclined plane. Indeed, one can derive (2.22) either from shallow water equations with friction at the bottom or free surface Navier-Stokes equations, both at the transition to instability of constant steady states (fluid height and velocity are constant in the shallow water description) for small amplitude disturbances and in the small wave number regime; see [W, YY] for more details on this derivation. In this case, periodic traveling waves solutions of (2.22) correspond to well-known hydrodynamical instabilities, known as *roll-waves*; see [NR1] and [JZN] for the spectral and nonlinear stability analysis of these roll-waves and for the analysis of their corresponding Whitham equations.

In the limit $\delta \to 0$, the governing equation (2.22) reduces to the integrable KdV equation

$$\partial_t u + u\partial_x u + \partial_x^3 u = 0 \tag{2.23}$$

where it is known that all periodic traveling wave solutions are spectrally stable to perturbations in $L^2(\mathbb{R})$ and nonlinearly (orbitally) stable in $L^2_{\text{per}}([0, nX])$ where X denotes the period of the underlying elliptic function solution; see [BD]. As discussed in detail in Appendix A.3, the elliptic function solutions given in (A.10) which satisfy the selection principle (A.12) may be continued for $0 < \delta \ll 1$ to a three-parameter family of periodic traveling wave solutions of (2.1) parameterized by translation, period, and spatial mean over a period.

Concerning the stability of these "near KdV profiles", we numerically observe that for $\delta > 0$ sufficiently small there exist numbers $X_L(\delta)$ and $X_U(\delta)$ such that the associated X-periodic traveling wave solution of (2.22) is spectrally stable to perturbations in $L^2(\mathbb{R})$ provided $X_L(\delta) < X < X_U(\delta)$, with $X_L \approx 8.49$ and $X_U \approx 26.17$; see Table 3 for details. This numerical observation complements the well known result that the "near KdV solitary wave" profiles of (2.22) are spectrally unstable to localized perturbations; see [PSU, BJNRZ2]. Analytical verification of these numerical observations, though outside the scope of the present work, would be a very interesting direction for future investigation. See [JNRZ4] for substantial progress in this direction.

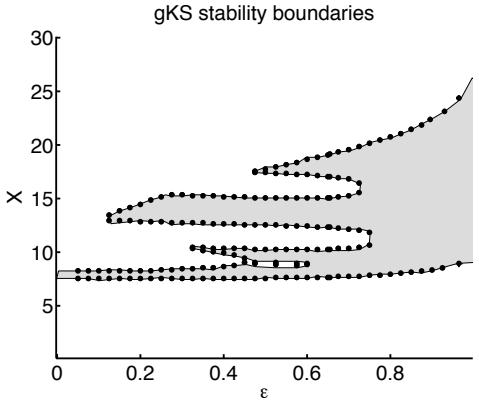

Figure 6: Plot of the stability boundaries (in the period X) versus the parameter ε. Here, $\delta = \sqrt{1-\varepsilon^2}$ is fixed by the choice of ε and the shaded regions correspond to spectrally stable periodic traveling waves. In the limits $\varepsilon \to 0$ and $\varepsilon \to 1$, we see the existence of only a single band of spectrally stable periodic traveling waves. For intermediate values, however, several bands emerge and the stability picture becomes much more complicated.

At first sight, one may attempt to deduce from the previous computations $\gamma = 1, \varepsilon = 0, 0.2$ or $\gamma = \delta \to 0, \varepsilon = 1$ that, generically, for a fixed set of parameters, there exists a band of spectrally stable periodic traveling waves. In fact, the situation is slightly more complicated and we carry out a spectral stability analysis for the full set of parameters $\varepsilon^2 + \delta^2 = 1$ and $\gamma = \delta$. Up to a time and space rescaling, this analysis includes all the particular cases treated previously: see Figure 6. This picture confirms that both for $\varepsilon \approx 0$ or $\delta \approx 0$ there is a single band of spectrally stable periodic waves. However for intermediate values of ε and δ, we clearly see that there a several bands of spectrally stable periodic waves and bounded bands of unstable periodic waves: this may be, among other things, connected to the various bifurcations of periodic waves occurring in this intermediate regime. Moreover, throughout this intermediate regime the nature of the transition to instability can be more complicated than previously seen. For example, it may happen that one diffusion coefficient β_j becomes positive while the other stays strictly negative; see Figure 7. This stands in contrast to the numerics in Tables 1 and 2.

Comparison with previous results. The results of our numerics agree very well with previous results of [BaN, CDK] obtained by completely different means. In particular, our estimates for the limiting stability boundaries X_L and X_U in the KdV limit are quite close to predictions obtained in [BaN] by formal singular perturbation analysis. Likewise, the global stability boundaries displayed in Figure 6 agree quite well with numerical results displayed in Figure 12 p. 316 of [CDK]. The methods used in [CDK] are again Galerkin-type as described in Remark 2.6, quite different from the Evans function methods used here, so give a useful independent check.

To connect our results to those of [CDK], we give a brief lexicon between our paper and that of Chang et al. The figure 12 in [CDK] involves α, δ, whereas our Figure is in terms of parameters X and ϵ. One has period $X = 2 * \pi/\alpha$ and coefficient $\epsilon = \delta/\sqrt{(}1 + \delta^2)$. On the right hand side of Figure 12 [CDK] ($\delta = 8/\epsilon = 0.99$), corresponding to the KdV limit, one finds stability region $\alpha \in (0.24, 0.74)$ which (after translation to our coordinates) agrees with the bounds found in this paper and in [BaN]. The first island of instability (starting from $\epsilon = 1$) is found at $\delta = 1.1$ which corresponds to $\epsilon = 0.74$. We note that $\delta = 1.1$ in [CDK] is found to represent also the transition where new branches of periodic wave trains are found as δ decreases below 1.1. There is also a nice discussion on the nature of the instabilities at this and other singularities of the stability boundary curves (p.316 [CDK] as well), which we recommend to the interested reader.

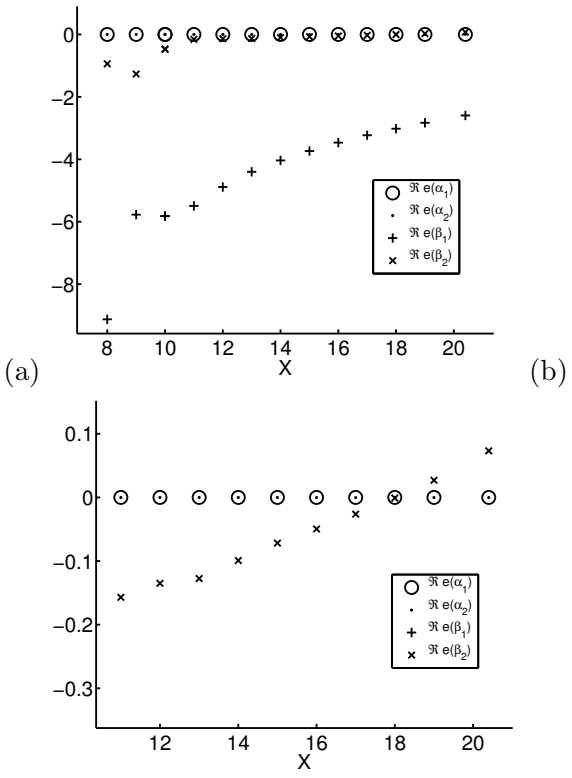

Figure 7: Plot of the real part of α_j and β_j from the spectral curves against the period X for gKS when $\varepsilon = 0.8$ and $\delta = 0.6$. Figure (b) is a zoom of figure (a).

2.3 The Whitham system and time evolution studies

In the previous section, we demonstrated numerically the existence of spectrally stable periodic traveling wave solutions of (2.1) in various circumstances, both in the classically studied case $\varepsilon = 0$ (Kuramoto-Sivashinsky equation) and in the case $\varepsilon \neq 0$ arising from general thin film flows. In each scenario considered, we found that all constant solutions are spectrally unstable and that, for a fixed period, an interval of the integration constant q (alternatively, of δ) corresponding to spectral stability; see Figure 1.

The goal of this final subsection is to shed light on the dynamics of the underlying periodic traveling wave when subject to a small integrable perturbation: in particular, we wish to connect the observed (numerical) behavior of solutions to the theoretical predictions given by Theorem 1.1. As we will see, the long-time behavior of such solutions to low-frequency perturbations can be well-approximated by a formal second-order Whitham modulation equation, with the dynamics intimately related to the properties of these derived amplitude equations.

We consider the behavior of a fixed periodic traveling wave solution $\bar{u}$ of (2.1), corresponding, say, to $\alpha = 0$ and $\beta = \bar{\beta}$ in (1.7), when subject to perturbations with characteristic wavenumber $|\nu| \ll 1$, on space and time scales $(X, T) = (x/\nu, t/\nu)$. Using a nonlinear optics (WKB) approximation

$$u(x,t) = u^0\left(X, T, \frac{\psi(X,T)}{\nu}\right) + \nu u^1\left(X, T, \frac{\psi(X,T)}{\nu}\right) + \mathcal{O}(\nu^2) \tag{2.24}$$

where $y \mapsto u^j(X, T, y)$ are unknown 1-periodic functions, to find approximate solutions of (1.1), it follows by substitution of the ansatz (2.24) into (1.1) in the re-scaled (X, T)-coordinates and collecting terms of leading order that we can take

$$u^0(X, T, y) = U\left(y - \alpha(X, T) - c(\beta(X, T))t; \beta(X, T)\right),$$

where $\alpha(X, 0) = 0$ and $\beta(X, 0) = \bar{\beta}$. For simplicity, we specialize now the discussion to the case where $\beta = (k, c)$, with k the wave number and c the wave speed.

As described in a more general setting in [Se], continuing the above calculation to higher orders, integrating over one period with respect to the fast variable y and noting by periodicity that integrals of perfect derivatives vanish, we find at first order in ν the modulation system

$$\begin{aligned} M(k,c)_t + F(k,c)_x &= 0, \\ k_t + (ck)_x &= 0 \end{aligned} \tag{2.25}$$

where $k = \psi_X$ is the local frequency, $c(X,T) = -\psi_T(X,T)/\psi_X(X,T)$ denotes the wave speed, $M(k,c)$ denotes the mean of u^0 over one period, and $F(k,c)$ is the mean of $f(u^0)$. Here, the second equation represents simply equality of mixed partial derivatives of ψ.

In the more specific setting of (2.1), $F(k,c)$ is the mean of $(u^0)^2/2$, and using the Galilean invariance $x \to x - ct$, $u \to u + c$, we may reduce (2.25) to

$$\begin{aligned} (m(k) + c)_T + (H(k) - m(k)c)_X &= 0 \\ k_T + (ck)_X &= 0, \end{aligned} \tag{2.26}$$

where $H(k) = F(k,0)$ and $m(k)$ denotes the mean over one period for a zero-speed wave of frequency k. In the classical situation, considered in [FST], where moreover $\varepsilon = 0$, symmetry of the governing equation ensures $m(k) = 0$ and (2.25) reduces to

$$\begin{aligned} c_t + (H(k))_x &= 0, \\ k_t + (ck)_x &= 0. \end{aligned} \tag{2.27}$$

Linearizing the latter about the constant $(\bar{k}, 0)$, corresponding to a background wave $\bar{u} = U(\cdot;(\bar{k},0))$, yields the linear *scalar* wave equation

$$k_{TT} \; - \; \bar{k}H'(\bar{k}) \; k_{XX} = 0 \tag{2.28}$$

in the local wave number k. In particular, the critical spectral curves $\lambda_j(\xi)$ bifurcating from the origin at the $\xi = 0$ state agree to first-order with the dispersion relation of (2.28). Clearly then, hyperbolicity of (2.28) is a necessary requirement for the spectral stability of the underlying periodic traveling wave $\bar{u}$.

Continuing to consider the classic case $\varepsilon = 0$ and a zero-speed wave, we may introduce similarly as in [NR2], higher order corrections to the WKB approximation (2.24) to find that the critical spectral curves $\lambda_j(\xi)$ actually agree to *second* order with the dispersion relation of the viscoelastic wave equation[13]

$$k_{TT} \; - \; \bar{k}H'(\bar{k}) \; k_{XX} = d(\bar{k}) \; k_{TXX} \tag{2.29}$$

for some $d(\bar{k})$ depending only on the underlying wave $U(.;\bar{\beta})$. As a result, we find that the diffusive spectral stability conditions (D1)–(D3) are equivalent

[13]The absence of terms like k_{XXX} originates in the symmetry of the governing equation under $(x,c) -> (-x,-c)$.

to $\bar{k}H'(\bar{k}) > 0$, corresponding to hyperbolicity of the linearized first-order Whitham averaged system (2.28), and $\mathrm{Re}(d(\bar{k})) < 0$, corresponding to diffusivity of the second-order linearized Whitham averaged system (2.29). Thus, the periodic traveling waves below the lower stability boundary ($\delta \approx 1.411$) in Table 1 correspond to a loss of hyperbolicity in the first-order Whitham system, while those above the upper stability boundary ($\delta \approx 1.701$) correspond to a "backward damping" effect corresponding to the amplification of the local wave-number $k(X,T)$ on time-scales of order $T = t/\nu$. These observations are discussed in more detail in [FST] and generalizations to cases $\varepsilon \neq 0$ (and $\bar{c}$ arbitrary) may be found in [NR2].

Equation (2.29) recovers the formal prediction of "viscoelastic behavior" of modulated waves carried out in [FST] and elsewhere, or "bouncing" behavior of individual periodic cells. Put more concretely, (2.29) predicts that the maximum of a perturbed periodic solution should behave approximately like point masses connected by viscoelastic springs. However, we emphasize that *such qualitative behavior*- in particular, the fact that the modulation equation is of second order- *does not derive only from Galilean or other invariance of the underlying equations*, as might be suggested by early literature on the subject, *but rather from the more general structure of conservative* (i.e., divergence) *form* [Se, JZ1].[14] Indeed, for any choice of f, $\lambda_j(\xi)$ may be seen to agree to second order with the dispersion relation for an appropriate diffusive correction of (2.25), a generalized viscoelastic wave equation. See [NR1, NR2] for further discussion of Whitham averaged equations and their derivation.

We now wish to connect the formal predictions of the above WKB analysis to the numerically observed time-evolution of a perturbed periodic traveling wave solution of (2.1). Keeping with the above theme, we fix $\varepsilon = 0$ throughout and consider waves with period $X = 6.3$ which, after an appropriate change of coordinates, have been taken to be initially stationary. In Figure 8 we have fixed three periodic traveling wave solutions of (2.1). The wave in Figure 8(a) corresponds to a periodic traveling wave below the lower stability boundary so that the associated linearized Whitham averaged system formally describing long-time behavior fails to be locally well-posed (hyperbolic). The resulting instability seems considerably more drastic than that observed for the wave in Figure 8(c), corresponding to a periodic traveling wave above the upper stability boundary. In this latter case, the first-order linearized Whitham system is locally well-posed but

[14] As discussed further in [Z3], conservation of mass lies outside the usual Noetherian formulation.

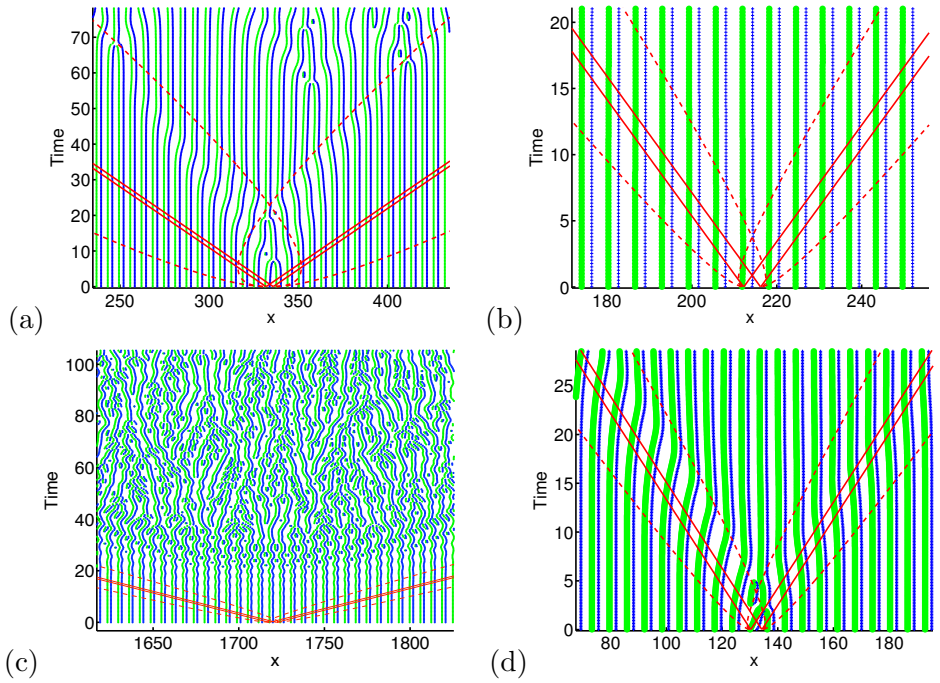

Figure 8: Here, we present the results of four time-evolution studies for the case when $\varepsilon = 0$. In Figures (a)-(c), we start with a small "Gaussian" type perturbation of the underlying 6.3-periodic wave (taken to be stationary by change of coordinates) and evolve the perturbation over time, with the vertical lines corresponding to the "peaks" and "troughs" between the waves. The wave-train in (a) corresponds to a wave below the lower stability boundary ($q = 3$), while the wave-train in (c) corresponds to a wave above the upper stability boundary ($q = 10$). The wave-train in (b) is spectrally stable and corresponds to $q = 5.5$. The "peaks" are plotted with thick green lines and the "troughs" are plotted with thin blue lines. In (a)-(d), the solid and dotted red lines indicate respectively the first order and second order approximations of bounds on the characteristics. They originate from a region enclosing three standard deviations from the mean of the perturbation. Finally, Figure (d) is the same as Figure (b) except for the initial perturbation is multiplied by a factor of 10. It is interesting to note that even when we subject the $q = 5.5$ wave to a large perturbation, lying well outside our stability theory, we observe a similar time asymptotic stability with analogous phase description as we developed for weak perturbations.

second-order diffusion coefficient, i.e. the coefficients β_j in (2.15), have real part with positive sign. This results in a type of "backward diffusion" where the amplitude of the local-wavenumber ψ grows with time, resulting in the forced visco-elastic behavior between the individual peaks and valleys in Figure 8(c). For more details on the instabilities in Figure 8(c), see Figure 9.

Finally, the wave in Figure 8(b) is spectrally stable and the resulting time-evolution of the perturbed wave at first sight appears to be of the form

$$u(x,t) = u(x + \psi(x,t))$$

where $\psi(\cdot,t)$ resembles the sum of well-separated Gaussian waves propagating in opposite directions. More precisely, it appears at first sight that our small initial perturbation simply divides its mass into two traveling Gaussian packets which convect in opposite directions and satisfies $\lim_{t\to\infty} u(x,t) = \bar{u}(x)$ for each $x \in \mathbb{R}$. In particular, this description would suggest that

$$\|u(\cdot,t) - \bar{u}\|_{L^p(\mathbb{R})} \approx \|\psi(\cdot,t)\|_{L^p(\mathbb{R})} \lesssim (1+t)^{-\frac{1}{2}(1-1/p)}, \quad p \geq 2.$$

However, while this intuition seems reasonable from our numerical experiments it is not correct: rather, the above "convecting Gaussian" description applies to the *wave number* ψ_x *and not the phase* ψ. As a result, ψ should roughly be described by the *integral* of Gaussian packets convecting in opposite directions, i.e. a small amplitude compactly supported (for each $t > 0$) sum of error functions of algebraically growing mass with $\lim_{t\to\infty} \psi(x,t) \neq 0$. In particular, we expect then that

$$\|u(\cdot,t) - \bar{u}(\cdot - \psi(\cdot,t))\|_{L^p(\mathbb{R})} \approx \|\psi_x(\cdot,t)\|_{L^p(\mathbb{R})} \lesssim (1+t)^{-\frac{1}{2}(1-1/p)}$$

for all $p \geq 2$, and that

$$\|u(\cdot,t) - \bar{u}\|_{L^p(\mathbb{R})} \approx \|\psi(\cdot,t)\|_{L^p(\mathbb{R})} \lesssim 1.$$

It is this observation that small localized perturbations of an underlying periodic traveling wave solution of (2.1) behave time-asymptotically as localized shifts of the original wave that drives our stability analysis in the next section, even in the general case when $\varepsilon \neq 0$; see Proposition 3.2, Corollary 1, and Lemma 3.3 below.

Finally, we remark that if one considers the more general case when $\varepsilon \neq 0$ it follows by similar considerations that the critical spectral curves $\lambda_j(\xi)$ agree to second-order with the dispersion relation of a second-order

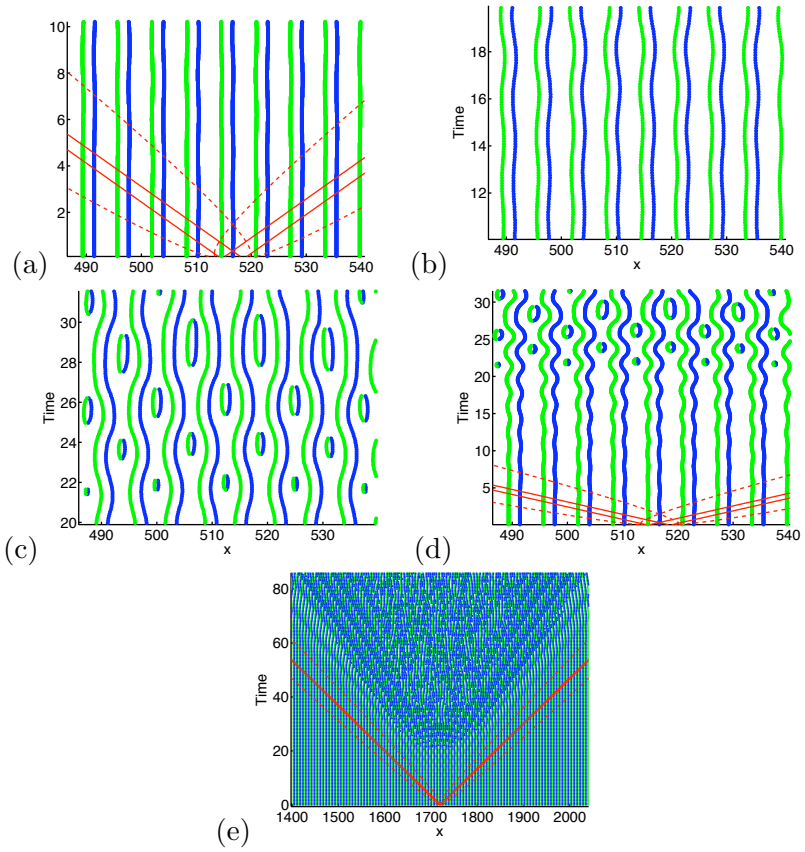

Figure 9: Here, we continue the time evolution study from Figure 8(c) (corresponding to $\varepsilon = 0$, $X = 6.3$, and $q = 10$). In particular, we highlight various aspects of the instability by zooming in on the evolution over different time intervals. Furthermore, due to the hyperbolicity of the first order Whitham equation (2.28) in this case the time scale on which the modulational instability (corresponding to Bloch frequencies $|\xi| \ll 1$) is observed is expected to be $\sim \eta^{-2}$, where η is the difference between X and the stability boundary X_*; see Appendix E.

Whitham modulation equation: see [NR2] for details of this derivation. However, the associated second order Whitham averaged system consists of a coupled system which, while sharing many of the properties of that of (2.26), is considerably more complicated to analyze directly. Nevertheless, when considering for definiteness again the case $\varepsilon = 0.2$, it is found that 6.3-periodic traveling wave solutions below the lower stability boundary ($\delta \approx 1.43$) in Table 2 correspond to a loss of hyperbolicity of the first-order Whitham system (2.26) while those corresponding to waves above the upper stability boundary ($\delta \approx 1.719$) correspond to a "backward damping" effect as described above.

Remark 2.7. As noted previously, the modulation ψ in the above discussion is not the same modulation presented in Theorem 1.1, although the two are very closely related; see Remark 1.4.

Remark 2.8. For rigorous justification of the Whitham equations at the nonlinear level, see [JNRZ1].

3 Proof of Theorem 1.1

In this section, we prove Theorem 1.1, showing that spectral stability of a given periodic traveling wave solution of (1.2) implies both linearized and nonlinear stability to small localized perturbations. The proof closely follows the analysis of [JZ1], concerning the analogous problem in the context of strictly parabolic second-order conservation laws. The main difference lies in the fact that the linear operator L defined in (1.8) is a fourth-order differential operator rather than second order. Nevertheless, the principles of [JZ1] readily extend to the present higher-order case with little modification.

3.1 Spectral preparation

Recall that in the statement of Theorem 1.1, we normalize $\bar{X}$ to 1. Our assumptions (H1)-(H2) and (D3) imply that the generalized kernel of the operator L_0, defined on $L^2_{\rm per}([0,1])$, is of dimension 2. A crucial part of our analysis of the linearized solution operator e^{Lt} relies on understanding how this zero-eigenspace bifurcates from this neutral state. As expected, the existence of a Jordan block at $\lambda = 0$ for the operator L_0, guaranteed by hypothesis (H4), greatly complicates matters as compared to the degenerate case when (H4) fails; see [JZ3]. We thus begin our linearized stability analysis with a careful study of the Bloch perturbation expansion of these critical eigenvalues and associated eigen-projections near $\xi = 0$.

Lemma 3.1. *Assuming (H1), (H2), and (D3), there exist constants $\xi_0 \in (0,\pi)$, $\varepsilon_0 > 0$ and two continuous curves, $j = 1,2$, $\lambda_j : [-\xi_0,\xi_0] \to B(0,\varepsilon_0)$ such that, when $|\xi| \le \xi_0$,*

$$\sigma(L_\xi) \cap B(0,\varepsilon_0) \;=\; \{\lambda_1(\xi),\lambda_2(\xi)\}\,. \tag{3.1}$$

Moreover these two critical curves are differentiable at 0 and can be expanded as

$$\lambda_j(\xi) = \; -ia_j\xi \; + o(\xi), \quad j = 1,2 \tag{3.2}$$

as $\xi \to 0$. Assuming also (H3), the curves λ_j are analytic in a neighborhood of $\xi = 0$. Thus, up to a possible change of ξ_0, there exist, for $0 < |\xi| \le \xi_0$, dual right and left eigenfunctions $\{q_j(\xi,\cdot)\}_{j=1,2}$ and $\{\tilde q_j(\xi,\cdot)\}_{j=1,2}$ of L_ξ associated with $\lambda_j(\xi)$, of form

$$q_j(\xi,\cdot) = (i\xi)^{-1}\beta_{j,1}(\xi)\, v_1(\xi,\cdot) + \beta_{j,2}(\xi)\, v_2(\xi,\cdot)$$

$$\tilde q_j(\xi,\cdot) = i\xi\tilde\beta_{j,1}(\xi)\, \tilde v_1(\xi,\cdot) + \tilde\beta_{j,2}(\xi)\, \tilde v_2(\xi,\cdot)$$

for $j = 1,2$, where

- *for $j = 1,2$, the functions $v_j : [-\xi_0,\xi_0] \to L^2_{\rm per}([0,1])$ and $\tilde v_j : [-\xi_0,\xi_0] \to L^2_{\rm per}([0,1])$ are analytic functions such that, when $|\xi| \le \xi_0$, $\{v_j(\xi,\cdot)\}_{j=1,2}$ and $\{\tilde v_j(\xi,\cdot)\}_{j=1,2}$ are dual bases of the total eigenspace of L_ξ associated with spectrum $\sigma(L_\xi) \cap B(0,\varepsilon_0)$, chosen to satisfy*

$$v_1(0,\cdot) = \bar u_x, \quad \text{and} \quad \tilde v_2(0,\cdot) \equiv 1;$$

- *for $j = 1,2$ and $k = 1,2$, the functions $\beta_{j,k} : [-\xi_0,\xi_0] \to \mathbb{C}$ and $\tilde\beta_{j,k} : [-\xi_0,\xi_0] \to \mathbb{C}$ are analytic.*

Finally, assuming in addition that (D2) holds, the spectral curves λ_j can be expanded as

$$\lambda_j(\xi) = -ia_j\xi - b_j\xi^2 + \mathcal{O}(|\xi|^3), \quad j = 1,2 \tag{3.3}$$

for some $a_j \in \mathbb{R}$ and $b_j > 0$.

Proof. (following [JZ1, JZN, NR2]) First, as already mentioned in Remark 1.3, assumptions (H1), (H2) and (D3) ensures the possibility of a parametrization $\beta = (k, M)$ by wave number and mean We adopt such a parametrization. This provides $L_0\bar u_x = 0$ and $L_0\partial_c U(\cdot;\bar\beta) = -\partial_M c(\bar\beta)\bar u_x$ with $\langle\tilde v, \bar u_x\rangle_{L^2_{\rm per}([0,1])} = 0$ and $\langle\tilde v, \partial_M U(\cdot;\bar\beta)\rangle_{L^2_{\rm per}([0,1])} = 1$, where $\tilde v \equiv 1$.

Since L_ξ has dense domain $H^4_{\rm per}([0,1])$ compactly embedded in $L^2_{\rm per}([0,1])$, its spectrum consists of isolated eigenvalues of finite multiplicity [He]. As 0 is separated from the rest of the spectrum of L_0, assumption (D3) and standard spectral theory for perturbations by relatively compact operators (see [K]) yields constants $\xi_0 \in (0,\pi)$, $\varepsilon_0 > 0$ and *continuous* functions λ_1, λ_2 such that, for $|\xi| < \xi_0$, $\sigma(L_\xi) \cap B(0,\varepsilon_0) = \{\lambda_1(\xi), \lambda_2(\xi)\}$. Moreover this also yields analytic dual right and left spectral projectors associated to spectrum in $B(0,\varepsilon_0)$. Analytic dual bases of the right and left eigenspaces may then be obtained by projecting dual bases for spectral spaces of the spectrum of L_0 in $B(0,\varepsilon_0)$. By the first paragraph of the proof and the conservation law structure of the governing equation, we may choose such bases in the form $\{\bar{u}_x, \partial_M U(\cdot;\bar\beta)\}$ and $\{*, \tilde v\}$ and obtain in this way the functions $\{v_j\}$ and $\{\tilde v_j\}$ of the lemma.

We have now reduced the infinite dimensional spectral perturbation problem for the operators L_ξ to the spectral analysis of

$$M_\xi = \left[\langle \tilde v_j(\xi,\cdot), L_\xi v_l(\xi,\cdot)\rangle_{L^2([0,1])}\right]_{j,l},$$

a 2×2 matrix perturbation problem. By direct calculation $M_0 = \begin{pmatrix} 0 & -\partial_M c(\bar\beta) \\ 0 & 0 \end{pmatrix}$. Below, however, we will scale M_ξ to blow up at the double eigenvalue. To do so, we expand the operator L_ξ as

$$L_\xi = L_0 + i\xi L^{(1)} + (i\xi)^2 L^{(2)} + (i\xi)^3 L^{(3)} + (i\xi)^4 L^{(4)} \tag{3.4}$$

and note, specifically, that

$$L^{(1)} = -(\bar u - \bar c) - 3\varepsilon\partial_x^2 - 2\delta\partial_x - 4\partial_x^3. \tag{3.5}$$

By either a direct calculation or by first scaling the parameterization then differentiating the profile equation with respect to k (see [NR1, NR2]), we find that $\left\langle \tilde v_2(0,\cdot), L^{(1)} v_1(0,\cdot)\right\rangle = 0$. Therefore, M_ξ can be expanded as $\xi \to 0$ as

$$M_\xi = \begin{pmatrix} 0 & -\partial_M c(\bar\beta) \\ 0 & 0 \end{pmatrix} + i\xi \begin{pmatrix} * & * \\ 0 & * \end{pmatrix} + \mathcal{O}(|\xi|^2)$$

so that, in particular, the scaling

$$\check M_\xi := (i\xi)^{-1} S(\xi) M_\xi S(\xi)^{-1}, \qquad S(\xi) := \begin{pmatrix} i\xi & 0 \\ 0 & 1 \end{pmatrix}, \tag{3.6}$$

preserves smoothness in ξ at $\xi = 0$. Since the eigenvalues $m_j(\xi)$ of $\check M_\xi$ are $(i\xi)^{-1}\lambda_j(\xi)$, their continuity implies the differentiability of the functions

$\lambda_j(\xi)$ at $\xi = 0$. Assuming, in addition to above, that assumption (H3) holds, it follows from the fact that $m_j(0) = -a_j$ that the eigenmodes of $\check{M}_\xi$ are analytic in ξ in a neighborhood of $\xi = 0$. Undoing the scaling finishes the proof, up to the observation that (3.3) follows from (D2) and $\overline{\lambda_j(\xi)} = \lambda_j(-\xi)$. □

3.2 Linearized bounds

We begin our stability analysis by deriving decay rates for the linearized solution operator e^{Lt} of the linearized equation (1.8). Recalling the inverse Bloch transform representation (1.13) of the linearized solution operator, we first introduce, as in the proof of Lemma 3.1, for each $\xi \in (-\xi_0, \xi_0)$ the spectral projection $P(\xi)$, analytic in ξ, onto the total eigenspace associated with spectrum $\sigma(L_\xi) \cap B(0, \varepsilon_0) = \{\lambda_1(\xi), \lambda_2(\xi)\}$ of the Bloch operator L_ξ. We also choose a smooth cutoff function $\phi : [-\pi, \pi) \to [0, 1]$ such that

$$\phi(\xi) = \begin{cases} 1, & \text{if } |\xi| \le \xi_0/2 \\ 0, & \text{if } |\xi| \ge \xi_0 \end{cases}$$

and split the solution operator $S(t) := e^{Lt}$ into its low Floquet-number critical part

$$S^I(t)g(x) := \int_{-\pi}^{\pi} e^{i\xi x}\phi(\xi)[P(\xi)e^{L_\xi t}\check{g}(\xi,\cdot)](x)d\xi \tag{3.7}$$

and exponentially-stable part

$$S^{II}(t)g(x) := \int_{-\pi}^{\pi} e^{i\xi x}[(1-\phi(\xi)P(\xi))\, e^{L_\xi t}\check{g}(\xi,\cdot)](x)d\xi. \tag{3.8}$$

As the analysis of the critical part is considerably more delicate, we being by deriving L^p bounds on $S^{II}(t)$. By standard sectorial bounds [Pa, He], the fact that L^2 and H^r spectra coincide and the spectral separation of the $\lambda_j(\xi)$ from the remaining spectrum of L_ξ we have bounds

$$\|L_\xi^m e^{L_\xi t}\,(1-\phi(\xi)P(\xi))\, g\|_{H^r_{\rm per}([0,1]),\xi} \le Ct^{-m}e^{-\theta t}\|g\|_{H^r_{\rm per}([0,1]),\xi} \tag{3.9}$$

for some constants $\theta, C > 0$, with $\|g\|^2_{H^r_{\rm per}([0,1]),\xi} = \sum_{j=0}^r \|(\partial_x+i\xi)^j g\|^2_{L^2_{\rm per}([0,1])}$. Using the fact that L_ξ is a relatively compact perturbation of the fourth order differential operator $(-1-(\partial_x+i\xi)^4)$, in conjunction with (1.14), we immediately have the H^r bounds of the following Proposition.

Proposition 3.1. *Under assumptions (H1)–(H4) and (D1)–(D3), there exist constants $C, \theta > 0$ such that for all $2 \le p \le \infty$, $0 \le 4l_1 + l_2 = l_3 \le K+1$, $0 \le 4m_1 + m_2 + m_3 \le K$, K as in (H1), $r = 0, 1$ and $t > 0$*

$$\begin{aligned}
\left\| \partial_t^{l_1} \partial_x^{l_2} S^{II}(t) \partial_x^{l_3} g \right\|_{H^r(\mathbb{R})} &\le C t^{-\frac{4l_1+l_2+l_3}{4}} e^{-\theta t} \|g\|_{H^r(\mathbb{R})}, \\
\left\| \partial_t^{m_1} \partial_x^{m_2} S^{II}(t) \partial_x^{m_3} g \right\|_{L^p(\mathbb{R})} &\le C t^{-\frac{1}{4}\left(\frac{1}{2}-\frac{1}{p}\right)-\frac{4m_1+m_2+m_3}{4}} e^{-\theta t} \|g\|_{L^2(\mathbb{R})}, \\
\left\| S^{II}(t) g \right\|_{L^p(\mathbb{R})} &\le C e^{-\theta t} \|g\|_{H^1(\mathbb{R})}.
\end{aligned}$$

Proof. By the above discussion, all that is left is to explain how to verify the stated L^p bounds. These follow from L^2 and H^1 bounds and the Sobolev embedding inequality $\|g\|_{L^p(\mathbb{R})} \le C \|g\|_{L^2(\mathbb{R})}^{1-(1/2-1/p)} \|\partial_x g\|_{L^2(\mathbb{R})}^{1/2-1/p}$. □

Next, we analyze the critical part of the solution operator $S(t)$. For this purpose, it is convenient to introduce the (critical) Green kernel

$$G^I(x,t;y) := S^I(t)\delta_y(x)$$

associated with S^I and

$$\left[G_\xi^I(\cdot,t;y)\right](x) := \phi(\xi) P(\xi) e^{L_\xi t} \left[\delta_y\right](x)$$

the corresponding integral kernel appearing within the Bloch-Fourier representation of G^I, where $[\cdot]$ denotes the 1-periodic extension of the given function onto the whole real line. We first prove the following lemma yielding a spectral representation of G^I incorporating the results of Lemma 3.1.

Lemma 3.2. *Under the hypothesis (H1)–(H4) and (D1)–(D3), we have*

$$\begin{aligned}
\left[G_\xi^I(\cdot,t;y)\right](x) &= \phi(\xi) \sum_{j=1}^{2} e^{\lambda_j(\xi)t} q_j(\xi,x) \tilde{q}_j(\xi,y)^*, \\
G^I(x,t;y) &= \int_{-\pi}^{\pi} e^{i\xi(x-y)} \left[G_\xi^I(\cdot,t;y)\right](x) d\xi \\
&= \int_{-\pi}^{\pi} e^{i\xi(x-y)} \phi(\xi) \sum_{j=1}^{2} e^{\lambda_j(\xi)t} q_j(\xi,x) \tilde{q}_j(\xi,y)^* d\xi,
\end{aligned} \tag{3.10}$$

where $*$ denotes the matrix adjoint, or complex conjugate transpose, and $q_j(\xi,\cdot)$ and $\tilde{q}_j(\xi,\cdot)$ are right and left eigenfunctions of L_ξ associated with the eigenvalues $\lambda_j(\xi)$ defined in (3.1)*, normalized so that $\langle \tilde{q}_j(\xi,\cdot), q_j(\xi,\cdot) \rangle_{L^2_{\mathrm{per}}([0,1])} = 1$.*

Proof. The first equality follows by the spectral decomposition of $e^{L_\xi t}$, and the spectral description of Lemma 3.1. The second equality follows by the inverse Bloch transform formula (3.7) and Fourier transform manipulations using the fact that both discrete and continuous transforms of the centered δ-function are constant equal to $(2\pi)^{-1}$ to get

$$\check{\delta_y}(\xi, x) \;=\; \frac{1}{2\pi} e^{-i\xi y} \sum_{l\in\mathbb{Z}} e^{2i\pi l(x-y)} \;=\; e^{-i\xi y}[\delta_y](x).$$

The third quality now follows by substitution; see [OZ4] for further details. □

Continuing, we point out that it seems unlikely that the low-frequency Green function G^I will satisfy $L^p \to L^p$ bounds which are suitable for our purposes. To see this, notice from Lemma 3.2 and Lemma 3.1 that we have the representation

$$G^I(x,t;y) = \int_{-\pi}^{\pi} e^{i\xi(x-y)}\phi(\xi) \sum_{j}^{2} e^{\lambda_j(\xi)t}\Big((i\xi)^{-1}\beta_{j,1}(\xi)\tilde{\beta}_{j,2}(\xi)v_1(\xi,x)\tilde{v}_2(\xi,y)^* + \mathcal{O}(1)\Big)d\xi$$

of the critical Green kernel. From assumption (D2) we expect, for example,

$$\left\|G^I(\cdot,t;y)\right\|_{L^\infty(\mathbb{R})} \approx \left\|\xi \mapsto |\xi|^{-1}e^{-\theta|\xi|^2 t}\phi(\xi)\right\|_{L^1([-\pi,\pi))},$$

where the right hand side is interpreted in the principal value sense, which is merely bounded and hence does not decay in time. In order to compensate for this lack of decay arising from the Jordan block associated with the translation mode at $\xi = 0$, we separate out the bounded translation mode from the faster-decaying "good" part of the Green kernel. To this end, notice that by defining the function

$$\tilde{e}(x,t;y) := \int_{-\pi}^{\pi} e^{i\xi(x-y)}\phi(\xi) \sum_{j=1}^{2} e^{\lambda_j(\xi)t}(i\xi)^{-1}\beta_{j,1}(\xi)\tilde{q}_j(\xi,y)^* d\xi \tag{3.11}$$

we have

(3.12)

$$\begin{aligned} G^I(x,t;y) &- \bar{u}_x(x)\tilde{e}(x,t;y) \\ &= \int_{-\pi}^{\pi} e^{i\xi(x-y)}\phi(\xi) \sum_{j=1}^{2} e^{\lambda_j(\xi)t}\beta_{j,2}(\xi)v_2(\xi,x)\tilde{q}_j(\xi,y)^* d\xi \\ &+ \int_{-\pi}^{\pi} e^{i\xi(x-y)}\phi(\xi) \sum_{j=1}^{2} e^{\lambda_j(\xi)t}\beta_{j,1}(\xi)\frac{v_1(\xi,x)-v_1(0,x)}{i\xi}\tilde{q}_j(\xi,y)^* d\xi \end{aligned}$$

Now since all quantities involved in (3.12) are C^1 in ξ, from (D2) we deduce

(3.13)
$$\left\|G^I(\cdot,t;y)-\bar{u}_x(\cdot)\tilde{e}(\cdot,t;y)\right\|_{L^\infty(\mathbb{R})}\leq C\left\|\xi\mapsto e^{-\theta|\xi|^2t}\phi(\xi)\right\|_{L^1([-\pi,\pi))}\leq C(1+t)^{-1/2}$$

yielding algebraic decay of $G^I-\bar{u}_x\tilde{e}$ in time. The more general effect of this regularization is the content of the following proposition.

Proposition 3.2. *Under the assumptions (H1)–(H4) and (D1)–(D3), the critical Green kernel $G^I(x,t;y)$ of (1.8) may be decomposed as*

$$G^I(x,t;y)=\bar{u}_x(x)\tilde{e}(x,t;y)+\widetilde{G}^I(x,t;y)$$

where for all $t\geq 0$, $1\leq q\leq 2\leq p\leq\infty$, and $1\leq r\leq 4$ the residual $\widetilde{G}^I(x,t;y)$ satisfies

$$\begin{aligned}
\left\|\int_{\mathbb{R}}\widetilde{G}^I(\cdot,t;y)g(y)dy\right\|_{L^p(\mathbb{R})}&\leq C\,(1+t)^{-\frac{1}{2}\left(\frac{1}{q}-\frac{1}{p}\right)}\,\|g\|_{L^q(\mathbb{R})},\\
\left\|\int_{\mathbb{R}}\partial_y^r\widetilde{G}^I(\cdot,t;y)g(y)dy\right\|_{L^p(\mathbb{R})}&\leq C\,(1+t)^{-\frac{1}{2}\left(\frac{1}{q}-\frac{1}{p}\right)-\frac{1}{2}}\,\|g\|_{L^q(\mathbb{R})},\\
\left\|\int_{\mathbb{R}}\partial_t\widetilde{G}^I(\cdot,t;y)g(y)dy\right\|_{L^p(\mathbb{R})}&\leq C\,(1+t)^{-\frac{1}{2}\left(\frac{1}{q}-\frac{1}{p}\right)-\frac{1}{2}}\,\|g\|_{L^q(\mathbb{R})}.
\end{aligned}\tag{3.14}$$

Furthermore, for all $t\geq 0$, $1\leq q\leq 2\leq p\leq\infty$, $0\leq j,l$, $j+l\leq K$, and $1\leq r\leq 4$ we have

$$\left\|\int_{\mathbb{R}}\partial_x^j\partial_t^l\partial_y^r\tilde{e}(\cdot,t;y)g(y)dy\right\|_{L^p(\mathbb{R})}\leq C(1+t)^{-\frac{1}{2}\left(\frac{1}{q}-\frac{1}{p}\right)-\frac{(j+l)}{2}}\|g\|_{L^q(\mathbb{R})}\tag{3.15}$$

and, if in addition $j+l\geq 1$, or ($j=l=0$, $p=\infty$ and $q=1$),

$$\left\|\int_{\mathbb{R}}\partial_x^j\partial_t^l\tilde{e}(\cdot,t;y)g(y)dy\right\|_{L^p(\mathbb{R})}\leq C(1+t)^{\frac{1}{2}-\frac{1}{2}\left(\frac{1}{q}-\frac{1}{p}\right)-\frac{(j+l)}{2}}\|g\|_{L^q(\mathbb{R})}.\tag{3.16}$$

Proof. To begin, let $\widetilde{G}^I(x,t;y):=G^I(x,t;y)-\bar{u}_x(x)\tilde{e}(x,t;y)$ where the function $\tilde{e}$ is defined in (3.11). By interpolation, it is sufficient to consider only the cases $q=1$ and $q=2$.

(i) Case $q=1$. To prove bounds for $q=1$ we rely on Triangle Inequality

$$\left\|\int_{\mathbb{R}}F(\cdot,t;y)g(y)dy\right\|_{L^p(\mathbb{R})}\;\leq\;\|g\|_{L^1(\mathbb{R})}\sup_{y\in\mathbb{R}}\|F(\cdot,t;y)\|_{L^p(\mathbb{R})}.$$

Now, to generalize (3.13) and prove the first part of (3.14) in the case $q = 1$, we use (1.15) to get for any (t, y)

$$\left\|\tilde{G}^I(\cdot,t;y)\right\|_{L^p(\mathbb{R})} \leq C \left\|\xi \mapsto e^{-\theta|\xi|^2 t}\phi(\xi)\right\|_{L^{p'}([-\pi,\pi))} \leq C(1+t)^{-\frac{1}{2}(1-1/p)}$$

with p' the Hölder conjugate of p, $1/p + 1/p' = 1$. The second part of (3.14) comes in a similar way by observing that for $j = 1, 2$ and $r \geq 1$, the fact that $\tilde{q}_j(0, y) = \tilde{\beta}_{j,2}(0)$ implies

$$\partial_y^r \tilde{q}_j(\xi, y) \;=\; \partial_y^r \tilde{q}_j(\xi, y) - \partial_y^r \tilde{q}_j(0, y) = \mathcal{O}(\xi), \tag{3.17}$$

and thus

$$\left\|\partial_y^r \tilde{G}^I(\cdot,t;y)\right\|_{L^p(\mathbb{R})} \leq C \left\|\xi \mapsto |\xi| e^{-\theta|\xi|^2 t}\phi(\xi)\right\|_{L^{p'}([-\pi,\pi))} \leq C(1+t)^{-\frac{1}{2}(1-1/p)-\frac{1}{2}}.$$

Likewise the last part of (3.14) stems from the fact that the time derivative brings down factors $\lambda_j(\xi) = \mathcal{O}(\xi)$.

Using again (3.17), we obtain for $r \geq 1$

$$\partial_x^j \partial_t^l \partial_y^r \tilde{e}(x,t;y) = \int_{-\pi}^{\pi} e^{i\xi(x-y)}\phi(\xi) \sum_{j'=1}^{2} e^{\lambda_{j'}(\xi)t}(i\xi)^j \lambda_j(\xi)^l \beta_{j',1}(\xi) \frac{\partial_y^r \tilde{q}_{j'}(\xi,y)^* - \partial_y^r \tilde{q}_{j'}(0,y)^*}{i\xi} d\xi$$

and another use of (1.15) provides

$$\left\|\partial_x^j \partial_t^l \partial_y^r \tilde{e}(\cdot,t;y)\right\|_{L^p(\mathbb{R})} \leq C \left\|\xi \mapsto |\xi|^{j+l} e^{-\theta|\xi|^2 t}\phi(\xi)\right\|_{L^{p'}([-\pi,\pi))} \leq C(1+t)^{-\frac{1}{2}(1-1/p)-\frac{1}{2}(j+l)}.$$

This proves (3.15) in the case $q = 1$. Inequality (3.16) follows similarly when $j + l \geq 1$.

Finally, we must obtain (3.16) in the critical case $j = l = 0$, $p = \infty$ and

$q = 1$. Recalling (3.3) we introduce $\check{\lambda}(\xi) := -ia_j\xi - b_j\xi^2$ and expand (3.18)

$$\begin{aligned}\tilde{e}(x,t;y) = &\int_{-\pi}^{\pi} e^{i\xi(x-y)}\phi(\xi)\sum_{j=1}^{2} e^{\lambda_j(\xi)t}\frac{\beta_{j,1}(\xi)\tilde{q}_j(\xi,y)^* - \beta_{j,1}(0)\tilde{q}_j(0,y)^*}{i\xi}d\xi\\ &+ \int_{-\pi}^{\pi} e^{i\xi(x-y)}\phi(\xi)\sum_{j=1}^{2} e^{\check{\lambda}_j(\xi)t}\frac{e^{(\lambda_j(\xi)-\check{\lambda}_j(\xi))t}-1}{i\xi}\beta_{j,1}(0)\tilde{\beta}_{j,2}(0)d\xi\\ &+ \int_{-\pi}^{\pi} e^{i\xi(x-y)}\sum_{j=1}^{2} e^{\check{\lambda}_j(\xi)t}\frac{\phi(\xi)-1}{i\xi}\beta_{j,1}(0)\tilde{\beta}_{j,2}(0)d\xi\\ &- \int_{\mathbb{R}\setminus[-\pi,\pi]} e^{i\xi(x-y)}\sum_{j=1}^{2} e^{\check{\lambda}_j(\xi)t}\frac{1}{i\xi}\beta_{j,1}(0)\tilde{\beta}_{j,2}(0)d\xi\\ &+ \text{P.V.}\int_{\mathbb{R}} e^{i\xi(x-y)}\sum_{j=1}^{2} e^{\check{\lambda}_j(\xi)t}\frac{1}{i\xi}\beta_{j,1}(0)\tilde{\beta}_{j,2}(0)d\xi.\end{aligned}$$

All but the last term in (3.18) may be bounded using Haussdorff-Young estimates, either using the classical one or (1.15). To complete the proof then, we must derive an appropriate L^∞ bound on the last integral in (3.18). Since

$$\frac{1}{2\pi}\int_{\mathbb{R}} e^{i\xi\cdot(x-y)}e^{\check{\lambda}_j(\xi)t}d\xi = \frac{e^{-(x-y-a_jt)^2/4b_jt}}{\sqrt{4\pi b_jt}}, \quad j = 1,2,$$

the final principal value integral in (3.18) is recognized to be

$$2\pi\sum_{j=1}^{2}\beta_{j,1}(0)\tilde{\beta}_{j,2}(0)\,\text{errfn}\left(\frac{x-y-a_jt}{\sqrt{4b_jt}}\right),$$

hence is bounded in L^∞ as claimed.

(ii) Case $q = 2$. To prove bounds with $q = 2$ we directly apply (1.15) to Bloch formulations. For instance expand

$$\begin{aligned}\int_{\mathbb{R}}\tilde{G}^I(x,t;y)g(y)dy = &\int_{-\pi}^{\pi} e^{i\xi x}\phi(\xi)\sum_{j=1}^{2} e^{\lambda_j(\xi)t}\beta_{j,2}(\xi)v_2(\xi,x)\langle\tilde{q}_j(\xi,\cdot),\check{g}(\xi,\cdot)\rangle_{L^2_{\text{per}}([0,1])}d\xi\\ &+ \int_{-\pi}^{\pi} e^{i\xi x}\phi(\xi)\sum_{j=1}^{2} e^{\lambda_j(\xi)t}\beta_{j,1}(\xi)\frac{v_1(\xi,x)-v_1(0,x)}{i\xi}\langle\tilde{q}_j(\xi,\cdot),\check{g}(\xi,\cdot)\rangle_{L^2_{\text{per}}([0,1])}d\xi.\end{aligned}$$

The generalized Haussdorff-Young estimate (1.15) thus yields

$$\begin{aligned}\left\|\int_{\mathbb{R}} \tilde{G}^I(\cdot,t;y)g(y)dy\right\|_{L^p(\mathbb{R})} &\le C\left\|\xi \mapsto e^{-\theta|\xi|^2 t}\|\check{g}(\xi,\cdot)\|_{L^2_{\mathrm{per}}([0,1])}\right\|_{L^{p'}([-\pi,\pi])}\\ &\le C\left\|\xi \mapsto e^{-\theta|\xi|^2 t}\right\|_{L^{p''}([-\pi,\pi])}\|\check{g}\|_{L^2([-\pi,\pi),L^2_{\mathrm{per}}([0,1]))}\\ &\le C(1+t)^{-\frac{1}{2}\left(\frac{1}{2}-\frac{1}{p}\right)}\|g\|_{L^2(\mathbb{R})}\end{aligned}$$

where p' is such that $1/p+1/p'=1$, and p'' such that $1/p'=1/2+1/p''$. The other bounds on $\tilde{G}^I$ follows in the same way, observing that space derivatives ∂_y allow the use of (3.17) and thus provide an extra $\mathcal{O}(\xi)$ factor in the appropriate integrals. The bounds on $\tilde{e}$ can be obtained in an analogous way, completing the proof. □

Finally, we combine the above various exponentially-stable and critical bounds to obtain decay estimates on the Green function

$$G(x,t;y) = S(t)\delta_y(x)$$

associated with the full solution operator $S(t) = e^{Lt}$. Prior to that, we let $\chi : [0,\infty) \to [0,1]$ be a smooth real valued cutoff function such that

$$\chi(t) = \begin{cases} 0, & \text{if } 0 \le t \le 1 \\ 1, & \text{if } t \ge 2 \end{cases}$$

and define

$$e(x,t;y) := \chi(t)\tilde{e}(x,t;y); \tag{3.19}$$

the purpose of the time cutoff function χ will be made clear in Remark 3.4 below. The following result immediately follows from Lemma 3.2 and Proposition 3.2.

Corollary 1. *Under assumptions (H1)–(H4) and (D1)–(D3), the Green function $G(x,t;y)$ of (1.8) decomposes as*

$$G(x,t;y) = \bar{u}_x(x)e(x,t;y) + \widetilde{G}(x,t;y)$$

where, for some $C, \theta > 0$ *and all* $t > 0$, $2 \le p \le \infty$ *and* $1 \le r \le 4$,

(3.20)

$$\left\| \int_{\mathbb{R}} \partial_y^r \widetilde{G}(\cdot, t; y) g(y) dy \right\|_{L^p(\mathbb{R})} \le \min \begin{cases} Ce^{-\theta t} \|\partial_x^r g\|_{H^1(\mathbb{R})} + C(1+t)^{-\frac{1}{2}\left(\frac{1}{2}-\frac{1}{p}\right)-\frac{1}{2}} \|g\|_{L^2(\mathbb{R})} \\ Ct^{-\frac{1}{4}\left(\frac{1}{2}-\frac{1}{p}\right)-\frac{r}{4}} (1+t)^{-\frac{1}{4}\left(\frac{3}{2}-\frac{1}{p}\right)-\frac{1}{2}+\frac{r}{4}} \|g\|_{L^1(\mathbb{R})\cap L^2(\mathbb{R})} \end{cases}$$

(3.21)

$$\left\| \int_{\mathbb{R}} \widetilde{G}(\cdot, t; y) g(y) dy \right\|_{L^p(\mathbb{R})} \le C(1+t)^{-\frac{1}{2}\left(1-\frac{1}{p}\right)} \|g\|_{L^1(\mathbb{R})\cap H^1(\mathbb{R})}$$

Furthermore, $e(x, t; y) \equiv 0$ *for* $0 \le t \le 1$ *and there exists a constant* $C > 0$ *such that for all* $t \ge 0$, $1 \le q \le 2 \le p \le \infty$, $0 \le j, l$, $j + l \le K$, *and* $1 \le r \le 4$ *we have*

(3.22)

$$\left\| \int_{\mathbb{R}} \partial_x^j \partial_t^l \partial_y^r e(\cdot, t; y) g(y) dy \right\|_{L^p(\mathbb{R})} \le C(1+t)^{-\frac{1}{2}\left(\frac{1}{q}-\frac{1}{p}\right)-\frac{(j+k)}{2}} \|g\|_{L^q(\mathbb{R})}.$$

and, if in addition $j + l \ge 1$, *or* ($j = l = 0$, $p = \infty$ *and* $q = 1$),

$$\left\| \int_{\mathbb{R}} \partial_x^j \partial_t^l e(\cdot, t; y) g(y) dy \right\|_{L^p(\mathbb{R})} \le C(1+t)^{\frac{1}{2}-\frac{1}{2}\left(\frac{1}{q}-\frac{1}{p}\right)-\frac{(j+k)}{2}} \|g\|_{L^q(\mathbb{R})} \tag{3.23}$$

Remark 3.3. As may be clear from the proofs of various linear estimates discussed above, except for the critical bounds on e or $\tilde{e}$ in the case $j = l = 0$, $p = \infty$ and $q = 1$, the introduction of the critical Green kernel was a pure presentation device. Indeed, we adopted here it to mark proximity with [JZ1]. Yet, since almost all the above linear bounds were proved using Haussdorff-Young type estimates, there may be some gain in clarity and efficiency in presentation in keeping all descriptions at the level of semigroups and Bloch symbols. This latter approach was recently adopted in [JNRZ1, JNRZ2, JNRZ3], where further decompositions of the critical part of the solution operator are needed.

3.3 Nonlinear preparations

Given the linearized bounds on the linear solution operator $S(t) = e^{Lt}$ derived in the previous section, we are now in position to consider the effect of the small nonlinear terms that were omitted in obtaining the linearized equation (1.8). Our first task is to explain how to implement at the nonlinear level the separation of critical phase-shift contribution. To this end, let $\tilde{u}(x, t)$ be a solution of

$$\partial_t u - c\partial_x u + \partial_x^4 u + \varepsilon \partial_x^3 u + \delta \partial_x^2 u + \partial_x f(u) = 0 \tag{3.24}$$

and define the spatially modulated function $u(x,t) := \tilde{u}(x+\psi(x,t),t)$, where $\psi : \mathbb{R}\times\mathbb{R}_+ \to \mathbb{R}$ is a function to be determined later. Moreover, let $\bar{u}(x)$ be a stationary periodic solution of (3.24) and define the nonlinear perturbation function

$$v(x,t) := u(x,t) - \bar{u}(x). \tag{3.25}$$

Lemma 3.3. *For v as above, we have*

$$(\partial_t - L)(v - \psi\bar{u}_x) = \mathcal{N}, \quad \mathcal{N} = \partial_x\mathcal{Q} + \partial_x\mathcal{R} + \partial_t\mathcal{S} \tag{3.26}$$

where

$$\begin{aligned}
\mathcal{Q} &= -\left(f(\bar{u}+v) - f(\bar{u}) - df(\bar{u})v\right)\\
\mathcal{R} &= \psi_t v - \delta\frac{-\psi_x}{1+\psi_x}v_x - \varepsilon\frac{-\psi_x}{1+\psi_x}\partial_x\left(\frac{1}{1+\psi_x}v_x\right) - \varepsilon\partial_x\left(\frac{-\psi_x}{1+\psi_x}v_x\right)\\
&\quad - \frac{-\psi_x}{1+\psi_x}\partial_x\left(\frac{1}{1+\psi_x}\partial_x\left(\frac{1}{1+\psi_x}v_x\right)\right) - \partial_x\left(\frac{-\psi_x}{1+\psi_x}\partial_x\left(\frac{1}{1+\psi_x}v_x\right)\right)\\
&\quad - \partial_x^2\left(\frac{-\psi_x}{1+\psi_x}v_x\right) - \delta\frac{\psi_x^2}{1+\psi_x}\bar{u}_x - \varepsilon\frac{-\psi_x}{1+\psi_x}\partial_x\left(\frac{-\psi_x}{1+\psi_x}\bar{u}_x\right) - \varepsilon\frac{\psi_x^2}{1+\psi_x}\bar{u}_{xx}\\
&\quad - \varepsilon\partial_x\left(\frac{\psi_x^2}{1+\psi_x}\bar{u}_x\right) - \frac{-\psi_x}{1+\psi_x}\partial_x\left(\frac{-\psi_x}{1+\psi_x}\partial_x\left(\frac{1}{1+\psi_x}\bar{u}_x\right)\right) - \frac{-\psi_x}{1+\psi_x}\partial_x^2\left(\frac{-\psi_x}{1+\psi_x}v_x\right)\\
&\quad - \frac{\psi_x^2}{1+\psi_x}\bar{u}_{xxx} - \partial_x\left(\frac{-\psi_x}{1+\psi_x}\partial_x\left(\frac{-\psi_x}{1+\psi_x}\bar{u}_x\right)\right) - \partial_x\left(\frac{\psi_x^2}{1+\psi_x}\bar{u}_{xx}\right) - \partial_x^2\left(\frac{\psi_x^2}{1+\psi_x}\bar{u}_x\right)\\
\mathcal{S} &= -v\psi_x.
\end{aligned}$$

Proof. From the definition of u above, it follows that

$$\begin{aligned}
&(1+\psi_x)\partial_t u - (\psi_t + c)\partial_x u + \partial_x f(u) + \delta\partial_x\left(\frac{1}{1+\psi_x}\partial_x u\right)\\
&\qquad + \varepsilon\partial_x\left(\frac{1}{1+\psi_x}\partial_x\left(\frac{1}{1+\psi_x}\partial_x u\right)\right)\\
&\qquad + \partial_x\left(\frac{1}{1+\psi_x}\partial_x\left(\frac{1}{1+\psi_x}\partial_x\left(\frac{1}{1+\psi_x}\partial_x u\right)\right)\right) = 0.
\end{aligned}$$

Hence, subtracting the profile equation $-c\bar{u}_x + \bar{u}_{xxxx} + \varepsilon\bar{u}_{xxx} + \delta\bar{u}_{xx} +$

$(f(\bar{u}))_x = 0$ implies

$$\begin{aligned}(\partial_t - L)v - (\psi\bar{u}_x)_t = \partial_x\mathcal{Q} - \psi_x v_t + \psi_t v_x - \delta\partial_x\left(\frac{-\psi_x}{1+\psi_x}(\bar{u}+v)_x\right)\\ - \varepsilon\partial_x\left(\frac{-\psi_x}{1+\psi_x}\partial_x\left(\frac{1}{1+\psi_x}(\bar{u}+v)_x\right)\right) - \varepsilon\partial_x^2\left(\frac{-\psi_x}{1+\psi_x}(\bar{u}+v)_x\right)\\ - \partial_x\left(\frac{-\psi_x}{1+\psi_x}\partial_x\left(\frac{1}{1+\psi_x}\partial_x\left(\frac{1}{1+\psi_x}(\bar{u}+v)_x\right)\right)\right)\\ - \partial_x^2\left(\frac{-\psi_x}{1+\psi_x}\partial_x\left(\frac{1}{1+\psi_x}(\bar{u}+v)_x\right)\right) - \partial_x^3\left(\frac{-\psi_x}{1+\psi_x}(\bar{u}+v)_x\right)\end{aligned}$$

or, equivalently,

$$\begin{aligned}(\partial_t - L)v - (\psi\bar{u}_x)_t = \partial_x\mathcal{Q} + \partial_x\mathcal{R} + \partial_t\mathcal{S} - \delta\partial_x(-\psi_x\bar{u}_x) - \varepsilon\partial_x(-\psi_x\bar{u}_{xx}) - \varepsilon\partial_x^2(-\psi_x\bar{u}_x)\\ - \partial_x(-\psi_x\bar{u}_{xxx}) - \partial_x^2(-\psi_x\bar{u}_{xx}) - \partial_x^3(-\psi_x\bar{u}_x).\end{aligned}$$

Using the fact that $\psi L\bar{u}_x = 0$ completes the proof. □

Using Lemma 3.3 and applying Duhamel's principle, recalling that $\tilde{e}(x,t;y) = 0$ for $0 \le t \le 1$, we obtain the implicit integral representation

$$v(x,t) = \bar{u}_x(x)\psi(x,t) + \int_{\mathbb{R}} G(x,t;y)v(y,0)dy + \int_0^t\int_{\mathbb{R}} G(x,t-s;y)\mathcal{N}(y,s)dy\,ds$$

for the nonlinear perturbation variable v and some function ψ still to be determined. Recalling Corollary 1, it follows that by defining ψ implicitly via the integral formula

$$\psi(x,t) = -\int_{\mathbb{R}} e(x,t;y)v(y,0)dy - \int_0^t\int_{\mathbb{R}} e(x,t-s;y)\mathcal{N}(y,s)dyds \tag{3.27}$$

the perturbation variable v must satisfy the integral equation

$$v(x,t) = \int_{\mathbb{R}} \widetilde{G}(x,t;y)v(y,0)dy + \int_0^t\int_{\mathbb{R}} \widetilde{G}(x,t-s;y)\mathcal{N}(y,s)dy\,ds. \tag{3.28}$$

Furthermore, recalling that $e(x,s;y) = 0$ for $0 \le s \le 1$, we find by differentiating (3.27) that

(3.29)

$$\partial_t^j\partial_x^k\psi(x,t) = -\int_{\mathbb{R}} \partial_t^j\partial_x^k e(x,t;y)v(y,0)dy - \int_0^t\int_{\mathbb{R}} \partial_t^j\partial_x^k e(x,t-s;y)\mathcal{N}(y,s)dy\,ds.$$

for $0 \le j \le 1$ and $0 \le k \le K+1$.

Remark 3.4. The purpose of the time cutoff function χ introduced in (3.19) is precisely to ensure that $\psi(\cdot, 0) \equiv 0$, corresponding to the fact that we are dealing with perturbations that are initially localized in space. Yet, in this periodic context it is reasonable to consider also perturbations which affect the phase or wave number of the underlying periodic profile, which corresponds to perturbations which are *not* initially localized in space. Stability of periodic wave trains to such non-localized perturbations have been the focus of much recent study; see [SSSU, JNRZ2, JNRZ3] for analysis in the context of reaction diffusion systems, and [JNRZ1] for analysis in systems with a conservative structure.

Remark 3.5. As discussed in Remark 1.4, the implicit ψ-dependent change of variables performed above has the effect of introducing at the linear level the critical non-decaying translational mode $\psi\bar{u}_x$, while at the same time ensuring that only derivatives of ψ, which decay in $L^p(\mathbb{R})$, appear in the nonlinear terms $\mathcal{N}$ in Lemma 3.3, as opposed to non-decaying terms involving ψ itself.

Equations (3.28) and (3.29) together form a complete system in the variables (v, ψ_t, ψ_x) and from the solution of this system, if it exists, we may recover the phase modulation ψ through (3.27). Furthermore, the short-time existence and continuity with respect to t of solutions $(v, \psi_t, \psi_x) \in H^K(\mathbb{R}) \times H^K(\mathbb{R}) \times H^{K+1}(\mathbb{R})$ follows from (3.26) together with (3.29) and a standard contraction-mapping argument based on (3.27), (3.22), (3.23), and the following nonlinear damping estimate.

Proposition 3.4. *Assuming (H1), there exist positive constants θ, C and ε_0 such that if v and ψ solve* (3.26) *on $[0, T]$ for some $T > 0$ and*

$$\sup_{t\in[0,T]} \|(v, \psi_x)(t)\|_{H^K(\mathbb{R})} + \sup_{t\in[0,T]} \|\psi_t(t)\|_{H^{K-1}(\mathbb{R})} \leq \varepsilon_0$$

then, for all $0 \leq t \leq T$,

(3.30)

$$\|v(t)\|^2_{H^K(\mathbb{R})} \leq Ce^{-\theta t}\|v(0)\|^2_{H^K(\mathbb{R})} + C\int_0^t e^{-\theta(t-s)} \left(\|v(s)\|^2_{L^2(\mathbb{R})} + \|\psi_x(s)\|^2_{H^{K+1}(\mathbb{R})} + \|\psi_t(s)\|^2_{H^{K-2}(\mathbb{R})} \right) ds.$$

Proof. First rewrite (3.26) as

$$\begin{aligned}
v_t + \partial_x^4 v \;=\; & -\varepsilon\partial_x^3 v - \delta\partial_x^2 v + c\partial_x v - \partial_x(f(\bar u + v) - f(\bar u)) - \frac{-\psi_x}{1+\psi_x}\partial_x(f(\bar u + v)) \\
& + \frac{\psi_t - c\psi_x}{1+\psi_x}(\bar u_x + v_x) - \delta\frac{-\psi_x}{1+\psi_x}\partial_x\left(\frac{1}{1+\psi_x}(\bar u_x + v_x)\right) - \delta\partial_x\left(\frac{-\psi_x}{1+\psi_x}(\bar u_x + v_x)\right) \\
& - \varepsilon\frac{-\psi_x}{1+\psi_x}\partial_x\left(\frac{1}{1+\psi_x}\partial_x\left(\frac{1}{1+\psi_x}(\bar u_x + v_x)\right)\right) - \varepsilon\partial_x\left(\frac{-\psi_x}{1+\psi_x}\partial_x\left(\frac{1}{1+\psi_x}(\bar u_x + v_x)\right)\right) \\
& - \varepsilon\partial_x^2\left(\frac{-\psi_x}{1+\psi_x}(\bar u_x + v_x)\right) - \frac{-\psi_x}{1+\psi_x}\partial_x\left(\frac{1}{1+\psi_x}\partial_x\left(\frac{1}{1+\psi_x}\partial_x\left(\frac{1}{1+\psi_x}(\bar u_x + v_x)\right)\right)\right) \\
& - \varepsilon\partial_x\left(\frac{-\psi_x}{1+\psi_x}\partial_x\left(\frac{1}{1+\psi_x}\partial_x\left(\frac{1}{1+\psi_x}(\bar u_x + v_x)\right)\right)\right) \\
& - \varepsilon\partial_x^2\left(\frac{-\psi_x}{1+\psi_x}\partial_x\left(\frac{1}{1+\psi_x}(\bar u_x + v_x)\right)\right) - \varepsilon\partial_x^3\left(\frac{-\psi_x}{1+\psi_x}(\bar u_x + v_x)\right).
\end{aligned}$$

By taking scalar product against $\sum_{j=0}^K (-1)^j \partial_x^j v$ and using integration by parts and Sobolev embedding $\|g\|_{L^\infty(\mathbb{R})} \le C\|g\|_{H^1(\mathbb{R})}$, we obtain under a smallness assumption as in the statement of the proposition

$$\frac{1}{2}\frac{d}{dt}\left(\|v\|^2_{H^K(\mathbb{R})}\right)(t) + \frac{1}{2}\|v(t)\|^2_{H^{K+2}(\mathbb{R})} \;\le\; C(\|v(t)\|^2_{H^{K+1}(\mathbb{R})} + \|\psi_x(t)\|^2_{H^{K+1}(\mathbb{R})} + \|\psi_t(t)\|^2_{H^{K-2}(\mathbb{R})}).$$

Using now the Sobolev inequality

$$\|g\|^2_{H^{K+1}(\mathbb{R})} \;\le\; \eta\,\|\partial_x^{K+2} g\|^2_{L^2(\mathbb{R})} + C_\eta \|g\|^2_{L^2(\mathbb{R})}$$

with a sufficiently small η reduces the result to a simple integration. □

3.4 Nonlinear iteration

With the above preparations in hand, we are now prepared to state the main technical lemma leading to the proof of Theorem 1.1. For this purpose, associated with the solution (v, ψ_t, ψ_x) of the integral system (3.28) and (3.29) considered in the previous section, define

$$\eta(t) := \sup_{0\le s\le t} \|(v, \psi_t, \psi_x, \psi_{xx})(s)\|_{H^K(\mathbb{R})}\,(1+s)^{1/4}. \tag{3.31}$$

By standard short-time $H^K(\mathbb{R})$ existence theory, η is continuous so long as it remains sufficiently small. Using the linearized estimates of Section 3.2 we now prove that if $\eta(0)$ is small then $\eta(t)$ remains small for all $t > 0$.

Lemma 3.6. *Under assumptions (H1)–(H4) and (D1)–(D3), there exist positive constants C and ε_0 such that if $v(0)$ is such that*

$$E_0 := \|v(0)\|_{L^1(\mathbb{R})\cap H^K(\mathbb{R})} \leq \varepsilon_0 \quad \textit{and} \quad \eta(T) \leq \varepsilon_0$$

for some $T > 0$, then for all $0 \leq t \leq T$ we have

$$\eta(t) \leq C(E_0 + \eta(t)^2). \tag{3.32}$$

Proof. First, note that by Lemma 3.3, we have under the smallness assumption on η that

$$\|(\mathcal{Q}, \mathcal{R}, \mathcal{S})(t)\|_{L^1(\mathbb{R})\cap L^2(\mathbb{R})} \leq C\eta(t)^2(1+t)^{-1/2} \tag{3.33}$$

for some constant $C > 0$. The contribution of $\partial_t \mathcal{S}$ needs some special care. For this purpose, note that, integrating by parts in critical contribution, we obtain from previous linear bounds and $\mathcal{S}(0) = 0$

$$\begin{aligned}\left\| \int_0^t \int_{\mathbb{R}} \tilde{G}(\cdot, t-s; y)\partial_s \mathcal{S}(y,s)dy\, ds \right\|_{L^p(\mathbb{R})} &\leq C\|\mathcal{S}(t)\|_{L^2(\mathbb{R})} + C\int_0^t e^{-\theta(t-s)}\|\partial_t \mathcal{S}(s)\|_{H^1(\mathbb{R})}ds \\ &\quad + C\int_0^t (1+t-s)^{-\frac{1}{2}\left(1-\frac{1}{p}\right)-\frac{1}{2}}\|\mathcal{S}(s)\|_{L^1(\mathbb{R})}ds.\end{aligned}$$

Now, observe that, using (3.26) to bound v_t, we have under the same smallness assumption the estimate

$$\|\mathcal{S}(t)\|_{H^1(\mathbb{R})} \leq C\eta(t)^2(1+t)^{-1/2}. \tag{3.34}$$

Using then the second part of (3.20) and (3.21) to bound other terms, we obtain from (3.28) the estimate

(3.35)

$$\begin{aligned}\|v(t)\|_{L^p(\mathbb{R})} &\leq C\,(1+t)^{-\frac{1}{2}\left(1-\frac{1}{p}\right)}\,(E_0 + \eta(t)^2) \\ &\quad + C\eta(t)^2\int_0^t (t-s)^{-\frac{1}{4}\left(\frac{1}{2}-\frac{1}{p}\right)-\frac{1}{4}}\,(1+t-s)^{-\frac{1}{4}\left(\frac{3}{2}-\frac{1}{p}\right)-\frac{1}{4}}\,(1+s)^{-\frac{1}{2}}ds \\ &\leq C_p\left(E_0 + \eta(t)^2\right)(1+t)^{-\frac{1}{2}\left(1-\frac{1}{p}\right)}\end{aligned}$$

and similarly, using (3.22) and (3.23) with $q = 1$, we obtain from (3.29) the estimate

(3.36)

$$\begin{aligned}\|(\psi_t, \psi_x)\|_{W^{K+1,p}(\mathbb{R})} &\leq C(1+t)^{-\frac{1}{2}(1-\frac{1}{p})}E_0 \\ &\quad + C\eta(t)^2\int_0^t (1+t-s)^{-\frac{1}{2}(1-1/p)-\frac{1}{2}}\,(1+s)^{-1/2}ds \\ &\leq C_p\left(E_0 + \eta(t)^2\right)(1+t)^{-\frac{1}{2}\left(1-\frac{1}{p}\right)},\end{aligned}$$

valid for all[15] $2 \le p < \infty$. The assumed smallness guarantees that we may apply Proposition 3.4 and get

$$\begin{aligned}\|v(t)\|_{H^K(\mathbb{R})}^2 &\le Ce^{-\theta t}E_0^2 + C(E_0+\eta(t)^2)^2\int_0^t e^{-\theta(t-s)}(1+s)^{-1/2}ds\\ &\le C\left(E_0+\eta(t)^2\right)^2(1+t)^{-1/2}.\end{aligned}$$

Together with (3.36), this completes the proof. □

Proof of Theorem 1.1. We are free to assume the constant C in (3.32) is larger than 1. Since η is continuous and $\eta(0) = \|v(0)\|_{H^K(\mathbb{R})} \le E_0$, it follows by continuous induction that if $4C^2E_0 < 1$ then $\eta(t) \le 2CE_0$ for all $t \ge 0$. We may then use (3.35) and (3.36) to get uniform bounds for $p \in [2,4]$

$$\|v(t)\|_{L^p(\mathbb{R})} + \|(\psi_t,\psi_x)(t)\|_{W^{K+1,p}(\mathbb{R})} \le CE_0(1+t)^{-\frac{1}{2}\left(1-\frac{1}{p}\right)}.$$

Next, we rewrite $\mathcal{R}$ in form

$$\begin{aligned}\mathcal{R} &= \mathcal{R}_1 + \partial_x\mathcal{R}_2 + \partial_x^2\mathcal{R}_3 + \partial_x^3\mathcal{R}_4,\\ \mathcal{R}_j(x,t) &= \mathcal{R}_j^{(0)}(x,\psi_x(x,t),\psi_{xx}(x,t),\psi_{xxx}(x,t),\psi_{xxxx}(x,t))\\ &\quad + \mathcal{R}_j^{(1)}(x,\psi_x(x,t),\psi_{xx}(x,t),\psi_{xxx}(x,t),\psi_{xxxx}(x,t))v(x,t)\end{aligned}$$

so that

$$\|(\mathcal{Q},\mathcal{R}_1,\mathcal{R}_2,\mathcal{R}_3,\mathcal{R}_4,\mathcal{S})(t)\|_{L^2(\mathbb{R})} \le C(\|v(t)\|_{L^4(\mathbb{R})}^2 + \|(\psi_t,\psi_x)(t)\|_{W^{K+1,4}(\mathbb{R})}^2) \le CE_0(1+t)^{-\frac{3}{4}}$$

and

$$\left\|(\partial_x\mathcal{Q},\partial_x\mathcal{R}_1,\partial_x^2\mathcal{R}_2,\partial_x^3\mathcal{R}_3,\partial_x^4\mathcal{R}_4,\partial_t\mathcal{S})(t)\right\|_{H^1(\mathbb{R})} \le CE_0(1+t)^{-\frac{1}{2}}.$$

Using now the estimate

$$\begin{aligned}\left\|\int_0^t\int_{\mathbb{R}}\tilde{G}(\cdot,t-s;y)\partial_s\mathcal{S}(y,s)dy\,ds\right\|_{L^p(\mathbb{R})} &\le C\|\mathcal{S}(t)\|_{L^2(\mathbb{R})} + C\int_0^t e^{-\theta(t-s)}\|\partial_t\mathcal{S}(s)\|_{H^1(\mathbb{R})}ds\\ &\quad + C\int_0^t(1+t-s)^{-\frac{1}{2}\left(\frac{1}{2}-\frac{1}{p}\right)-\frac{1}{2}}\|\mathcal{S}(s)\|_{L^2(\mathbb{R})}ds,\end{aligned}$$

[15] Notice the above integral estimates fail in the case $p = \infty$ due to a term of size $\log(1+t)$ arising from integrating on $\left[\frac{t}{2},t\right]$.

together with the first part of (3.20) and (3.21), we obtain for all $p \in [2, \infty]$

$$\begin{aligned}\|v(t)\|_{L^p(\mathbb{R})} &\leq C(1+t)^{-\frac{1}{2}\left(1-\frac{1}{p}\right)}E_0 + CE_0\int_0^t (1+t-s)^{-\frac{1}{2}\left(\frac{1}{2}-\frac{1}{p}\right)-\frac{1}{2}}(1+s)^{-\frac{3}{4}}ds \\ &\leq CE_0(1+t)^{-\frac{1}{2}\left(1-\frac{1}{p}\right)}\end{aligned}$$

and, similarly, using (3.22) with $q = 2$ and (3.23) both with $q = 1$ and $q = 2$ we obtain the estimate

$$\begin{aligned}\|(\psi_t, \psi_x)(t)\|_{W^{K+1,p}(\mathbb{R})} &\leq C(1+t)^{-\frac{1}{2}\left(1-\frac{1}{p}\right)}E_0 + CE_0\int_0^t (1+t-s)^{-\frac{1}{2}\left(\frac{1}{2}-\frac{1}{p}\right)-\frac{1}{2}}(1+s)^{-\frac{3}{4}}\,ds \\ &\leq CE_0(1+t)^{-\frac{1}{2}\left(1-\frac{1}{p}\right)}.\end{aligned}$$

This completes the proof of (1.20).

To establish (1.21), note that (3.22) and (3.23) imply

$$\|\psi(t)\|_{L^\infty(\mathbb{R})} \leq CE_0 + CE_0^2\int_0^t (1+t-s)^{-\frac{1}{2}\left(1-\frac{1}{p}\right)}(1+s)^{-\frac{1}{2}}ds \leq CE_0.$$

Finally, notice that by definition we have that

$$\tilde{u}(x,t) - \bar{u}(x) = v(x,t) + (\tilde{u}(x,t) - \tilde{u}(x+\psi(x,t),t)),$$

hence

$$\|\tilde{u}(t) - \bar{u}\|_{L^\infty(\mathbb{R})} \leq \|v(t)\|_{L^\infty(\mathbb{R})} + \|\bar{u}_x\|_{L^\infty([0,1])}\|\psi(t)\|_{L^\infty(\mathbb{R})} \leq CE_0.$$

We thus obtain the final $L^1 \cap H^K \to L^\infty$ bound (1.21) of Theorem 1.1. This completes the proof of the main theorem, hence establishing the nonlinear $L^1 \cap H^K \to L^\infty$ stability of the underlying periodic traveling wave $\bar{u}$ under the structural and spectral assumptions (H1)–(H4) and (D1)–(D3).

Acknowledgement: The numerical stability computations in this paper were carried out using the STABLAB package developed by Jeffrey Humpherys and the first and last authors and the SpectrUW package developed by Bernard Deconinck and collaborators; see [BHZ2, CDKK] for documentation. We gratefully acknowledge their contribution. We thank also Indiana University Information Technology Service for the use of the Quarry computer with which some of our computations were carried out.

A Appendix: Survey of existence theory for generalized KS

In this appendix we give a brief survey of the existence theory for periodic traveling wave solutions of the generalized Kuramoto-Sivashinsky equation (1.1) with nonlinearity $f(u) = 3u^2$. For the forthcoming discussion we will also consider the particular scaling where $\gamma = \delta$, i.e. the equation

$$u_t + 6uu_x + \varepsilon\partial_x^3 u + \delta(\partial_x^2 u + \partial_x^4 u) = 0. \tag{A.1}$$

Under this scaling, there are three situations to consider: the rather generic case where $\varepsilon = 1$ and $\delta = \mathcal{O}(1)$; the classic Kuramoto-Sivashinsky limit $\delta = 1$ and $|\varepsilon| \ll 1$ and the (integrable) Korteweg-de Vries (KdV) limit $\varepsilon = 1$ and $0 < \delta \ll 1$. In the first two cases, we obtain only existence of small amplitude periodic wave trains through a normal form approach whereas we obtain existence of large amplitude periodic traveling waves in the KdV limit, by using Fenichel theory.

A.1 The generic case: Hopf bifurcation analysis

Traveling waves $u(x,t) = U(x - ct)$ of (A.1) are then readily seen to be solutions of the ODE

$$\delta(U''' + U') + \varepsilon U'' + 3U^2 - cU = q, \tag{A.2}$$

where $q \in \mathbb{R}$ is a constant of integration. We begin by considering the generic situation where $\varepsilon > 0$ and $\delta \neq 0$ are fixed and arbitrary. In this case, so long as $c^2 + 12q > 0$, (A.2) possess two stationary solutions $U_-(c,q) < U_+(c,q)$ such that $3U_\pm^2 - cU_\pm = q$. Linearizing (A.2) about a constant state $U = U_\pm$ thus yields

$$(6U_\pm - c)\tilde{U} + \varepsilon\tilde{U}'' + \delta\big(\tilde{U}' + \tilde{U}'''\big) = 0, \tag{A.3}$$

which is seen to undergo a Hopf bifurcation (necessarily) at U_+ when $c_{\text{Hopf}}(q) = 6U_+ - \varepsilon$. Denoting $V = U - U_+$ and $6U_+ - c = \varepsilon + \mu$ with $|\mu| \ll 1$, equation (A.2) then reads

$$(3V + \varepsilon + \mu)V + \varepsilon V'' + \delta(V' + V''') = 0, \tag{A.4}$$

from which we find, for sufficiently small μ on one side of zero, a family $V(\mu)$ of periodic orbits with amplitude $\mathcal{O}(|\mu|^{1/2})$ and frequency $k(\mu)$, with $k(0) = 1$ and $k'(0) \neq 0$. As a result, in the neighborhood of the Hopf

bifurcation we find a three dimensional manifold of small amplitude periodic traveling waves parameterized by translation, the wavenumber k, and the integration constant q.

Remark A.1. Note that when $c^2+12q = 0$, the equilibrium states coincide. The nature of the bifurcation occurring at this degenerate point requires a more delicate normal form analysis, which we postpone to the next section.

Finally, notice that for $|\mu| \ll 1$ the solution U of (A.2) satisfies

$$U = \langle U \rangle + \mathcal{O}(|\mu|^{1/2}),$$

where $\langle U \rangle$ denotes the spatial mean of U over a period, so that, by the definition of q, we find

$$3 \langle U \rangle^2 - c \langle U \rangle = q + \mathcal{O}(|\mu|^{1/2}).$$

Setting $M(k, q) = \langle U \rangle$ it follows that $\partial_q M$ is non-zero by the definition of μ. Here, we are using that $\varepsilon > 0$ is fixed. In particular, in a neighborhood of the Hopf bifurcation, we can switch from the (k, q) parametrization of the local manifold of periodic traveling waves (here identified up to translation) to the (k, M) parametrization; see Remark 1.3. This provides the following proposition.

Proposition A.2. *Let $M \in \mathbb{R}$ be fixed and $k < 1$ be such that $1 - k$ is small. Then there exist a unique $c(k, M)$ and a unique $q(k, M)$ such that there exists a 1-periodic $U(\,\cdot\,; k, M)$ solution of*

$$k\left(3U^2 - cU\right) + \varepsilon k^3 U'' + \delta\left(k^2 U' + k^4 U'''\right) \;=\; q, \quad \langle U \rangle = M \;. \tag{A.5}$$

Moreover this solution is unique up to translation.

A.2 The classic KS limit: a normal form analysis

Here, we complement the above bifurcation analysis in the previous section with a normal form analysis near the degenerate case $|\varepsilon| \ll 1$. In order to find periodic solutions, we necessarily work in the neighborhood of $0 < c^2 + 12q \ll 1$. Setting $V = U - U_+$ then we see that V must satisfy (A.4) which we can rewrite here as the first order differential system

$$\begin{pmatrix} x' \\ y' \\ z' \end{pmatrix} = \begin{pmatrix} 0 & 1 & 0 \\ -1 & 0 & 0 \\ 0 & 0 & 0 \end{pmatrix} \begin{pmatrix} x \\ y \\ z \end{pmatrix} + \mu(x+z) \begin{pmatrix} 1 \\ 0 \\ -1 \end{pmatrix} + \varepsilon z \begin{pmatrix} 1 \\ 0 \\ -1 \end{pmatrix} + 6(x+z)^2 \begin{pmatrix} 1 \\ 0 \\ -1 \end{pmatrix} \tag{A.6}$$

where $x = 2V + V''$, $y = V'$, $z = V + V''$, and $\varepsilon > 0$ and μ are small.

Next we compute the normal form of (A.6). By finding an appropriate change of variables of the form

$$(x, y, z) = (Id + \mu T_1 + \varepsilon T_2 + Q)(\tilde{x}, \tilde{y}, \tilde{z})$$

where the T_i are linear operators and Q a quadratic vector field, we obtain after a lengthy but straightforward computation

$$\begin{aligned} \tilde{x}' &= \tilde{y} + \mu\tilde{x}/2 + \Gamma\tilde{x}\tilde{z} + \mathcal{O}(3) \\ \tilde{y}' &= -\tilde{x} + \mu\tilde{y}/2 + \Gamma\tilde{y}\tilde{z} + \mathcal{O}(3) \\ \tilde{z}' &= -(\varepsilon + \mu)\tilde{z} - \Gamma\big(\tilde{z}^2 + (\tilde{x}^2 + \tilde{y}^2)/2\big) + \mathcal{O}(3). \end{aligned} \tag{A.7}$$

where $\mathcal{O}(3)$ denotes terms cubic order or higher terms. Finally, using polar coordinates $r^2 = \tilde{x}^2 + \tilde{y}^2$ and $\theta = \cos^{-1}\left(\frac{\tilde{x}}{r}\right)$, and dropping all resulting $\mathcal{O}(3)$ terms we obtain the normal form

$$\begin{aligned} r' &= \mu\frac{r}{2} + \Gamma r z \\ z' &= -(\varepsilon + \mu)z - \Gamma\big(z^2 + \frac{r^2}{2}\big) \\ \theta' &= -1 \end{aligned} \tag{A.8}$$

valid in a neighborhood of $(\varepsilon, \mu) = (0, 0)$.

The dynamics of the normal form equation (A.8) is quite easy to describe. In the corresponding three dimensional phase plane we find two fixed points in the r-z plane with $r = 0$: namely, $(r, z) = (0, 0)$ and $(r, z) = (0, -(\varepsilon + \mu)/\Gamma)$. By definition, these correspond to the steady solutions $U_\pm$ of the original system (A.2). The Jacobian matrix J at these points are, respectively,

$$J(0,0) = \begin{pmatrix} \mu/2 & 0 \\ 0 & -(\varepsilon+\mu) \end{pmatrix} \text{ and } J\left(0, \frac{-(\varepsilon+\mu)}{\Gamma}\right) \begin{pmatrix} -\varepsilon - \mu/2 & 0 \\ 0 & \varepsilon + \mu \end{pmatrix}.$$

Furthermore, nontrivial stationary solutions of (A.8) in the r-z plane exist only if $\mu^2 + 2\mu\varepsilon$ is positive, in which case there is only one possible stationary point P given by

$$(r, z) = \left(\sqrt{\frac{\mu^2 + 2\varepsilon\mu}{2\Gamma^2}}\,, -\frac{\mu}{2\Gamma}\right),$$

which is a non-trivial stationary solution of (A.8) corresponding to a periodic solution to the original system (A.2). We readily find that the trace and

determinant of the Jacobian matrix J_P are

$$\mathrm{tr}(J_P) = -\varepsilon, \quad \det(J_P) = \frac{\mu^2 + 2\varepsilon\mu}{2}$$

so that the periodic point P undergoes a Hopf bifurcation (in the r-z plane) at $\varepsilon = 0$, which corresponds precisely to the Kuramoto-Sivashinsky equation. To determine whether it is a sub or supercritical bifurcation, one would need to compute higher order terms in the normal form, which is beyond the scope of this paper. These periodic orbits emerging from P in the r-z plane correspond to quasiperiodic solutions of the original system (A.2).

Finally, note that in [CD] a similar normal form was derived in the case when $\varepsilon = 0$, corresponding to the "classic" KS equation of the form

$$\tilde{r}' = -\tilde{\mu}\tilde{r}/2 + 2\tilde{r}\tilde{z}, \quad \tilde{z}' = \tilde{\mu}\tilde{z} - 2\tilde{z}^2 - 4\tilde{r}^2, \quad \theta' = 1$$

from which we can recover (A.8) in this case by a simple rescaling. In both cases, if $\det(J_P) = \frac{\mu^2+2\varepsilon\mu}{2} \neq 0$, a straightforward application of the implicit function theorem shows that the point P, corresponding to a periodic wave train of (A.1), persists under higher order perturbations.

We further note that in [CD] a full family of periodic solutions to (A.8) for the Poincaré return map around the point P and ending with a solitary wave was found. However, it was not proved that such a family of quasi periodic solutions persists under higher order perturbations. This is not surprising since we are precisely at the Hopf bifurcation point and ε is the additional parameter needed in KS to carry out a codimension 2 bifurcation analysis. In contrast when $0 < |\varepsilon| \ll 1$, there is a selection of the periodic orbit of the Poincaré return map and this structure persists for higher order perturbations.

Let us mention that the full bifurcation analysis for KS is far more complicated: indeed Kent and Elgin [KE] proved the occurrence of a Shi'lnikov bifurcation which leads to cascades of period doubling, period multiplying k-bifurcations and oscillatory homoclinic as period is increased. The computation of the bifurcation diagram was also investigated numerically for KS [BKJ] and work is still in progress to carry out a similar program for gKS by using AUTO continuation software.

A.3 The KdV limit: singular perturbation analysis

We finally conclude our survey of relevant existence results for periodic traveling wave solutions of (A.1) by considering a particular singular limit arising

in applications to pattern formation analysis. In this context, it is usually assumed that $\varepsilon = 1$ and $0 < \delta \ll 1$ in which case (A.1) can be treated as a singular perturbation of the integrable KdV equation

$$u_t + uu_x + u_{xxx} = 0. \tag{A.9}$$

As is well known, (A.9) admits a four parameter family of periodic traveling wave solutions of the form

(A.10)

$$U_{\mathrm{KdV}}(x - c(u_0,\kappa,p)t; x_0, u_0, \kappa, p) = u_0 + 12p^2\kappa^2 \,\mathrm{cn}^2\left(\kappa(x - x_0 - c(u_0,\kappa,p)t), p\right)$$

with wave speed $c(u_0,\kappa,p) := 8\kappa^2p^2 - 4\kappa^2 + u_0$, where $\mathrm{cn}(\cdot,p)$ denotes the standard Jacobi elliptic cosine function with elliptic modulus $p \in [0,1)$, and x_0, u_0, and κ are arbitrary real numbers corresponding, respectively, to the translation, Galilean, and scaling symmetries of the KdV equation (A.9).

Here, we are interested in the continuation of these explicit solutions to the KdV equation in the singular limit $\delta \to 0^+$ in (A.1). In this limit, it was shown in [EMR], by using Fenichel theory, that periodic solutions to (A.1) remain close to the above elliptic function solutions of the KdV and, in particular, an expansion of these solutions with respect to δ was obtained. Furthermore, we point out that in [BaN] a formal spectral analysis of these perturbed KdV waves was conducted. We now briefly describe the associated expansions of the periodic traveling waves in the limit $\delta \to 0^+$; see [EMR, BaN, NR2, JNRZ4] for more details.

Without loss of generality, we can restrict to zero-mean solutions of (A.1). We seek an expansion of the associated periodic traveling wave solution of the form

$$U^\delta(x,t) = U_{\mathrm{KdV}}(x,t; x_0, u_0^*, \kappa, p) + \delta\tilde{U}(x,t) + \mathcal{O}(|\delta|^2)$$

where u^* is chosen so that the mean of U_{KdV} over one spatial period vanishes. Notice at order δ^0 the parameters p and κ are completely arbitrary, yielding a three parameter family of periodic traveling wave solutions of (A.9) with zero mean. When $0 < \delta \ll 1$ however, we expect only a *two* parameter family to persist, hence we expect a selection principle to manifest itself at the next order between the parameters p and κ.

At the next order one finds that the first-order correction $\tilde{U}$ must satisfy the equation

$$\kappa^2\tilde{U}''' + (6U_{\mathrm{KdV}}\tilde{U} - c(u_0^*,\kappa,p)\tilde{U})' - \tilde{c}_1 U'_{\mathrm{KdV}} + \kappa U''_{\mathrm{KdV}} + \kappa^3 U''''_{\mathrm{KdV}} = 0, \tag{A.11}$$

where $\tilde{c}_1$ denotes the first order δ-correction to the wave speed of U^δ. As the linear operator

$$\mathcal{L} := \kappa^2 \frac{d^3}{dx^3} + \frac{d}{dx}\left((6U_{\rm KdV} - c(u_0^*, \kappa, p)).\right)$$

has Fredholm index 0 and the kernel of its adjoint operator is spanned by constant functions and $U_{KdV}(\cdot; x_0, u_0^*, \kappa, p)\}$, it follows that (A.11) will have a solution precisely when the solvability condition

$$\left\langle \left(U'_{\rm KdV}\right)^2 \right\rangle = \kappa^2 \left\langle \left(U''_{\rm KdV}\right)^2 \right\rangle \tag{A.12}$$

is satisfied. Condition (A.12) yields an explicit selection principle between the elliptic modulus p and the scaling parameter κ and, as a result, we find for $0 < \delta \ll 1$ a two-parameter family of periodic traveling wave solutions of (A.1) parameterized by translation and the elliptic modulus p or, equivalently, by translation and period.

Coming back to the more general case where we allow $U_{\rm KdV}$ to have nonzero mean, we have obtained for $0 < \delta \ll 1$ a three dimensional manifold of periodic traveling wave solutions of (A.1) parameterized by translation, period, and spatial mean over a period.

The numerical tests carried out here and in [CDK] suggests that there are finite limit for lower and upper bounds of stability as $\delta \to 0$, in agreement with results predicted by formal singular perturbation analysis in [BaN]. The purpose of the recent work [JNRZ4], although still finally relying on elliptic integrals numerical computations of [BaN], is precisely to go a step further towards a complete analytic proof of these observations.

B Appendix: The Swift-Hohenberg equation

In this appendix, we demonstrate a streamlined proof that spectrally modulationally stable periodic traveling wave solutions of the Swift-Hohenberg equation (1.3) are nonlinearly stable to small localized perturbations. While this problem has been previously solved by Schneider in [Sc] by using a combination of weighted energy estimates, renormalization theory, and spectacular nonlinear cancellation technique, all carried out in the Bloch frequency domain, our nonlinear analysis rather relies on spatial domain techniques developed in [OZ4, JZ1, JZ3] in the context of systems of viscous conservation laws. We also carry out a numerical spectral stability analysis, demonstrating generality of our techniques. In particular, in a specific parameter regime we obtain nice agreement with stability curves found by Mielke [M1].

B.1 Setup and main result

The traveling wave solutions of (1.3) are stationary solutions of the PDE

$$\partial_t u - c\partial_x u + (1+\partial_x^2)^2 u - ru + f(u) = 0 \tag{B.1}$$

for some wave speed $c \in \mathbb{R}$, i.e. they are solutions of the traveling wave ODE

$$-cu' + u'''' + 2u'' + (1-r)u + f(u) = 0. \tag{B.2}$$

Due to the presence of the non-conservative terms, this equation can not be further integrated, hence the orbits of (B.2) lie in the phase space $\mathbb{R}^4$. In particular, it follows that periodic orbits u of (B.2) correspond to values $(b, c, X) \in \mathbb{R}^6$, where $X, c \in \mathbb{R}$ denote the period and speed, respectively, and the vector $b = (b_1, b_2, b_3, b_4)$ denotes the values of (u, u', u'', u''') at $x = 0$ such that

$$(u, u', u'', u''')(X; b, c) = b,$$

where $(u, u', u'', u''')(\cdot; b, c)$ is the unique solution of (B.2) so that $(u, u', u'', u''')(0; b, c) = b$. As usual then, we make the following technical assumptions:

(H1') $f \in C^K$, $K \geq 5$.

(H2') The map $H : \mathbb{R}^6 \to \mathbb{R}^4$ taking $(b, c, X) \mapsto (u, u', u'', u''')(X; b, c) - b$ is full rank at $(\bar{b}, \bar{c}, \bar{X})$.

By the Implicit Function Theorem, conditions (H1')–(H2') imply that the set of periodic solutions of (1.3) in the vicinity of $\bar{u}$, with parameters $(\bar{b}, \bar{c}, \bar{X})$, forms a smooth 2-dimensional manifold

$$\{\ (x,t) \mapsto U(x - \alpha - c(\beta)t; \beta) \mid (\alpha, \beta) \in \mathbb{R} \times \mathcal{I}\ \}, \quad \text{with } \mathcal{I} \subset \mathbb{R}.$$

In particular, in contrast to the Kuramoto-Sivashinsky equation (1.2), the lack of conservative structure implies a loss in dimension of the periodic solution manifold. As we will see, this has the effect that there are no longer "enough" periodic orbits around to make variations in wave speed an admissible perturbation, hence the corresponding linearization does not have a (co-periodic) Jordan block at the origin.

Remark B.1. As noted in [JZN], transversality, (H2'), is necessary for our notion of spectral stability hence there is no loss of generality in making this assumption.

To begin our stability analysis we consider the linearization of (B.1) about a fixed $\bar{X}$-periodic traveling wave solution $\bar{u} = u(\cdot; \bar{b}, \bar{c})$. Here we assume without loss of generality $\bar{X} = 1$. To this end, consider a nearby solution of (B.1) of the form $\bar{u}(x)+v(x,t)$ with v small. Directly substituting this into (B.1) and neglecting quadratic order terms in v leads us to the linearized equation $(\partial_t - L)v = 0$ with

$$Lv := cv_x - v_{xxxx} - 2v_{xx} + (r-1)v - f'(\bar{u})v. \tag{B.3}$$

Introducing the one-parameter family of Bloch operators

$$L_\xi := e^{-i\xi x} L e^{i\xi x}, \;\; \xi \in [-\pi, \pi)$$

operating on $L^2_{\text{per}}([0,1])$ parameterizes the spectrum of L as

$$\sigma_{L^2(\mathbb{R})}(L) = \bigcup_{\xi\in[-\pi,\pi)} \sigma_{L^2_{\text{per}}([0,1])}(L_\xi).$$

Thus, we assume the following spectral stability conditions:

(D1') $\sigma(L) \subset \{\lambda \in \mathbb{C} | \text{Re}(\lambda) < 0\} \cup \{0\}$.

(D2') $\sigma(L_\xi) \subset \left\{\lambda \in \mathbb{C} \middle| \text{Re}(\lambda) \leq -\theta|\xi|^2\right\}$, for some $\theta > 0$ and any $\xi \in [-\pi, \pi)$.

(D3') $\lambda = 0$ is a simple eigenvalue of L_0.

By standard spectral perturbation theory [K], (D3') implies that the critical eigenvalue $\lambda(\xi)$ bifurcating from $\lambda = 0$ at $\xi = 0$ is analytic in ξ. In particular, under assumption (D2') and the symmetry $\lambda(\xi) = \overline{\lambda(-\xi)}$, the $\lambda(\xi)$ admits an expansion as $\xi \to 0$ of the form

$$\lambda(\xi) = -ia\xi - b\xi^2 + \mathcal{O}(|\xi|^3), \quad a \in \mathbb{R}, \quad b > 0. \tag{B.4}$$

Remark B.2. More generally, assume that a real valued, periodic coefficient differential operator $\mathcal{L}$ whose essential spectrum near the origin admits a Bloch representation as a single analytic curve of the form $\lambda(\xi) = \sum_{j\in\mathbb{N}} \alpha_j \xi^j$. Then the symmetry $\lambda(\xi) = \overline{\lambda(-\xi)}$ implies that $\alpha_{2j} \in \mathbb{R}$ and $\alpha_{2j+1} \in i\mathbb{R}$ for each $j \in \mathbb{N}$. Finally, we note that this observation is related to properties of the associated Whitham modulation equations as well; see [JNRZ1] for details.

With these preparations in hand, we now state the main theorem of this appendix.

Theorem B.1. *Let $\bar{u}$ be any steady 1-periodic solution of* (B.1) *such that (H1')–(H2') and (D1')–(D3') hold. Then there exist constants $\varepsilon_0 > 0$ and $C > 0$ such that for any $\tilde{u}_0$ with $\|\tilde{u}_0 - \bar{u}\|_{L^1(\mathbb{R})\cap H^K(\mathbb{R})} \le \varepsilon_0$, where K is as in assumption (H1'), there exist $\tilde{u}$ a solution of* (B.1) *satisfying $\tilde{u}(\cdot,0) = \tilde{u}_0$ and a function $\psi(\cdot,t) \in W^{K,\infty}(\mathbb{R})$ such that for all $t \ge 0$ and $2 \le p \le \infty$ we have the estimates*

(B.5)

$$\begin{aligned}
\|\tilde{u}(\cdot+\psi(\cdot,t),t) - \bar{u}(\cdot)\|_{L^p(\mathbb{R})} &\le C\,(1+t)^{-\frac{1}{2}\left(1-\frac{1}{p}\right)-\frac{1}{2}}\,\|\tilde{u}(\cdot,0)-\bar{u}(\cdot)\|_{L^1(\mathbb{R})\cap H^K(\mathbb{R})}\,,\\
\|(\psi_t,\psi_x)(\cdot,t)\|_{L^p(\mathbb{R})} &\le C\,(1+t)^{-\frac{1}{2}\left(1-\frac{1}{p}\right)-\frac{1}{2}}\,\|\tilde{u}(\cdot,0)-\bar{u}(\cdot)\|_{L^1(\mathbb{R})\cap H^K(\mathbb{R})}\,,\\
\|\tilde{u}(\cdot+\psi(\cdot,t),t) - \bar{u}(\cdot)\|_{H^K(\mathbb{R})} &\le C\,(1+t)^{-\frac{3}{4}}\,\|\tilde{u}(\cdot,0)-\bar{u}(\cdot)\|_{L^1(\mathbb{R})\cap H^K(\mathbb{R})}\,,\\
\|(\psi_t,\psi_x)(\cdot,t)\|_{H^K(\mathbb{R})} &\le C\,(1+t)^{-\frac{3}{4}}\,\|\tilde{u}(\cdot,0)-\bar{u}(\cdot)\|_{L^1(\mathbb{R})\cap H^K(\mathbb{R})}\,.
\end{aligned}$$

Moreover, we have the $L^1(\mathbb{R}) \cap H^K(\mathbb{R}) \to L^p(\mathbb{R})$, $2 \le p \le \infty$, nonlinear stability estimate

(B.6)

$$\|\tilde{u}(\cdot,t) - \bar{u}(\cdot)\|_{L^p(\mathbb{R})}\,,\ \ \|\psi(\cdot,t)\|_{L^p(\mathbb{R})} \le C\,(1+t)^{-\frac{1}{2}\left(1-\frac{1}{p}\right)}\,\|\tilde{u}(\cdot,0)-\bar{u}(\cdot)\|_{L^1(\mathbb{R})\cap H^K(\mathbb{R})}$$

valid for all $t \ge 0$.

The outline of the proof is as follows. Given a fixed periodic solution $\bar{u}(x)$ of the traveling wave ODE (B.2), nearby solutions of the traveling SH equation (B.1) $\tilde{u}$ are investigated by defining a nonlinear perturbation variable

$$v(x,t) := \tilde{u}(x+\psi(x,t),t) - \bar{u}(x), \tag{B.7}$$

where $\psi : \mathbb{R}\times\mathbb{R}_+ \to \mathbb{R}$ is a spatial-temporal phase modulation ψ to be chosen later such that $\psi(\cdot,0) \equiv 0$, corresponding to perturbations which are initially spatially localized. By a direct calculation, we find that (B.1) is then written

$$(\partial_t - L)\,(v - \bar{u}_x\psi) = \mathcal{N}[v,\psi]$$

where L is the linearized operator defined in (B.3) and $\mathcal{N}$ denotes a nonlinear remainder term depending on derivatives of v and ψ: see (B.15) below. By an application of Duhamel's principle, it follows that (B.1) reads

$$v(\cdot,t) - \bar{u}_x\psi(\cdot,t) = e^{Lt}v(\cdot,0) + \int_0^t e^{L(t-s)}\mathcal{N}[v,\psi](\cdot,s)ds. \tag{B.8}$$

Of course, we need then a detailed study of the linearized solution operator e^{Lt}. In the present periodic context, this is complicated by the fact that the spectrum of L agrees with the essential spectrum and contains a spectral curve touching the imaginary axis. We are thus led to separate the exponentially-stable spectrum from this low-Floquet critical curve for which, at best, one should only expect polynomial decay of small perturbations. A full separation at the linear level would lead to a separation of the nonlinear equation into a decay-critical equation and an exponentially-slaved equation. Although we perform the linear separation only in an approximate way, the purpose of the introduction of ψ is to ensure that $\psi\bar{u}_x$ contains at the linear level the main contribution of the algebraically decaying part of the semigroup, decay of v being essentially slaved.

B.2 Linearized estimates

We begin our analysis deriving decay rates for the semigroup e^{Lt} of the linearized operator L defined in (B.3). With the inverse Bloch transform representation (1.13) of the solution operator in mind, we begin by making more precise the statements about the critical curve. Since 0 is separated from the rest of the spectrum of L_0, we first note that by standard spectral perturbation theory [K], assumption (D3') implies that there exist $\xi_0 \in]0,\pi[$, $\varepsilon_0 > 0$, an analytic curve $\lambda : [-\xi_0,\xi_0] \to B(0,\varepsilon_0)$ such that, when $|\xi| \leq \xi_0$, $\sigma(L_\xi) \cap B(0,\varepsilon_0) = \{\lambda(\xi)\}$. and, when $|\xi| \leq \xi_0$, dual right and left eigenfunctions $q(\xi,\cdot)$ and $\tilde{q}(\xi,\cdot)$ of L_ξ associated with $\lambda(\xi)$, analytic in ξ and such that $q(0,\cdot) = \bar{u}_x$. We may thus define the critical spectral projection $P(\xi)$ through

$$P(\xi)g = q(\xi)\langle \tilde{q}(\xi), g\rangle_{L^2_{\rm per}([0,1])}.$$

Symmetry of the spectrum and (D2') imply that λ satisfies (B.4).

Now, we choose a smooth cutoff function $\phi : [-\pi,\pi) \to [0,1]$ such that

$$\phi(\xi) = \begin{cases} 1, & \text{if } |\xi| \leq \xi_0/2 \\ 0, & \text{if } |\xi| \geq \xi_0 \end{cases}$$

and decompose the linearized solution operator $S(t) = e^{Lt}$ as $S(t) = S^I(t) +$

$S^{II}(t)$, with

$$\begin{aligned} S^I(t)g(x) &:= \int_{-\pi}^{\pi} e^{i\xi x}\phi(\xi)[P(\xi)e^{L_\xi t}\check{g}(\xi,\cdot)](x)d\xi \\ &= \int_{-\pi}^{\pi} e^{i\xi x}\phi(\xi)e^{\lambda(\xi)t}q(\xi,x)\langle\tilde{q}(\xi,\cdot),\check{g}(\xi,\cdot)\rangle_{L^2_{\mathrm{per}}([0,1])}d\xi \\ S^{II}(t)g(x) &:= \int_{-\pi}^{\pi} e^{i\xi x}[(1-\phi(\xi)P(\xi))\,e^{L_\xi t}\check{g}(\xi,\cdot)](x)d\xi. \end{aligned}$$

Note by the way that the Green kernel

$$G^I(x,t;y) := S^I(t)\delta_y(x)$$

is given by

$$G^I(x,t;y) = \int_{-\pi}^{\pi} e^{i\xi(x-y)}\phi(\xi)e^{\lambda(\xi)t}q(\xi,x)\tilde{q}(\xi,y)^*d\xi;$$

see the proof of Lemma 3.2 for some details. General considerations about semigroups leads for S^{II} to the following bounds, whose proof is essentially the same as Proposition 3.1.

Proposition B.2. *Under assumptions (H1')-(H2') and (D1')–(D3'), there exist constants $C,\theta>0$ such that for all $2\le p\le\infty$, $0\le 4l_1+l_2=l_3\le K+1$, $0\le 4m_1+m_2+m_3\le K$, K as in (H1'), $s=0,1$ and $t>0$*

$$\begin{aligned} \left\|\partial_t^{l_1}\partial_x^{l_2}S^{II}(t)\partial_x^{l_3}g\right\|_{H^s(\mathbb{R})} &\le Ct^{-\frac{4l_1+l_2+l_3}{4}}e^{-\theta t}\|g\|_{H^s(\mathbb{R})}, \\ \left\|\partial_t^{m_1}\partial_x^{m_2}S^{II}(t)\partial_x^{m_3}g\right\|_{L^p(\mathbb{R})} &\le Ct^{-\frac{1}{4}\left(\frac{1}{2}-\frac{1}{p}\right)-\frac{4m_1+m_2+m_3}{4}}e^{-\theta t}\|g\|_{L^2(\mathbb{R})}, \\ \left\|S^{II}(t)g\right\|_{L^p(\mathbb{R})} &\le Ce^{-\theta t}\|g\|_{H^1(\mathbb{R})}. \end{aligned}$$

Aiming at identifying up to remainders terms in form $S^I(t)g$ with terms in form $\bar{u}_x h$, we decompose further by expanding $q(\xi,\cdot)=\bar{u}_x+\mathcal{O}(\xi)$ and thus write $G^I(x,t;y)=\bar{u}_x(x)\tilde{e}(x,t;y)+\tilde{G}^I(x,t;y)$ with

$$\begin{aligned} \tilde{e}(x,t;y) &= \int_{-\pi}^{\pi} e^{i\xi(x-y)}\phi(\xi)e^{\lambda(\xi)t}\tilde{q}(\xi,y)^*d\xi \\ \tilde{G}^I(x,t;y) &= \int_{-\pi}^{\pi} e^{i\xi(x-y)}\phi(\xi)e^{\lambda(\xi)t}\,(q(\xi,x)-q(0,x))\,\tilde{q}(\xi,y)^*d\xi. \end{aligned}$$

Since then

$$\int_{\mathbb{R}} \tilde{e}(x,t;y)g(y)dy = \int_{-\pi}^{\pi} e^{i\xi x}\phi(\xi)e^{\lambda(\xi)t}\langle \tilde{q}(\xi,\cdot),\check{g}(\xi,\cdot)\rangle_{L^2_{\rm per}([0,1])}d\xi$$
$$\int_{\mathbb{R}} \tilde{G}^I(x,t;y)dy = \int_{-\pi}^{\pi} e^{i\xi x}\phi(\xi)e^{\lambda(\xi)t}\left(q(\xi,x)-q(0,x)\right)\langle \tilde{q}(\xi,\cdot),\check{g}(\xi,\cdot)\rangle_{L^2_{\rm per}([0,1])}d\xi,$$

a direct application of Hausdorff-Young inequality (1.15) yields the following bounds.

Proposition B.3. *Under the assumptions (H1')-(H2') and (D1)–(D3), the low-frequency Green function $G^I(x,t;y)$ of* (B.3) *may be decomposed as*

$$G^I(x,t;y) = \bar{u}'(x)\tilde{e}(x,t;y) + \widetilde{G}^I(x,t;y)$$

where for all $t \geq 0$ and $1 \leq q \leq 2 \leq p \leq \infty$, $0 \leq j,l,s, j+l \leq K+1$, the residual $\widetilde{G}^I(x,t;y)$ satisfies

(B.9)
$$\left\| \int_{\mathbb{R}} \partial_x^j \partial_t^l \partial_y^s \widetilde{G}^I(\cdot,t;y)g(y)dy \right\|_{L^p(\mathbb{R})} \leq C\,(1+t)^{-\frac{1}{2}\left(\frac{1}{q}-\frac{1}{p}\right)-\frac{1}{2}-\frac{l}{2}}\,\|g\|_{L^q(\mathbb{R})}.$$

Furthermore, for all $t \geq 0$, $1 \leq q \leq 2 \leq p \leq \infty$, $0 \leq j,l,s, j+l \leq K+1$,we have

$$\left\| \int_{\mathbb{R}} \partial_x^j \partial_t^l \partial_y^s \tilde{e}(\cdot,t;y)\; g(y)dy \right\|_{L^p(\mathbb{R})} \leq C(1+t)^{-\frac{1}{2}\left(\frac{1}{q}-\frac{1}{p}\right)-\frac{(j+l)}{2}}\|g\|_{L^q(\mathbb{R})}. \tag{B.10}$$

Finally, we combine the various exponential and algebraic bounds to obtain decay estimates on the Green function

$$G(x,t;y) = S(t)\delta_y(x) \tag{B.11}$$

associated with the full solution operator $S(t) = e^{Lt}$. To this end, we let χ be a smooth real valued cutoff function defined on $[0,\infty)$ such that $0 \leq \chi \leq 1$ and

$$\chi(t) = \begin{cases} 0, & \text{if } 0 \leq t \leq 1 \\ 1, & \text{if } t \geq 2 \end{cases}$$

and define

$$e(x,t;y) := \chi(t)\tilde{e}(x,t;y).$$

Using the Hausdorff-Young inequality (1.15) and the triangle inequality

$$\left\| \int_{\mathbb{R}} F(\cdot,t,y)g(y)dy \right\|_{L^p(\mathbb{R})} \leq C\|g\|_{L^1(\mathbb{R})} \sup_{y\in\mathbb{R}} \|F(\cdot,t,y)\|_{L^p(\mathbb{R})},$$

we obtain the following estimates.

Corollary B.4. *Under assumptions (H1')-(H2') and (D1')–(D3'), the Green function $G(x,t;y)$ of* (B.11) *decomposes as*

$$G(x,t;y) = \bar{u}'(x)e(x,t;y) + \widetilde{G}(x,t;y)$$

where, for some $C, \theta > 0$ and all $t > 0$, $2 \le p \le \infty$, and $0 \le j, l, s, j+l \le K+1$ we have

(B.12)
$$\left\| \int_{\mathbb{R}} \partial_y^s \widetilde{G}(\cdot,t;y) g(y) dy \right\|_{L^p(\mathbb{R})} \le C t^{-\frac{1}{4}\left(\frac{1}{2}-\frac{1}{p}\right)-\frac{s}{4}} (1+t)^{-\frac{1}{4}\left(\frac{3}{2}-\frac{1}{p}\right)-\frac{1}{2}+\frac{s}{4}} \|g\|_{L^1(\mathbb{R})\cap L^2(\mathbb{R})}$$

(B.13)
$$\left\| \int_{\mathbb{R}} \widetilde{G}(\cdot,t;y) g(y) dy \right\|_{L^p(\mathbb{R})} \le C (1+t)^{-\frac{1}{2}\left(1-\frac{1}{p}\right)-\frac{1}{2}} \|g\|_{L^1(\mathbb{R})\cap H^1(\mathbb{R})}$$

(B.14)
$$\left\| \int_{\mathbb{R}} \partial_x^j \partial_t^l \partial_y^s e(\cdot,t;y) g(y) dy \right\|_{L^p(\mathbb{R})} \le C (1+t)^{-\frac{1}{2}\left(1-\frac{1}{p}\right)-\frac{(j+k)}{2}} \|g\|_{L^1(\mathbb{R})}.$$

and $e(x,t;y) \equiv 0$ for $0 \le t \le 1$.

B.3 Nonlinear analysis

Given the linearized bounds on the linearized solution operator $S(t) = e^{Lt}$ derived in the previous section, we are now in position to consider the effect of the small nonlinear terms that were omitted in obtaining the linearized equation. For this purpose, we introduce $v(x,t) = \tilde{u}(x+\phi(x,t),t) - \bar{u}(x)$ as in (B.7). Direct calculations similar to those detailed in the proof of Lemma 3.3 provide the following lemma.

Lemma B.5. *For v as above, the equation is*

$$(\partial_t - L)(v - \psi \bar{u}_x) = \mathcal{N}, \quad \mathcal{N} = \mathcal{Q} + \partial_x \mathcal{R} + \partial_t \mathcal{S} + \mathcal{T} \tag{B.15}$$

where

$$\begin{aligned}
\mathcal{Q} &= -\left(f(\bar{u}+v) - f(\bar{u}) - df(\bar{u})v\right)\\
\mathcal{R} &= \psi_t v - 2\frac{-\psi_x}{1+\psi_x}v_x - \frac{-\psi_x}{1+\psi_x}\partial_x\left(\frac{1}{1+\psi_x}\partial_x\left(\frac{1}{1+\psi_x}v_x\right)\right) - \partial_x\left(\frac{-\psi_x}{1+\psi_x}\partial_x\left(\frac{1}{1+\psi_x}v_x\right)\right)\\
&\quad - \partial_x^2\left(\frac{-\psi_x}{1+\psi_x}v_x\right) - 2\frac{\psi_x^2}{1+\psi_x}\bar{u}_x - \frac{-\psi_x}{1+\psi_x}\partial_x\left(\frac{-\psi_x}{1+\psi_x}\partial_x\left(\frac{1}{1+\psi_x}\bar{u}_x\right)\right) - \frac{-\psi_x}{1+\psi_x}\partial_x^2\left(\frac{-\psi_x}{1+\psi_x}v_x\right)\\
&\quad - \frac{\psi_x^2}{1+\psi_x}\bar{u}_{xxx} - \partial_x\left(\frac{-\psi_x}{1+\psi_x}\partial_x\left(\frac{-\psi_x}{1+\psi_x}\bar{u}_x\right)\right) - \partial_x\left(\frac{\psi_x^2}{1+\psi_x}\bar{u}_{xx}\right) - \partial_x^2\left(\frac{\psi_x^2}{1+\psi_x}\bar{u}_x\right)\\
\mathcal{S} &= -v\psi_x\\
\mathcal{T} &= -\psi_x\left((1-r)v + f(\bar{u}+v) - f(v)\right).
\end{aligned}$$

By Duhamel's principle, we obtain the announced implicit representation (B.8), so that we may express the phase ψ and the nonlinear perturbation variable v implicitly as

$$\psi(x,t) = -\int_{\mathbb{R}} e(x,t;y)v(y,0)dy - \int_0^t\int_{\mathbb{R}} e(x,t-s;y)\mathcal{N}(y,s)dyds \tag{B.16}$$

and

$$v(x,t) = \int_{\mathbb{R}} \widetilde{G}(x,t;y)v(y,0)dy + \int_0^t\int_{\mathbb{R}} \widetilde{G}(x,t-s;y)\mathcal{N}(y,s)dy\ ds. \tag{B.17}$$

Furthermore, recalling that $e(x,s;y) = 0$ for $0 \le s \le 1$, we find by differentiating (B.16) that

(B.18)

$$\partial_t^j\partial_x^k\psi(x,t) = -\int_{\mathbb{R}} \partial_t^j\partial_x^k e(x,t;y)v(y,0)dy - \int_0^t\int_{\mathbb{R}} \partial_t^j\partial_x^k e(x,t-s;y)\mathcal{N}(y,s)dy\ ds.$$

for $0 \le j \le 1$ and $0 \le k \le K+1$. To apply a standard contraction-mapping argument and solve locally in time our Cauchy problem (B.17)-(B.18) with $(v,\psi_t,\psi_x) \in H^K(\mathbb{R}) \times H^K(\mathbb{R}) \times H^{K+1}(\mathbb{R})$, we only need besides our linear bounds the following nonlinear damping energy estimate whose proof is entirely similar to the one of Proposition 3.4.

Proposition B.6. *Assuming (H1'), there exist positive constants θ, C and ε_0 such that if v and ψ solve* (B.15) *on $[0,T]$ for some $T > 0$ and*

$$\sup_{t\in[0,T]} \|(v,\psi_x)(t)\|_{H^K(\mathbb{R})} + \sup_{t\in[0,T]} \|\psi_t(t)\|_{H^{K-1}(\mathbb{R})} \le \varepsilon_0$$

then, for all $0 \le t \le T$,

(B.19)

$$\|v(t)\|^2_{H^K(\mathbb{R})} \le Ce^{-\theta t}\|v(0)\|^2_{H^K(\mathbb{R})} + C\int_0^t e^{-\theta(t-s)}\left(\|v(s)\|^2_{L^2(\mathbb{R})} + \|\psi_x(s)\|^2_{H^{K+1}(\mathbb{R})} + \|\psi_t(s)\|^2_{H^{K-2}(\mathbb{R})}\right) ds.$$

With the above preparations in hand, we are now prepared to state the main technical lemma leading to the proof of Theorem B.1. To this end, associated with the solution (u, ψ_t, ψ_x) of the integral system (B.17) and (B.18) considered in the previous section, define

$$\eta(t) := \sup_{0\le s\le t} \|(v, \psi_t, \psi_x, \psi_{xx})(s)\|_{H^K(\mathbb{R})} (1+s)^{3/4}. \tag{B.20}$$

By standard short-time $H^K(\mathbb{R})$ existence theory, the function η is continuous so long as it remains sufficiently small. Using the linearized estimates of Section B.2 we now prove that if $\eta(0)$ is sufficiently small then $\eta(t)$ remains small for all $t > 0$.

Lemma B.3. *Under assumptions (H1')-(H2') and (D1')–(D3'), there exist positive constants* C *and* ε_0 *such that if* $v(0)$ *is such that for some* $T > 0$

$$E_0 := \|v(0)\|_{L^1(\mathbb{R})\cap H^K(\mathbb{R})} \le \varepsilon_0 \quad \textit{and} \quad \eta(T) \le \varepsilon_0$$

then, for all $0 \le t \le T$,

$$\eta(t) \le C(E_0 + \eta(t)^2). \tag{B.21}$$

Proof. First, note that under the above smallness assumption

$$\|\mathcal{N}(t)\|_{L^1(\mathbb{R})\cap L^2(\mathbb{R})} \le C\eta(t)^2(1+t)^{-3/2}.$$

Applying now the bounds of Corollary B.4 to representations (B.17)–(B.18), we obtain for any $2 \le p \le \infty$ the bounds

(B.22)

$$\begin{aligned}\|v(t)\|_{L^p(\mathbb{R})} &\le C\,(1+t)^{-\frac{1}{2}\left(1-\frac{1}{p}\right)-\frac{1}{2}} E_0 \\ &\quad + C\eta(t)^2\int_0^t (t-s)^{-\frac{1}{4}\left(\frac{1}{2}-\frac{1}{p}\right)} (1+t-s)^{-\frac{1}{4}\left(\frac{3}{2}-\frac{1}{p}\right)-\frac{1}{2}} (1+s)^{-\frac{3}{2}} ds \\ &\le C\left(E_0+\eta(t)^2\right)(1+t)^{-\frac{1}{2}\left(1-\frac{1}{p}\right)-\frac{1}{2}}\end{aligned}$$

and

(B.23)

$$\begin{aligned}\|(\psi_t,\psi_x)\|_{W^{K+1,p}(\mathbb{R})} &\leq C(1+t)^{-\frac{1}{2}(1-\frac{1}{p})-\frac{1}{2}}E_0 \\ &\quad + C\eta(t)^2\int_0^t (1+t-s)^{-\frac{1}{2}(1-1/p)-\frac{1}{2}}(1+s)^{-3/2}ds \\ &\leq C\left(E_0+\eta(t)^2\right)(1+t)^{-\frac{1}{2}\left(1-\frac{1}{p}\right)-\frac{1}{2}}.\end{aligned}$$

Finally, since the smallness assumption guarantees that we can apply Proposition (B.6) it follows that

$$\begin{aligned}\|v(t)\|^2_{H^K(\mathbb{R})} &\leq Ce^{-\theta t}E_0^2 + C\left(E_0+\eta(t)^2\right)^2\int_0^t e^{-\theta(t-s)}(1+s)^{-3/2}ds \\ &\leq Ce^{-\theta t}E_0^2 + C\left(E_0+\eta(t)^2\right)^s(1+t)^{-3/2} \\ &\leq C\left(E_0+\eta(t)^2\right)^2(1+t)^{-3/2},\end{aligned}$$

which, together with (B.23) , completes the proof. □

Assuming without loss of generality that the constant C in (B.21) is larger than 1, we obtain, since η is continuous and $\eta(0) = \|v(0)\|_{H^K(\mathbb{R})} \leq E_0$, by continuous induction that if $4C^2E_0 < 1$ then $\eta(t) \leq 2CE_0$ for all $t \geq 0$. Recalling (B.22), (B.23) and the definition of η yields (B.5).

Using Corollary B.4 again gives for $2 \leq p \leq \infty$

$$\begin{aligned}\|\psi(t)\|_{L^p(\mathbb{R})} &\leq CE_0(1+t)^{-\frac{1}{2}\left(1-\frac{1}{p}\right)} + CE_0^2\int_0^t (1+t-s)^{-\frac{1}{2}\left(1-\frac{1}{p}\right)}(1+s)^{-\frac{3}{2}}ds \\ &\leq CE_0(1+t)^{-\frac{1}{2}\left(1-\frac{1}{p}\right)}.\end{aligned}$$

Now by definition we have that

$$\tilde{u}(x,t) - \bar{u}(x) = v(x,t) + (\tilde{u}(x,t) - \tilde{u}(x+\psi(x,t),t)),$$

hence

$$\|\tilde{u}(t)-\bar{u}\|_{L^p(\mathbb{R})} \leq \|v(t)\|_{L^p(\mathbb{R})} + \|\bar{u}_x\|_{L^\infty([0,1])}\|\psi(t)\|_{L^p(\mathbb{R})} \leq CE_0(1+t)^{-\frac{1}{2}\left(1-\frac{1}{p}\right)}.$$

This completes the proof of Theorem B.1, establishing the nonlinear $L^1 \cap H^K \to L^p$ asymptotic stability of the underlying periodic traveling wave $\bar{u}$ under the structural and spectral assumptions (H1')-(H2') and (D1')–(D3').

B.4 Numerical stability analysis

We demonstrate the numerical stability verification method described in Section 2.1.3 in the context of the Swift-Hohenberg equation. To match with [Sc], we choose $f(u) = u^3$, set $\varepsilon = \sqrt{r}$ and rewrite (1.3) as

$$\partial_t u = (\varepsilon^2 - 1)u - 2\partial_x^2 u - \partial_x^4 u - u^3. \tag{B.24}$$

Stationary traveling wave solutions of (B.24) satisfy,

$$(\varepsilon^2 - 1)u - 2u'' - u'''' - u^3 = 0. \tag{B.25}$$

When ε is small there is a three parameter family of stationary periodic solutions approximated by

$$u_0(\omega, \phi, \varepsilon)[x] = 2\mathrm{Re}(\varepsilon(\sqrt{1 - 4\omega^2}/\sqrt{3})e^{i(1+\varepsilon\omega)x}e^{i\phi}) \tag{B.26}$$

and with period $X = 2\pi/(1 + \varepsilon\omega)$; see [Sc]. About $\bar{u}$, a periodic stationary wave solution of (B.24), the linearized evolution is described by $(\partial_t - L) = 0$ where

$$Lu := (\varepsilon^2 - 1)u - 2u_{xx} - u_{xxxx} - 3\bar{u}^2 u, \tag{B.27}$$

Note that the fact we deal with stationary solutions make L and L_0 self-adjoint. In particular, assumption (D1') of the previous section is a consequence of (D2') and the spectrum of L lies in $\mathbb{R}$ so that any transition to stability/instability must be marked by an eigenvalue passing through the origin for some possibly non-zero Bloch frequency. Furthermore, in [Eck, M1, MS] it was analytically verified that for $\varepsilon > 0$ small in (B.24) the solutions approximated by $u_0(\omega, \phi, \varepsilon)$ are spectrally stable, i.e. $\sigma_{L^2(\mathbb{R})}(L) \subset (-\infty, 0]$, provided that

$$\left|4\omega^2\right| < \frac{1}{3} + \mathcal{O}(\varepsilon). \tag{B.28}$$

Below, we apply an appropriate modification of the numerical protocol introduced in Section 2.1.3 above to analyze the stability of such small amplitude periodic wave trains of (B.24).

Modifying adequately the proof of Lemma 2.2, we find that $\sigma_{L^2(\mathbb{R})}(L) \subset (-\infty, \varepsilon^2]$. We first check that there is only one spectral branch of the associated Bloch operators L_ξ bifurcating from the origin at $\xi = 0$, and then track its location. In this case, the Evans function $D(\lambda, \xi)$ can be expanded to second order as

$$D(\lambda, \xi) = a_0\lambda + a_1\xi + a_2\lambda^2 + a_3\lambda\xi + a_4\xi^2 + \mathcal{O}\left(|\lambda|^3 + |\xi|^3\right).$$

Assuming that indeed only one critical spectral branch bifurcates from the $(\lambda, \xi) = (0, 0)$ state, expanding the critical spectral branch as $\lambda(\xi) = \alpha\xi + \beta\xi^2 + \mathcal{O}(|\xi|^3)$ it follows that the coefficients α and β are related to the above Evans function expansion via the formulas

$$\alpha = -\frac{a_1}{a_0} \quad \text{and} \quad \beta = -\frac{a_2\alpha^2 + a_3\alpha + a_4}{a_0}.$$

Recalling Remark B.2 together with the fact that here the spectrum is real, we note that $\alpha = 0$ so that $\beta = -\frac{a_4}{a_0}$, and thus there are only two coefficients of the Taylor expansion of the Evans function that need to be computed in order to check stability for $|(\lambda, \xi)| \ll 1$ with stability in this small-Floquet regime corresponding to the condition that $\beta < 0$.

For $\varepsilon = 0.187$, $\omega = 0.1$, and $X = 6.1678$ we compute the Evans function on a contour $\partial(B(0, R)/B(0, r_0) \cap \{\lambda \,|\, \mathrm{Re}(\lambda) \geq 0\})$ where $R = \varepsilon^2$ and $r_0 = 10^{-3}$ using 1001 Floquet parameters, ξ, evenly spaced in the interval $[-\pi/X, \pi/X]$, and an adaptive mesh in the λ contour requiring relative error be less than 0.2 between consecutive contour points. We then use the Taylor coefficients method to find $\beta = -3.874 + 0.000i$ via a convergence study requiring convergence in relative error between successive iterations of β be less than 0.01. As a check on the accuracy of our computation, we note that $\alpha = 5.2664e - 11 + 1.9970e - 07i \approx 0$. Next we determine the maximum modulus root of the Evans function for $|\xi| = 0.2$, $\xi \in \mathbb{C}$ using a λ contour of radius 2, yielding the bound, $\max(\lambda(\xi)) = 1.1099$.

We find that $k_0 = 1.7420e{-}4$ suffices for breaking the Floquet parameter interval into small and large modulus values. For $|\xi| > k_0$ we compute the Evans function on a semicircle of radius 0.1 passing through the origin requiring that the relative error between consecutive contour points not exceed 0.2. Then we compute the Evans function on the same semicircle shifted left by $1e - 4$, this time taking $|\xi| < k_0$. In all computations, we find the winding number is consistent with spectral stability.

We also find the stability boundary, though this time we do not use Taylor coefficients because the algorithm for α and β becomes numerically poor conditioned since a becomes small near much of the stability boundary; see Remark 2.4 above. To circumvent this difficulty, we find the stability boundary as given by computing the Evans function on a contour $\partial(B(0, \varepsilon^2)/B(0, r_0) \cap \{\lambda \,|\, \mathrm{Re}(\lambda) \geq 0\})$, $r_0 < \varepsilon^2$, to determine the presence of spectra as ω varies, and then take the limit of the location of the stability boundary found in this way as $r_0 \to 0$. We take care to choose via a convergence study a sufficiently tight tolerance setting in the RKF integration routine to obtain accurate results. We plot the stability boundary and

a comparison with the analytical bound given by Eckhaus, Schneider, and Mielke [Eck, M1, Sc] in Figure 10.

Finally, we verify numerically the eigenvalue picture given in Figure 1 of [Sc] by computing the Evans function on a circle and then solving for the roots using the method of moments as described in Section 2.1.5; see Figure 11.

C Appendix: Computational statistics

In this short appendix we detail computational statistics for some typical values in the numerical studies reported in previous sections. All numerical computations were performed on either a Mac Pro with 2 Quad-Core Intel Xeon processors with speed 2.26 GHz, the super computer Quarry[16] at Indiana University, an Intel(R) Pentium(R) 4 CPU with speed 2.80 GHz running Windows XP, or a MacBook with an Intel Core 2 Duo processor with speed 2.0 GHz.

Carrying out the stability study for the classical Kuramoto-Sivashinsky equation with $q = 6$ and $X = 6.3$, corresponding to the $q = 6$ row of Table 1, with the MacPro using 8-cores via MATLAB's parallel computing toolbox, it took 11.46 seconds to perform the High Frequency Evans function computation, 159.0 seconds to compute the Taylor coefficients $\{\alpha_j\}_{j=1,2}$ and $\{\beta_j\}_{j=1,2}$, 26.85 seconds to compute $\max_\xi |\lambda_j(\xi)|$, 169.5 seconds to compute the Evans function when[17] $k_0 < |\xi| < \pi/X$, and 40.89 sec to compute the Evans function for $|\xi| < k_0$. For these same parameters computing SpectrUW on the Windows machine using the Maple kernel took 26 seconds using 5 Fourier modes and 30 Floquet parameters. It took 55 seconds using 10 Fourier modes and 30 Floquet parameters.

The stability study computation times for the Swifth-Hohenberg equation, those discussed in Appendix B.4 using the MacPro with 8-cores are as follows. The High Frequency Evans function computation took 5.638 seconds, the Taylor coefficients took 81.73 seconds to compute, finding $\max |\lambda_j(\xi)|$ took 1.110 seconds, computing the Evans function for $k_0 < |\xi| < \pi/X$ took 11.30 seconds, and computing the Evans function for $|\xi| < k_0$ took 8.589 seconds.

The stability diagram in Figure 6 for the full parameter study of the

[16] This is a cluster composed of IBM HS21 Bladeservers and IBM iDataPlex dx340 rack-mounted servers.

[17] Here, we are following Section 2.1.3. In particular, k_0 is the low-frequency cutoff in Step 2(b) of the numerical procedure outlined in Section 2.1.3.

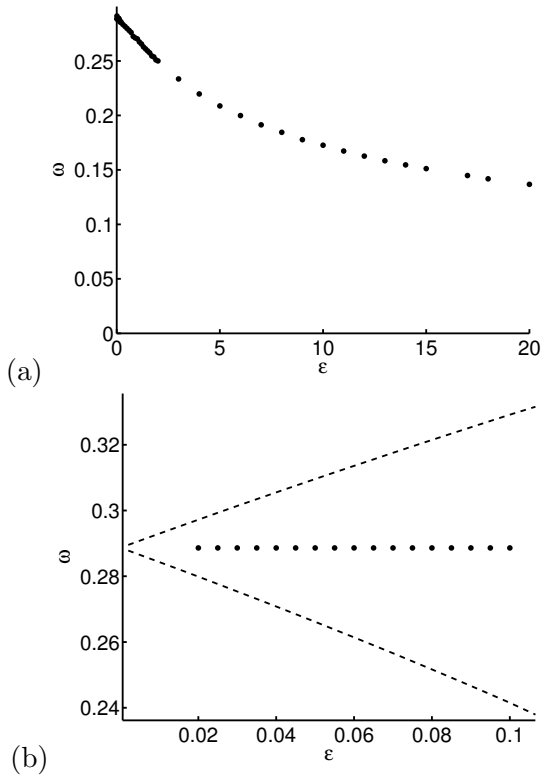

Figure 10: In (a) we plot the stability boundary for the Swift-Hohenberg equation, and in (b) we compare the numerical stability boundary with the analytic one in (B.28), plotted here using dashed lines, found by Eckhaus, Schneider, and Mielke [M1, MS]. This provides a check on our numerics against a well known result. The analytic curve is found by rigorous perturbation analysis in [Eck, M1, MS]. Our numerics give a nice extension to large amplitudes in the non-perturbative regime. We find the stability boundary with relative error tolerance of 0.01. In (a) we do a convergence study as $r_0 \to 0$ as described previously. In (b) we compute the Evans function on the contour $\partial(B(0,\varepsilon^2)/B(0,r_0) \cap \{\lambda \,|\, \mathrm{Re}(\lambda) \geq 0\})$, $r_0 = 1e-8$, with tolerance set at 1e-12 in the RKF routine.

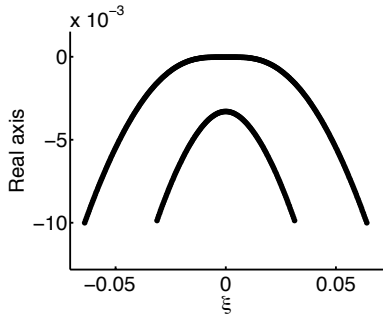

Figure 11: Plot of two smallest eigenvalues of the Swift-Hohenberg system against the Floquet parameter ξ for $\varepsilon = 0.05$, $\omega = 0.28858$; cf. Figure 1 in [Sc].

generalized Kuramoto-Sivashinsky equation took roughly 6 days on 6 nodes with 8 cores each on Quarry using MATLAB'S parallel computing capabilities. We took steps sizes of 0.25 in ε and 0.1 in period X to check for stability. Furthermore, the stability picture in Figure 10 for the Swift-Hohenberg equation took roughly 3 days running on the MacPro. Finally, concerning the time evolution studies in Section 2.3, those over time intervals of less than 50 took between 5-30 minutes each to run while those on larger time intervals took approximately 5 hours each to complete on the Macbook described at the beginning of this section.

D Appendix: Numerical Evans algorithm

Here, we briefly describe the numerical algorithm on which our Evans function computations are based, and explain the terminology (scaled lifted polar coordinate method; unscaled lifted polar coordinate method) used elsewhere in the paper. Recall the standard definition (2.13) of the periodic Evans function as $D(\xi, \lambda) := \det(\Psi(X) - e^{i\xi X}\mathbf{I})$, where $\Psi(x, \lambda)$ is the monodromy matrix of eigenvalue ODE (2.12), that is, a matrix-valued solution with initial condition $\Psi(0, \lambda) = \mathbf{I}$.

As pointed out in [OZ2], this is deceptively simple to code as compared to the homoclinic or front-type Evans function defined on the whole line [AGJ, PW, GZ], in the sense that there are no issues with infinite domains and imposition of asymptotic boundary conditions at $x = \pm\infty$, so that one may in a matter of moments develop a naive algorithm that is serviceable for

moderate values of λ and X, using any standard ODE evolution algorithm.

However, as described in [BJNRZ1], for the type of global parameter exploration carried out here, inherently involving large λ and X values, such a naive algorithm is essentially useless. This is most easily seen by the asymptotic relation [G2, SS, Z4] between the periodic and homoclinic Evans functions as period $X \to \infty$, as we now describe.

D.1 Balanced and rescaled Evans functions

Start with the eigenvalue equation $\mathbf{Y}'(x;\lambda) = \mathbb{H}(x,\lambda)\mathbf{Y}(x;\lambda)$, $x \in [0,X]$, Away from a finite set of curves $\zeta_j(k)$ determined by the dispersion relation $ik \in \sigma(\mathbb{H}(0,\lambda))$, $k \in \mathbb{R}$, where σ denotes spectrum, the eigenvalues of $\mathbb{H}(0,\lambda)$ have non-vanishing real part. For each $j \in \mathbb{N}$, set

$$\mathcal{C}_j := \{\lambda \in \mathbb{C} \mid \lambda = \zeta_j(k) \text{ for some } k \in \mathbb{R}\}$$

and let $\mathcal{C}$ denotes the compliment in $\mathbb{C}$ of the set $\cup_j \mathcal{C}_j$. On $\mathcal{C}$, we can define the real-valued function n such that $n(\lambda)$ equals the number of eigenvalues of $\mathbb{H}(0,\lambda)$ with negative real part noting, in particular, that n is locally constant on each connected component of $\mathcal{C}$. Similarly, we define the real valued functions $\alpha_\pm$ such that $\alpha_+(\lambda)$, respectively $\alpha_-(\lambda)$, equals the sum of the positive, respectively negative, real part eigenvalues of $\mathbb{H}(0,\lambda)$: as above, the functions $\alpha_\pm$ are locally constant on each connected component of $\mathcal{C}$. Following [G2], we note that, by Abel's formula, $D(\lambda,\xi)$ may be written alternatively as

$$D(\lambda,\xi) = \tilde{D}(\lambda,\xi)e^{-\int_0^{X/2} \mathrm{tr}(\mathbb{H}(y,\lambda))dy}, \tag{D.1}$$

where

$$\tilde{D}(\lambda,\xi) := \det(\Psi(0)\Psi(-X/2)^{-1} - e^{i\xi X}\Psi(0)\Psi(X/2)^{-1}) \tag{D.2}$$

is a "balanced" periodic Evans function defined symmetrically about $x = 0$.

Definition D.1. *For $\lambda \in \mathcal{C}$ and $\xi \in [-\pi/X, \pi/X)$, we define the rescaled balanced periodic Evans function as*

$$\check{D}(\lambda,\xi) := e^{(\alpha_-(\lambda)-\alpha_+(\lambda))X/2}e^{-n(\lambda)i\xi X}\tilde{D}(\lambda,\xi). \tag{D.3}$$

The rescaling in (D.3) is designed to cancel the exponential growth in (D.2) with respect to the period X of the pieces $\Psi(0)\Psi(-X/2)^{-1}$ and $\Psi(0)\Psi(X/2)^{-1}$ in the constant-coefficient case $\mathbb{H} \equiv$ constant. Indeed, suppose that $\bar{u}^X$ are a sequence of periodic waves with period X, converging

as $X \to \infty$ to a solitary wave, or homoclinic, solution $\bar{u}^\infty$, and index the associated sequence of periodic Evans functions by $D^X(\lambda, \xi)$. Then, under mild assumptions, we have [Z4]:

$$\lim_{X\to\infty} \check{D}^X(\lambda, \xi) = D_{\hom}(\lambda), \tag{D.4}$$

where $D_{\hom}(\lambda)$ denotes the associated homoclinic Evans function defined in [PW, GZ].

Comparing with (D.1) and (D.3), we see that if $\check{D}^X$ is uniformly bounded then D^X and $\tilde{D}^X$ exhibit exponential growth with respect to X. Thus, by (D.4), together with the well-known fact (see, e.g., [GZ]) that the homoclinic Evans function $D_{\hom}$, hence also $\check{D}^X$, is uniformly bounded on compact λ-domains, that both the usual and balanced Evans functions D^X and $\tilde{D}^X$ exhibit exponential growth with respect to X as $X \to \infty$, hence become numerically impractical for large X or for moderate periods X and large λ (leading to large $\alpha_\pm$) in the sense that even small variations in λ will lead to excessive winding in the image $D(\lambda, \xi)$ that requires fine resolution to track for purposes of winding number computations.

For our high-frequency winding number estimates, therefore, it is crucial to use the rescaled Evans function $\check{D}$ in place of D or $\tilde{D}$. Near $\lambda = 0$ on the other hand there are several curves on which the spectra of $\mathbb{H}(0)$ becomes imaginary, across which n, α_-, and α_+ undergo discontinuities. This does not occur on $\{\lambda \,|\, \mathrm{Re}\lambda \geq 0\}\backslash\{0\}$, so does not come into play in high-frequency estimates; however, for our tracking of spectral curves $\zeta_j(\xi)$ near zero using analyticity/the method of moments, it is evidently a problem. *Thus, for our low-frequency computations, we use the unrescaled Evans function, to avoid loss of analyticity that would otherwise occur near $\lambda = 0$,* a subtle but important point.

D.2 The lifted Evans function

Up to this point we have only discussed winding with respect to λ, ignoring questions of numerical conditioning. However, these are quite relevant also for large X, given the exponential growth already described. Indeed, one faces all of the issues described for homoclinic or front-type Evans functions in [Z1], arising from variations in growth rate of various scalar modes in the solution operator $\Psi(\lambda, x)$, in which faster-growing modes dominate slower-growing modes through cancellation/loss of significant digits.

Similarly as in the homoclinic case [Br, BrZ, HuZ], these can be avoided by the device introduced in [BJNRZ1] of working with "lifted equations"

for which the periodic Evans function appears as a *Wronskian* of certain bases of solutions. Namely, we may recall Gardner [G1], and his simple but important observation

$$D(\xi,\lambda) := \det(\Psi(X) - e^{i\xi X}\mathrm{Id}) = \det \begin{pmatrix} \Psi(X) & e^{i\xi X}\mathrm{Id} \\ \mathrm{Id} & \mathrm{Id} \end{pmatrix} \tag{D.5}$$

expressing D as an exterior product of evolving solutions for equations

$$\begin{pmatrix} Y \\ \alpha \end{pmatrix}' = \begin{pmatrix} \mathbb{H}(\lambda,\cdot)Y \\ 0 \end{pmatrix}, \tag{D.6}$$

with data $\begin{pmatrix} \mathrm{Id} \\ \mathrm{Id} \end{pmatrix}$ at $x = 0$ and $\begin{pmatrix} e^{i\xi X}\mathrm{Id} \\ \mathrm{Id} \end{pmatrix}$ at $x = X$.

Working with (D.5) allows us to apply any of the efficient algorithms that have been developed in the homoclinic Evans function setting for evaluation of Wronskians, in particular the *exterior product method* of [Br, BrZ] in which minors of columns in (D.5) are computed as evolving exterior products, or the *polar coordinate method* of [HuZ], in which they are computed instead as evolving orthonormal subspace/scalar "radius" pairs; see [HuZ] for further details. Both of these methods are by now standard and have been implemented in STABLAB, a Matlab-based platform for numerical Evans function computations; see [BHZ2]. These methods can thus readily be implemented once we have made the reformulation (D.5), and the resulting algorithm is numerically well-conditioned by the same analysis sed in [Z1] to study the homoclinic case.

The results of this apparently simple change are dramatic, *extending the range of $|\lambda|$ values that can be computed by up to three orders of magnitude*; see [BJNRZ1]. Indeed, the efficiency of the lifted balanced periodic method appears to be quite comparable with that of the well-established algorithms used to evaluate the homoclinic Evans function, making the numerical Evans function approach a practical alternative to the Galerkin methods that have been used in past literature [FST, CKTR, CDK].

D.3 Optimization across ξ

Finally, we mention for the reader who may wish to perform such computations independently a final detail that greatly speeds up computations with varying Bloch frequency ξ. Namely, rather than computing a new solution of (D.6) for each value of ξ, we may, by the decoupled nature of the flow in first and second coordinates, compute the result for a single solution initialized

as $\begin{pmatrix} \mathrm{Id} \\ \mathrm{Id} \end{pmatrix}$ at $x = X$, then multiply the first entry of the resulting solution by $e^{i\xi X}$ to obtain the desired suite of solutions for varying ξ. This means that we need in practice only compute solutions of the eigenvalue ODE once for each value of λ, with variation in ξ introduced by computationally negligible linear algebraic manipulations, for a considerable savings.

See [BJNRZ1] for further discussion/comparison of results.

E Appendix: Behavior near stability boundaries

Finally, we consider the difference in behavior expected as we cross a stability boundary across which hyperbolicity of the first-order Whitham system is lost vs. behavior expected as we cross a stability boundary where strict hyperbolicity is maintained but the second-order diffusion coefficient changes sign.

Introduce a bifurcation parameter η, with the stability boundary assumed to correspond to $\eta = 0$. In the second case, by standard spectral perturbation theory/separation to first order of modes, we have $\lambda_j(\xi, \eta) = ia_j(\eta)\xi - b_j(\eta)\xi^2 + ic_j(\eta)\xi^3 - d_j(\eta)\xi^4 + \mathcal{O}(\xi^5)$, where a_j, b_j, c_j, d_j (by complex symmetry of eigenvalues of real-valued operators) are real and

$$b_j = -b_*\eta + o(\eta), \quad d_j = d_* + o(1),$$

so that $\mathrm{Re}\lambda_j(\xi, \eta) \sim \eta b_*\xi^2 - d_*\xi^4$ and (after a brief calculation)

$$\max_\xi \mathrm{Re}\lambda_j(\xi, \eta) \sim \eta^2. \tag{E.1}$$

In the first case, we note, rather, that, by the connection to the second-order Whitham approximation, $\lambda_j(\xi, \eta) = \pm\sqrt{\eta}a_*\xi + b_*\xi^2 + o(\xi^2)$, whence

$$\max \mathrm{Re}\lambda_j(\xi, \eta) \sim \eta. \tag{E.2}$$

We may conclude that the transition involving loss of hyperbolicity is more drastic, featuring exponential growth at rate roughly the square root of the rate expected for a comparable transition across a boundary involving loss of diffusivity.

References

[AGJ] J. Alexander, R. Gardner and C.K.R.T. Jones, *A topological invariant arising in the analysis of traveling waves*, J. Reine Angew. Math. 410 (1990), 167–212.

[BaN] D. E. Bar and A. A. Nepomnyashchy. *Stability of periodic waves governed by the modified Kawahara equation.* Phys. D 86 (1995), no. 4, 586–602.

[BD] N. Bottman and B. Deconinck *KdV cnoidal waves are linearly stable*, Discrete Contin. Dyn. Syst. 25 (2009) no. 4, 1163-1180.

[BHZ1] B. Barker, J. Humpherys, and K. Zumbrun, *One-dimensional stability of parallel shock layers in isentropic magnetohydrodynamics,* J. Diff. Eq. 249 (2010) Issue 9, 21752213.

[BHZ2] B. Barker, J. Humpherys, and K. Zumbrun, *STABLAB: A MATLAB-based numerical library for Evans function computation,* Available at: http://impact.byu.edu/stablab/.

[BJNRZ1] B. Barker, M. Johnson, P. Noble, M. Rodrigues, and K. Zumbrun, *Efficient numerical evaluation of the periodic Evans function of Gardner and spectral stability of periodic viscous roll waves*, in preparation.

[BJNRZ2] B. Barker, M. Johnson, P. Noble, M. Rodrigues, and K. Zumbrun, *Whitham averaged equations and modulational stability of periodic solutions of hyperbolic-parabolic balance laws,* Journées équations aux dérivées partielles (2010), Exp. No. 3.

[BJNRZ3] B. Barker, M. Johnson, P. Noble, M. Rodrigues, and K. Zumbrun, *Stability of periodic Kuramoto-Sivashinsky waves*, Appl. Math. Lett. 25 (2012) no. 5, 824-829.

[BJRZ] B. Barker, M. Johnson, M. Rodrigues, and K. Zumbrun, *Metastability of solitary roll wave solutions of St. Venant equations,* Phys. D 240 (2011) no. 16, 1289-1310.

[BJZ] B. Barker, M. Johnson, and K. Zumbrun, *A posteriori estimates for Hill's method,* in preparation.

[BZ] B. Barker and K. Zumbrun, *Numerical stability analysis of ZND detonations,* in preparation.

[BrJZ] J. C. Bronski, M. Johnson, K. Zumbrun, *On the Modulation Equations and Stability of Periodic GKdV Waves via Bloch Decompositions* Phys. D 239 (2010), 2037-2065.

[BKJ] H.S. Brown, I.G. Kevrekidis, M.S. Jolly, *A minimal model for spatio-temporal patterns in thin film flows*, Pattern and Dynamics in reactive media, IMA Volumes in Mathematics and its applications (1991), vol 37.

[BMS] A.L. Bertozzi, A. Muensch, M. Shearer, *Undercompressive shocks in thin film flows.* Phys. D 134 (1999) no. 4, 431-464.

[Br] L. Q. Brin, *Numerical testing of the stability of viscous shock waves.* Math. Comp. 70 (2001) 235, 1071–1088.

[BrZ] L. Brin and K. Zumbrun, *Analytically varying eigenvectors and the stability of viscous shock waves.* Seventh Workshop on Partial Differential Equations, Part I (Rio de Janeiro, 2001). Mat. Contemp. 22 (2002), 19–32.

[CDKK] J. D. Carter, B. Deconick, F. Kiyak, and J. Nathan Kutz, *SpectrUW: a laboratory for the numerical exploration of spectra of linear operators*, Mathematics and Computers in Simulation 74 (2007), 370–379.

[CD] H-C. Chang and E.A. Demekhin, *Complex wave dynamics on thin films,* (Elsevier, 2002).

[CDK] H.C. Chang, E.A. Demekhin, D.I. Kopelevich, *Laminarizing effects of dispersion in an active-dissipative nonlinear medium,* Phys. D 63 (1993), 299–320.

[CKTR] B.I. Cohen, J.A. Krommes, W.M. Tang, and M.N. Rosenbluth, *Non-linear saturation of the dissipative trapped-ion mode by mode coupling* Nucl. Fusion 16 (1976) 971.

[DSSS] A. Doelman, B. Sandstede, Ab. Scheel, and G. Schneider. *The dynamics of modulated wave trains.* Mem. Amer. Math. Soc. 199 (2009) 934,viii+105.

[Eck] W. Eckhaus, *Studies in nonlinear stability theory*, Springer Tracts in Nat. Phil. Vol 6, 1965.

[E] S. Ei. *The motion of weakly interacting pulses in reaction-diffusion systems.* J. Dyn. Diff. Eq., 14 (1992), no. 1, 85–137.

[EMR] N. M. Ercolani, D. W. McLaughlin, and H. Roitner. *Attractors and transients for a perturbed periodic KdV equation: a nonlinear spectral analysis.* J. Nonlinear Sci. 3 (1993) 4, 477–539.

[FST] U. Frisch, Z.S. She, and O. Thual, *Viscoelastic behaviour of cellular solutions to the Kuramoto–Sivashinsky model* J. Fluid Mech. 168 (198) 221–240.

[G1] R. Gardner, *On the structure of the spectra of periodic traveling waves*, J. Math. Pures Appl. 72 (1993), 415-439.

[G2] R.A. Gardner, *Spectral analysis of long wavelength periodic waves and applications*, J. Reine Angew. Math. 491 (1997), 149–181.

[GZ] R. Gardner and K. Zumbrun, *The Gap Lemma and geometric criteria for instability of viscous shock profiles*, Comm. Pure Appl. Math. 51 (1998) no. 7, 797–85.

[He] D. Henry, *Geometric theory of semilinear parabolic equations*, Lecture Notes in Mathematics, Springer–Verlag, Berlin (1981).

[Ho] P. Howard, *Spectral analysis for periodic solutions of the Cahn-Hilliard equation on R* NoDEA Nonlinear Differential Equations and Applications 18 (2011) 1–26.

[HuZ] J. Humpherys and K. Zumbrun, *An efficient shooting algorithm for Evans function calculations in large systems,* Phys. D 220 (2006) no. 2, 116–126.

[KL] J. Kierzenka and L. F. Shampine, *A BVP solver that controls residual and error.* J. Numer. Anal. Ind. Appl. Math., 3 (2008) no. 1-2, 27–41.

[HLZ] J. Humpherys, O. Lafitte, and K. Zumbrun, *Stability of viscous shock profiles in the high Mach number limit,* Comm. Math. Phys. 293 (2010) no. 1, 1–36.

[HLyZ1] J. Humpherys, G. Lyng, and K. Zumbrun, *Spectral stability of ideal-gas shock layers*, Arch. Ration. Mech. Anal. 194 (2009) no. 3, 1029–1079.

[JNRZ1] M. Johnson, P. Noble, L.-M. Rodrigues, K. Zumbrun, *Behavior of periodic solutions of viscous conservation laws under Localized and nonlocalized perturbations* in preparation (2011).

[JNRZ2] M. Johnson, P. Noble, L.-M. Rodiruges, K. Zumbrun, *Non-Localized Modulation of Periodic Reaction Diffusion Waves: Nonlinear Stability*, preprint (2011), arXiv:1105.5040.

[JNRZ3] M. Johnson, P. Noble, L.-M. Rodiruges, K. Zumbrun, *Non-Localized Modulation of Periodic Reaction Diffusion Waves: The Whitham Equation*, preprint (2011), arXiv:1105.5044.

[JNRZ4] M. Johnson, P. Noble, L.-M. Rodrigues, K. Zumbrun, *Spectral stability of periodic wave trains of the Korteweg-de Vries/Kuramoto-Sivashinsky equation in the Korteweg-de Vries limit*, preprint (2012), arXiv:1202.6402.

[JZ1] M. Johnson and K. Zumbrun, *Nonlinear stability of periodic traveling waves of viscous conservation laws in the generic case*, J. Diff. Eq. 249 (2010) no. 5, 1213-1240.

[JZ2] M. Johnson and K. Zumbrun, *Nonlinear stability of periodic traveling waves of systems of reaction diffusion equations*, Annales de l'Institut Henri Poincare - Analyse non linéaire, 28 (2011) no. 4, 471-483.

[JZ3] M. Johnson and K. Zumbrun, *Nonlinear stability of periodic traveling wave solutions of viscous conservation laws in dimensions one and two*, SIAM J. Appl. Dynam. Syst. 10 (2011) no. 1, 189-211.

[JZ4] M. Johnson and K. Zumbrun, *Rigorous justification of the Whitham modulation equations for the generalized Korteweg-de Vries equation*, Stud. in Appl. Math. 125 (2010) no. 1, 69-89.

[JZ5] M. Johnson and K. Zumbrun, *Convergence of Hill's method for nonselfadjoint operators,* SIAM J. Num. Analysis, 50 (2012) no. 1, 64-78.

[JZN] M. Johnson, K. Zumbrun, and P. Noble, *Nonlinear stability of viscous roll waves,* SIAM J. Math. Anal. 43 (2011) no. 2, 577-611.

[KE] P. Kent and J. Elgin, *traveling-waves of the Kuramoto-Sivashinsky equation: period-multiplying bifurcations.* Nonlinearity 5 (1992) no. 4, 899-919.

[K] Y. Kuramoto, *Chemical oscillations, waves, and turbulence,* Springer-Verlag, Berlin, 1984, 164 p.

[KT] Y. Kuramoto and T. Tsuzuki, *On the formation of dissipative structures in reaction-diffusion systems,* Progress of Theoretical Physics, 1975. 54:3.

[LP] R. Laugesen and M. Pugh, *Linear stability of steady states for thin film and Cahn- Hilliard type equations,* Arch. Ration. Mech. Anal. 154 (2000) no. 1, 3-51.

[M1] A. Mielke, *Instability and stability of rolls in the Swift-Hohenberg equation,* Comm. Math. Phys. 189 (1997) no. 3, 829-853

[MS] A. Mielke and G. Schneider, *Attractors for modulation equations on unbounded domains – Existence and comparison,* Nonlinearity 8 (1995), 743-768.

[N1] P. Noble, *On the spectral stability of roll waves,* Indiana Univ. Math. J. 55 (2006) 795–848.

[N2] P. Noble, *Linear stability of viscous roll waves,* Comm. Partial Differential Equations 32 (2007) no. 10-12, 1681–1713.

[NR1] P. Noble, and M. Rodrigues, *Whitham's equations for modulated roll-waves in shallow flows*, preprint (2010), arXiv:1011.2296.

[NR2] P. Noble, and M. Rodrigues, *Modulated wave trains in a generalized Kuramoto–Sivashinsky equation*, preprint (2010), arXiv:1012.1733.

[OZ2] M. Oh and K. Zumbrun, *Stability of periodic solutions of viscous conservation laws with viscosity- 1. Analysis of the Evans function*, Arch. Ration. Mech. Anal. 166 (2003) no. 2, 99–166.

[OZ3] M. Oh and K. Zumbrun, *Stability of periodic solutions of viscous conservation laws with viscosity: pointwise bounds on the Green function* Arch. Ration. Mech. Anal. 166 (2003) no. 2, 167-196.

[OZ4] M. Oh and K. Zumbrun, *Stability and asymptotic behavior of periodic traveling wave solutions of viscous conservation laws in several dimensions* Arch. Ration. Mech. Anal. 196 (2010) no. 1, 1-20.

[Pa] A. Pazy, *Semigroups of linear operators and applications to partial differential equations,* Applied Mathematical Sciences, 44, Springer-Verlag, New York-Berlin, (1983) viii+279 pp. ISBN: 0-387-90845-5.

[PSU] R. Pego, H. Schneider, and H. Uecker, *Long-time persistence of Korteweg-de Vries solitons as transient dynamics in a model of*

inclined film flow, Proc. Royal Soc. Edinburg 137A (2007), 133–146.

[PW] R. L. Pego and M.I. Weinstein, *Eigenvalues, and instabilities of solitary waves*, Philos. Trans. Roy. Soc. London Ser. A 340 (1992), 47–94.

[SS] B. Sandstede and A. Scheel, *On the stability of periodic traveling waves with large spatial period,* J. Differential Equations 172 (2001), 134–188.

[SSSU] B. Sandstede, A. Scheel, G. Schneider, and H. Uecker, *Diffusive mixing of periodic wave trains in reaction-diffusion systems*, J. Differential Equations, to appear.

[Sc] G. Schneider, *Diffusive Stability of Spatial Periodic Solutions of the Swift-Hohneberg Equation*, Commun. Math. Phys. 178 (1996), 679–702.

[Se] D. Serre, *Spectral stability of periodic solutions of viscous conservation laws: Large wavelength analysis*, Comm. Partial Differential Equations 30 (2005) no. 1-3, 259–282.

[S1] G.I. Sivashinsky, *Nonlinear analysis of hydrodynamic instability in laminar flame. I. Derivation of basic equations,* Acta Astron. 4 (1977) no. 11-12, 1177–1206.

[S2] G.I. Sivashinsky, *Instabilities, Pattern Formation, and Turbulence in Flames*, Annual Review of Fluid Mechanics, January 1983. 15. Pp.179-199.

[W] H. A. Win, *Model equation of surface waves of viscous fluid down an inclined plane*, J. Math. Kyoto Univ. 33 (1993) no. 3, 803-824.

[YY] J. Yu, Y. Yang, *Evolution of small periodic disturbances into roll waves in channel flow with internal dissipation*, Stud. Appl. Math. 111 (2003) no. 1, 1-27.

[Z1] K. Zumbrun, *Numerical error analysis for evans function computations: a numerical gap lemma, centered-coordinate methods, and the unreasonable effectiveness of continuous orthogonalization,* preprint, 2009.

[Z2] K. Zumbrun, 2-*modified characteristic Fredholm determinants, Hill's method, and the periodic Evans function of Gardner,* to appear, Z. Anal. Anwend.

[Z3] K. Zumbrun, *A sharp stability criterion for soliton-type propagating phase boundaries in Korteweg's model*, Z. Anal. Anwend. 27 (2008) no. 1, 11–30.

[Z4] K. Zumbrun, *Stability of periodic traveling waves in the homoclinic limit,* in preparation.

q	δ	α_1	α_2	β_1	β_2
4.5	1.41	0.695+1.34e-05i	-0.695+1.33e-05i	-6.32-0.000214i	-6.32+0.000209i
4.6	1.42	6.86e-09+0.267i	7.83e-09-0.267i	-5.98-2.02e-07i	-5.98-3.91e-07i
4.7	1.43	-4.66e-09-0.792i	-5.37e-09+0.792i	-5.66-2.05e-08i	-5.66+9.42e-08i
4.8	1.44	2.44e-09-1.09i	1.89e-09+1.09i	-5.34-2.9e-07i	-5.34+2.15e-07i
4.9	1.45	2.38e-09-1.32i	1.57e-09+1.32i	-5.04-1.15e-07i	-5.04+8.15e-08i
5	1.46	-9.44e-09-1.52i	-9.9e-09+1.52i	-4.74+5.02e-07i	-4.74-2.85e-07i
5.1	1.47	4.21e-09-1.7i	3.06e-09+1.7i	-4.45-3.9e-07i	-4.45+2.9e-07i
5.2	1.48	8.39e-10-1.86i	2.29e-10+1.86i	-4.17-9.99e-09i	-4.17-7.39e-09i
5.3	1.49	-1.81e-07+2i	1.89e-07-2i	-3.9+1.95e-05i	-3.9+2.13e-05i
5.4	1.51	-1.37e-07+2.14i	1.67e-07-2.14i	-3.64-4.97e-05i	-3.64-4.72e-05i
5.5	1.52	-4.29e-07-2.27i	3.88e-07+2.27i	-3.38-2.82e-05i	-3.38-3.23e-05i
5.6	1.53	-3.99e-09-2.4i	-4.91e-09+2.4i	-3.13+4.78e-07i	-3.13-3.34e-07i
5.7	1.54	2.48e-10-2.52i	-4.01e-10+2.52i	-2.88-3.05e-08i	-2.88+2.41e-08i
5.8	1.55	-7.36e-10-2.63i	-1.31e-09+2.63i	-2.64+1.54e-07i	-2.64-5.01e-07i
5.9	1.56	-1.79e-09-2.74i	-2.24e-09+2.74i	-2.41+6.27e-08i	-2.41-1.07e-07i
6	1.57	-1.08e-09-2.84i	-1.79e-09+2.85i	-2.18+3.14e-09i	-2.18+1.26e-08i
6.1	1.58	3.79e-10-2.95i	2.89e-10+2.95i	-1.95+3.54e-07i	-1.95-3.47e-07i
6.2	1.59	1.91e-10-3.05i	-7.21e-10+3.05i	-1.73-4.21e-08i	-1.73-2.22e-08i
6.3	1.61	-1.14e-08-3.14i	1.18e-08+3.14i	-1.52+2.47e-07i	-1.52-2.87e-08i
6.4	1.62	-1.28e-08-3.24i	1.37e-08+3.24i	-1.3+2.88e-07i	-1.3+2.36e-08i
6.5	1.63	-3.76e-08-3.33i	3.67e-08+3.33i	-1.09+6.92e-07i	-1.09-1.71e-07i
6.6	1.64	-4.03e-08-3.42i	3.99e-08+3.42i	-0.885+6.99e-07i	-0.885-2.95e-07i
6.7	1.65	-4.33e-08-3.51i	4.33e-08+3.51i	-0.681+7.4e-07i	-0.681-2.83e-07i
6.8	1.66	-2.36e-09+3.6i	1.73e-08-3.6i	-0.476-8.45e-05i	-0.476-8.36e-05i
6.9	1.68	-2.66e-06+3.68i	2.66e-06-3.68i	-0.281+0.000738i	-0.281+0.000671i
7	1.69	-1.41e-08-3.77i	1.36e-08+3.77i	-0.0849+1.26e-07i	-0.0843-2.38e-07i
7.1	1.7	-1.5e-08-3.85i	1.39e-08+3.85i	0.109+1.6e-07i	0.11-1.23e-07i

Table 1: This table collects the coefficients of the Taylor expansions (2.15) of the critical modes bifurcating from the origin at $\xi = 0$ in the case $\varepsilon = 0$ and $X = 6.3$. Here, we vary the integration constant q in (2.3) and note then that $\delta = \delta(q)$ is determined from q via the periodic boundary conditions. This table demonstrates a range of values of q corresponding to spectrally stable 6.3-periodic traveling wave solutions of (2.1). In these computations, the evaluation of the integrals (2.17) was performed using an absolute tolerance of $1e-10$ and relative tolerance of $1e-8$ for the integration in the Floquet parameter, and an absolute tolerance of $1e-8$ with relative tolerance of $1e-6$ in the integration in λ. Furthermore, the value of the Evans function along the contour was found with absolute tolerance of $1e-8$ with relative tolerance of $1e-10$.

q	δ	α_1	α_2	β_1	β_2
4.6	1.41	0.694+0.272i	-0.694+0.272i	-6.46-1.05i	-6.46+1.05i
4.7	1.42	5.44e-08+0.518i	-6.31e-09+0.0311i	-9.16+1.37e-06i	-3.11-1.56e-07i
4.8	1.43	-2.91e-09-0.499i	-4.35e-09+1.05i	-4.86+9.51e-10i	-6.77+2.62e-07i
4.9	1.44	3.51e-09+1.35i	2.21e-09-0.791i	-6.2+3.6e-07i	-4.82-1.93e-07i
5	1.45	-2.02e-07+1.58i	7.16e-08-1.02i	-5.78-1.52e-05i	-4.64-4.23e-06i
5.1	1.46	9.62e-10-1.21i	9.17e-10+1.78i	-4.43-6.08e-08i	-5.42+1.06e-07i
5.2	1.47	1.55e-10-1.38i	-4.18e-10+1.96i	-4.2+1.05e-07i	-5.08-1.52e-07i
5.3	1.49	2.81e-09-1.54i	2.59e-09+2.12i	-3.97-1.89e-07i	-4.77+2.67e-07i
5.4	1.5	1.43e-09-1.68i	1.16e-09+2.27i	-3.74-1.73e-08i	-4.47-1.77e-08i
5.5	1.51	6.84e-10-1.81i	3.05e-10+2.41i	-3.51-3.51e-08i	-4.19+2.86e-08i
5.6	1.52	-9.72e-11-1.94i	-8.41e-10+2.54i	-3.28+2.7e-08i	-3.92-5.11e-08i
5.7	1.53	-1.05e-07+2.67i	5.65e-08-2.06i	-3.65+5.4e-06i	-3.06+2.24e-06i
5.8	1.54	2.55e-09-2.17i	2.12e-09+2.79i	-2.84-9.26e-08i	-3.39+6.11e-08i
5.9	1.55	-2.51e-09+2.9i	5.59e-09-2.28i	-3.14-2.14e-06i	-2.63-1.01e-06i
6	1.56	-4.8e-10-2.38i	-1.25e-09+3.01i	-2.42+6.1e-08i	-2.9-5.96e-08i
6.1	1.57	-4.61e-07-2.48i	6.86e-07+3.12i	-2.21-5.33e-05i	-2.66-0.000108i
6.2	1.58	-1.66e-09-2.58i	1.4e-09+3.22i	-2.01+2.63e-07i	-2.43+1.72e-07i
6.3	1.59	-8.86e-10-2.67i	-1.57e-09+3.32i	-1.81+1.27e-07i	-2.2-1.13e-07i
6.4	1.6	-4e-09+3.42i	5.31e-10-2.76i	-1.98+4.16e-06i	-1.61+2.22e-06i
6.5	1.62	-5.27e-10-2.85i	-7.42e-10+3.52i	-1.42+1.32e-07i	-1.76+3.66e-07i
6.6	1.63	1.34e-09-2.94i	3.55e-10+3.61i	-1.23+2.29e-07i	-1.55-2.84e-07i
6.7	1.64	-1.61e-09+3.7i	1.98e-09-3.02i	-1.34+5.22e-08i	-1.05+7.35e-09i
6.8	1.65	-6.87e-08+3.8i	4.71e-08-3.1i	-1.13+4.11e-06i	-0.865+1.19e-06i
6.9	1.66	-8.73e-07-3.18i	1.39e-06+3.88i	-0.688-3.38e-05i	-0.925-6.86e-05i
7	1.67	-9.68e-09+3.97i	8.81e-09-3.26i	-0.72-6.88e-06i	-0.51-4.02e-06i
7.1	1.68	-5.29e-09+4.06i	4.25e-09-3.33i	-0.521+1.23e-05i	-0.337+6.76e-06i
7.2	1.7	-2.46e-08-3.41i	3.62e-08+4.14i	-0.167+3.29e-07i	-0.324-2.02e-07i
7.3	1.71	-5.07e-07-3.48i	6.83e-07+4.23i	0.0037+0.000203i	-0.124+0.000359i
7.4	1.72	-2.72e-08-3.55i	4.14e-08+4.31i	0.167+1.17e-06i	0.0642+1.07e-06i

Table 2: Similar to Table 1, this table collects the Taylor coefficients of the critical modes in (2.15) in the case $\varepsilon = 0.2$ and $X = 6.3$. This table indicates the existence of a range of values of q corresponding to spectrally stable 6.3-periodic traveling wave solutions of (2.1). These computations were preformed with the same absolute and relative tolerances used for the computations discussed in Table 1.

δ	X_L	X_U		δ	X_L	X_U
0.1	9.03125	25.7188		0.045	8.98047	25.9219
0.095	9.03125	25.7188		0.04	8.98047	26.1406
0.09	9.03125	25.7188		0.035	8.98047	26.1406
0.085	9.03125	25.9062		0.03	8.98047	26.1406
0.08	9.03125	25.9062		0.025	8.98047	26.1406
0.075	9.03125	25.9062		0.02	8.98047	26.1406
0.06	8.98047	25.9219		0.015	8.98047	26.1406
0.055	8.98047	25.9219		0.01	8.98047	26.1406
0.05	8.98047	25.9219		0.005	8.98047	26.1406

Table 3: Table of the periods X_L and X_U corresponding respectively to the lower and upper stability boundary of the generalized KS system, $\partial_t u + \partial_x(u^2/2) + \partial_x^3 u + \delta(\partial_x^2 u + \partial_x^4 u) = 0$ as $\delta \to 0^+$.